The behaviour of drops of water moving through a superheated steam atmosphere

Klaus Peter Staskiewicz

THE BEHAVIOUR OF DROPS OF WATER MOVING THROUGH A SUPERHEATED STEAM ATMOSPHERE.

by

Klaus Peter Staskiewicz.,Ing.grd.(Berlin)

Thesis submitted for the degree of

Doctor of Philosophy

in the

University of Durham.

Department of Engineering Science
The University
Durham

December 1970

ABSTRACT

An experimental investigation has been made into the evaporation of large freely falling, oscillating water drops in an atmosphere composed entirely of its own vapour at varying pressures. Experiments were carried out at pressures of 2, 4, 5 and 6 x 10^5 N/m^2.

A photographic record was obtained of the drop at six observation points down the pressure vessel. From the drop diameter and the velocity of fall measured at the observation point the mass, Nusselt number, Reynolds number and coefficient of drag were calculated.

With an increase in pressure the Nusselt numbers were found to increase and were much higher in value than those obtained by other investigators who had, however, used anchored drops in a moving atmosphere. Values obtained for small, freely falling drops were not comparable with the large drops investigated in this study due to the difference in dynamics of the larger drop falling within a pressurised atmosphere composed entirely of its own superheated vapour.

From the experimental results it has been shown how the obtained heat-transfer coefficient decreased with the increase in excess temperature above the boiling point.

ACKNOWLEDGEMENTS

The author wishes to thank Professor R. Hoyle for his invaluable guidance and supervision throughout this work, and for granting facilities to carry out research in the Department.

The author also wishes to gratefully acknowledge the help of the academic and technical staff of the Department.

Thanks are due to Mr. K. Gordon (Newcastle University) and Mr. T. Brown for their help in the development of the experimental technique, and also to Mr. Venmore and his technical staff for building the apparatus.

TABLE OF CONTENTS

LISTS OF FIGURES

CHAPTER I

INTRODUCTION

There are many contexts in which the subject of the evaporation of drops is important. Consider the evaporation of petrol drops in air. In a combustion engine for instance, the petrol is drawn from the jet into the choke tube in the form of liquid drops of varying sizes, and it is important that these should be completely evaporated by the time the inlet valve is reached. To assist this process a common surface between exhaust and inlet manifolds is usually provided.

For the purpose of manufacturing dried milk, liquid milk is sprayed from an atomiser into a heated chamber. This process is known as spray-drying. Evaporation from each drop takes place until all the water content is removed and only the colloidal fat particle remains.

In the following examples it is attempted to demonstrate to the reader how very important the evaporation of water drops is in a superheated steam atmosphere.

The steam raised in a boiler is never dry saturated, there is invariably a small amount of liquid dispersed through the vapour as it enters the superheater. The question then arises how long this water drop may survive in the superheater and especially whether under any circumstance it has a chance to enter a high pressure turbine with the admission of superheated steam.

In spite of the usual warming through period steam, on entering a relatively cool turbine will form a condensate layer on the turbine components. The condensate will drain off, mostly due to gravity,

and will be pumped out from a drainage point. However, gravity will not be the main cause of drainage from the surface of the rotor. Rotation will cause a centrifugal force which will raise protrusions on the free surface of the condensate film. These protrusions will increase in size and will eventually be thrown off the rotor surface in the form of drops which will fly through the steam atmosphere until they strike some stationary part of the turbine where they will join other condensate, drained off by gravity and be removed from the casing by the extractor pump. The drop diameter varies with rotational acceleration as shown by the work of Matthew and Hoyle.(1) It is important how long these water drops survive in the superheated steam atmosphere. If their behaviour were accurately known, it might be possible under certain conditions to reduce the warming-up-period of the turbine.

During the operation of a high pressure turbine drops may be formed in the following ways:

a) High pressure turbines are driven by superheated steam at a high pressure-level and exhausted at a low pressure-level, thus developing steam power and reducing temperature. This reduction of steam energy may cause the formation of water drops. These drops may impinge on the rotating turbine blades and cause erosion, thus reducing the life span of the turbine.

b) The pressure difference across the guide vanes will cause condensation on the turbine inward edge of the vanes. Modern turbine designs have allowed for these condensate pools by producing hollow, slotted vanes. The condensate is drawn off through these slots, but the situation may arise when the vibrations of the rotor may cause

drops to be carried into the rotating turbine and they also may erode the blades.

c) Water may also form behind a rotating blade due to a pressure difference caused by rotation. This water may be thrown off the blades by centrifugal force, and in the form of drops, towards the turbine casing, but if their relative velocity is less than that of the rotating blades, they will impinge on a neighbouring blade. The impact of a water drop on a turning turbine blade can be very hard, and errosive effects will take place. This erosion may so weaken the blade that it breaks. The centrifugal forces resulting from loss of a blade are enormous; they can lead to complete destruction of the turbine.

In stationary condensers, for instance, using internally cooled tubes, the steam in contact is cooled by loosing energy to the cold surface. The condensate layer so formed will in turn act as a cold layer on which more steam condenses. In this way a liquid film is built up at an ever diminishing rate, and if no action intervened the film would grow so thick that condensation would virtually cease. However, drainage intervenes, whereby liquid is removed, thinning the film and allowing condensation to continue. The thicker the film, the more difficult is condensation, and good drainage of the film is therefore very important in condensers. In conventional stationary condensers drainage is by gravity. The liquid is pulled away from the tubes by its own weight and falls in a continuous stream, thus thinning the film. Continuous stream drainage prevails only in conditions of very heavy condensation - e.g. when steam enters the condenser very wet, when the condenser tubes are very large, etc. We are interested in the case of a fairly dry conden-

ser in which the drainage is by drops falling from the film. In any case, even if a continuous falling stream started from the film and conditions existed that provoked evaporation of the stream, the stream would soon become thin and break up into a series of drops. The atmosphere in the condenser will be that of water vapour, through which drops of water are falling. It is the subsequent history of one such drop, falling through an atmosphere of water vapour in which the author was interested.

Other examples from engineering and applied science could be quoted, but those already mentioned are sufficient to show that the problem of the evaporation of water drops in superheated steam occurs widely.

For evaporation to take place the drop must fulfil the following requirements:

a) there must be a temperature difference between the drop and its surroundings for energy to be transferred to the drop, and

b) there must be a pressure difference between the drop and its surroundings to promote mass diffusion from the drop surface into the atmosphere.

When a water drop evaporates in a superheated steam atmosphere the energy transferred to the drops is by conduction and convection. Starting in the centre of the drop and moving outward, the temperature rises as one passes through the first zone until, at the boundary, the evaporation temperature is reached. Moving further outward through the evaporation zone the temperature remains the same, although the fluid is saturated at the inner boundary, and dry

saturated steam at the outer, the change from one to the other is not made linearly. In this zone the vapour is wet, and its degree of wetness is decided by the motion of its molecules relative to the whole mass of fluid in the zone. In the boundary layer the temperature has been assumed to increase with the radial distance from the centre of the drop.

The condition of a drop at rest evaporating into a still atmosphere is a ficticious one, and greatly over-simplifies the process that is usually the case. Thus, for example, a drop being thrown off a rotor in a high pressure turbine may be travelling towards a turning blade, to the turbine casing or may be blown about by the superheated steam entering the rotating turbine. The drop is therefore in continual relative motion to the surrounding atmosphere; this effect sweeps away the surrounding saturated vapour cloud. An increased pressure difference is promoted at certain areas between the drop surface and the atmosphere, thus accelerating the mass transfer rate. Boundary layer theory indicates that the rate is a maximum at the forward stagnation point and reaches a minimum at the boundary layer separation point. An attempt to calculate in detail the evaporation behaviour of a water drop would be very difficult; there are no theoretical solutions to the problem of heat and mass transfer from a spherical surface. This problem is further complicated for high concentration gradients as the mass leaving the drop surface affects the flow pattern around the drop.

Semi-empirical correlations have been obtained for cases of small concentration gradients. Frössling[7] presented an equation

in which the Sherwood number, corresponding to a transfer coefficient, was related to the Schmidt and Reynolds number; a similar equation was obtained by Ranz and Marshall[8] relating the Nusselt number to the Prandtl and Reynolds number. These equations were adequate for evaporation into air atmospheres at temperatures up to 220°C and a Reynolds number range of 2 - 800.

The majority of experiments on the evaporation of drops has been carried out with anchored drops in a moving high and low temperature atmosphere. Such experiments showed that the square of the drop diameter decreased linearly with time of exposure. The drop diameter used was usually 100 - 200 μm and the medium hot air. Lee and Ryley[9], however, blew superheated steam past an anchored water drop. Their work agreed closely with the work of Frössling, Ranz and Marshall, and a similar equation relating the Nusselt number to the Prandtl and Reynolds number was obtained.

The dynamics of an evaporating drop falling freely in superheated steam has received little attention in the past. When evaporation occurs the drag is expected to decrease as there is a thickening of the boundary layer with a reduction in the relative velocity at the drop surface. This drag reduction has been shown by Ingebo.[13] Many investigators have ignored this fact and used standard drag coefficient curves which apply to smooth, spherical, solid particles, moving in a steady state without heat or mass transfer. Due to experimental and theoretical difficulties the study of freely falling water drops in a superheated steam atmosphere has been limited.

As a step nearer to a practical system, the object of this work has been to study single water drops approximately 4 mm in diameter as they evaporate falling freely through a superheated steam atmosphere.

In order to study the effect of heat transfer the experiments have covered a water drop in a superheated steam atmosphere at 200°C at 6 bar and to 200°C at 2 bar. The Reynolds number range varied from 600 to 1600 (based on physical properties of surrounding atmosphere). The trajectory of the drops have been recorded to calculate the drag coefficients under these conditions.

The drop size and distance travelled were obtained by repetetively photographing the drop as it travelled down the chamber. The change of the square of the drop diameter was donstant but varied with pressure.

CHAPTER II.

LITERATURE SURVEY.

So many investigators have studied the evaporation of drops that it is of advantage to separate the literature in the following sections:

1. Evaporation of stationary drops in a still air atmosphere.
2. Evaporation of stationary drops in moving atmosphere.
   a) air (low temperature, high temperature).
   b) superheated steam.
3. Evaporation of freely falling drops in a still air atmosphere.
4. The drag of liquid drops undergoing heat and mass transfer.

II.1. Evaporation of stationary drops in a still air atmosphere.

Many investigators have shown that the decrease of surface area, due to simultaneous heat and mass transfer, from a stationary drop in low temperature surroundings is directly proportional to the time of exposure to the atmosphere.

This may be written as:

$$r_o^2 - r_t^2 = C.t \qquad 2.1$$

r_o is the initial drop radius

r_t is the drop radius at the time t

t is the time, and

C is the evaporation constant

Kumagai and Iseda[10] obtained data for single drops of cetane, heptane, benzene and ethyl alcohol evaporating into a high temperature air atmosphere suspended on a silica filament. The data

obtained showed that equation 1.1. is also valid over most of the evaporation period in a high temperature air atmosphere.

A complete survey on the evaporation and growth of drops in gaseous media has been written by N. A. Fuchs[2] and the N.A.C.A. Report No. 1300 [3] deals with evaporation and combustion of droplets. Some of the more relevant results are discussed in this section.

Nichiwaki and Haghi[4] experimentally measured the variation of diameter with time of liquid drops suspended on a fine silica filament. The filament, 0.1 mm diameter, was inserted into a hot chamber and motion pictures taken of the drop. Initial drop diameters ranged from 0.8 mm to 1.2 mm and the liquids used were water, benzene, ethyl alcohol and methyl alcohol. The results showed that the square of the diameter decreased linearly with time. Kobayasi[5] mounted a furnace on wheels so that it could be moved quickly into position around a suspended drop, and achieved similar results. Spalding [6] investigated the combustion of liquid fuels using model drops made by fluid flowing continuously over solid spheres. He obtained the following expression for the mass transfer rate from a liquid sphere in an infinite atmosphere:

$$\frac{dm}{dt} = - \frac{2\pi D.k.\ln(1 + B)}{c} \qquad 2.2.$$

D is the drop diameter.

k is the mean thermal conductivity

B is the transfer number of the fuel

c is the specific heat of the medium

For evaporation into high temperature atmospheres, Spalding stated that the transfer number B is given by $B = \frac{Cm \,.\, \Delta T}{L}$

where C_m is the mean specific heat of the medium, ΔT is the temperature difference between the atmosphere and drop surface, and L is the latent heat of the liquid, assuming the drop has reached a steady temperature.

2.2.a. Evaporation of stationary drops in a moving air atmosphere.

Frössling [7] studied drops of water, aniline, naphtalene and nitrobenzene evaporating into airstreams at room temperature. The data were obtained over a range of Reynolds Numbers from 2 to 750 and correlated by an empirical equation of the form:

$$Sh = 2.0 + C_1 S_c^m Re^n \qquad 2.3$$

where Sh is the Sherwood Number corresponding to an overall transfer coefficient.

Sc is the Schmidt Number corresponding to the ratio ϑ/D; ϑ = viscosity; D = diffusivity.

Re is the flow parameter for convective heat transfer (Reynolds Number)

C_1 is a constant.

$m = \frac{1}{3}$

$n = \frac{1}{2}$

"m" is an index of the effect of convective velocity on mass transfer, and "n" an index of the ratio of momentum and diffusion boundary layer thickness on mass transfer.

Many molecules, because of their irregular movement, return to the drop surface and in turn are partially accepted by it. Frössling showed this irregular transfer rate along the drop surface.

Ranz and Marshall [8] carried out investigations of the rate of evaporation of water drops and water drops containing dissolved and suspended solids up to 220° C using high-speed photography to

record the decrease in drop diameter. They expressed their mass-transfer correlation by the equation:

$$Nu' = 2.0 + 0.6\ Sc^{\frac{1}{3}}\ Re^{\frac{1}{2}} \qquad 2.4.$$

Nu' = Nusselt Number for mass transfer.

By analogy heat-transfer data should be correlated by a corresponding equation:

$$Nu = 2.0 + 0.6\ Pr^{\frac{1}{3}}\ Re^{\frac{1}{2}} \qquad 2.5.$$

Their results of studies on pure liquid drops confirmed the analogy between heat and mass transfer at low Reynolds numbers. They pointed out that this correlation does not apply in high temperature surroundings and large concentration gradients, as sensible heat gained by the vapour and diffusion due to thermal gradients in the transfer path will have to be taken into account.

Toei, Okuzahi and Kubota[30] studied the evaporation of supported water drops into a stream of steam-air mixture. They worked with drop sizes of 1.2 mm to 2.1 mm, an atmosphere temperature of up to 140°C and a Reynolds number range of 0 to 120. They correlated their results for heat transfer by the equation:

$$Nu = 2.0 + 0.65\ Re^{\frac{1}{2}}\ Pr^{\frac{1}{3}} \qquad 2.6$$

Their results for the small Reynolds number range used agreed well with the work done by Frössling and Ranz and Marshall.

For high rates of mass transfer in forced convective flow, no theoretical solutions have been obtained. Such solutions would involve the simultaneous solving of the generalized equation of heat conduction together with the Navier-Stokes equation and the equation of continuity under the boundary conditions defining the evaporative

flow of the vapour at the drop surface with the general gas motion equation in the neighbourhood of the drop.

Gohrbrandt[11] however studied the evaporation of camophor spheres mounted in a hot air stream and derived an expression for the mass transfer of a hemisphere, which may be written over the whole sphere as

$$\frac{dm}{dt} = -K \frac{k.D}{C} \frac{B}{1+B} Re^{\frac{1}{2}} \qquad 2.7$$

where K is a constant, k the thermal conductivity of the medium, D the drop diameter, C the specific heat of the medium at constant pressure and B the transfer number. It was found that at temperatures up to 760 °C the heat transfer coefficient decreased with increase in temperature difference.

Rasbach and Stark [12] measured the evaporation rate of a water drop suspended on a quartz fibre in a bunsen flame. The value for the heat transfer agreed with that calculated from the equation of Ranz and Marshall how, if the calculated value were multiplied by a constant factor of 0.63

$$Nu = 0.63(2 + 0.60 \ Pr^{\frac{1}{3}} \ Re^{\frac{1}{2}}) \qquad 2.8.$$

The constant factor accounts for the mass flow of vapour which acquires sensible heat as it passes through the boundary layer surrounding the drop surface.

2.2.b. Evaporation of stationary drops in a moving superheated steam atmosphere.

K. Lee and D. J. Ryley[9] made a study of water drops suspended in a stream of superheated steam. The data were obtained over a range of Re numbers from 64 to 250 and an ambient temperature of up to 143°C.

They accepted the corrolation of 1.5, but the constant $C_1 = 0.738$ exceeded the Ranz and Marshall value of 0.6. This they attributed to the fact that the water drop was evaporating into an atmosphere composed entirely of its own vapour. Their correlating equation was

$$\overline{Nu} = 2.0 + 0.74 \; Re^{\frac{1}{2}} \; Pr^{\frac{1}{3}} \qquad 2.9.$$

$\overline{Nu}$ is the mean Nusselt number for heat transfer. The drop was observed to oscillate slightly in certain circumstances, but it was not known how this influenced the evaporation.

2.3. Evaporation of freely falling drops in a stationary atmosphere.

Eisenklam[26] studied the mass transfer from drops with simultaneous heat transfer in an air atmosphere. The experiments were carried out with a wide range of liquids (methyl alcohol, ethyl alcohol, benzene, heptone, pentane and water) with air temperatures from 200°C to 1000°C and with drop sizes from 25 μm to 2 mm. For comparative purposes mean physical property values of the fluid surrounding the drop were used in their calculations. The transfer number B was used to characterize the effect of intense mass transfer. This transfer number corresponds to the one used by Spalding.[6] Their correlating equation is:

$$Nu^{*} \; (1 + Bm) = 2 + 1.6 \; (Re_m)^{\frac{1}{2}} \qquad 2.10$$

m denotes an evaluation of B or Re at mean temperatures.

Topps[17] carried out an investigation of the evaporation of drops 300 μm to 500 μm diameter, falling at their terminal velocity in air at temperatures of up to 800°C. Quantitative results for the pure hydrocarbons showed a rate of evaporation

$\frac{dm}{dt}$, which varied approximately as the (radius), [4.6]. He suggested that the temperature of the vapour leaving the surface of the drop boundary layer is below the ambient level, but that ambient temperature can always be attained in the wake. Also that the variation of evaporation rate with temperature is affected by the outward flow of vapour from the drop surface reducing the transfer rate of heat to it.

2.4. The drag of liquid drops undergoing heat and mass transfer.

The laws governing a spherical particle moving freely through an undisturbed fluid have been expressed by means of a drag coefficient, C_D, defined by:

$$C_D = \frac{F}{A_p \rho_o V^2} \qquad 2.11$$

where F = drag force.

ρ_o = density of fluid.

V = velocity of particle

A_p = projected area of particle.

The standard drag coefficient curve having C_D and Re as ordinates applies to smooth solid spheres, moving at a constant velocity in an incompressible fluid of sufficient extent to eliminate the effects of the confining walls. The resistance to a sphere in motion is due to friction effects consisting of film friction and form friction. ~~In~~ Outside Stokes Low region, Re $>$ 0.1, form friction caused by pressure variation on drop surface contributes the major part of the total drag and its relative importance decreases steadily as the Re number of the particle increases.

The Navier-Stokes equations are the basis of any theoretical description of a fluid system so that their specific solutions would predict all flow properties of that system. However, a general solution is unjustified since major assumptions have to be made of the physical properties and motion of the droplet. Under conditions of mass transfer a solution would become even more complex, since the boundary condition of zero velocity in the drop surface is no longer true.

Ingebo[13] studied the drag coefficients for droplets and solid spheres in an accelerating air stream. Diameter and velocity data for individual drops and solid spheres were obtained with a high-speed camera. The drag coefficients for water is octane and trichlorethylene drops were found to correlate by the equation:

$$C_D = 27/Re^{0.84} \qquad 2.12$$

for $6 < Re < 400$

He states that when evaporation rates were low, solid-sphere equations were applicable.

Eisenklam[26] also studied the effect of mass transfer on the drag coefficient and found that it was greatly reduced. This reduction was due to the boundary layer thickness increasing, separation occurs at a different place, and the separation wake is changing.

The correlating equation for a sphere with mass transfer was found to be:

$$C_D^* \quad (1 + B) \quad = C_D$$

$C_d^{\equiv}$ = Drag coefficient with mass transfer

B = transfer number

C_d = Drag coefficient without mass transfer.

It can be seen that the evaporation of small supported water drops in an air atmosphere has been well established, but the evaporation of freely falling water drops in a pressurised steam atmosphere has received little attention. In order to come near a practical system, methods and apparatus were devised to study a drop travelling freely through a pressurised superheated steam atmosphere as encountered in condensers or steam turbines. The object of the work was to study the effect of pressure on the evaporation of a drop of water at terminal velocity in a superheated steam atmosphere.

Experimenters.	Year.	Mode of transfer.	Diameter of sphere mm.	Material of sphere.	Medium.	Re.	Motion.	Correlation.
Frössling	1938	Mass	0.2-1.8	Water. Nitro-benzene aniline	Air	2.3-1280	anchored	$\bar{Sh} = 2+0.552\ Re^{0.5}Sc^{0.33}$
Ranz & Marshall	1952	Mass Heat	0.6-1.1	Water	Air	0-200	anchored	$\bar{Sh} = 2+0.6\ Re^{0.5}Sc^{0.33}$ $\bar{Nu} = 2+0.6\ Re^{0.5}Pr^{0.33}$
Rasbach & Stark		Heat	1.3-2.3	Water	Bunsen flame	100-2,000	anchored	$\bar{Nu} = 0.63(2+0.6\ Re^{0.5}Pr^{0.33})$
Eisenklam	1966	Mass	0.025-2.00	methyl alcohol, benzene, heptane, petane and water	Air	0.2-10	free fall	$\bar{Nu}\ (1+B_m) = 2.16\ Re_m^{0.5}$ 17.
Ingebo	1951	Mass	6.88	Benzene acetone ethonal	Air	1600-5700	anchored	$\bar{Nu} = (\frac{ka}{kv})^{0.5}[2+0.303(ReSc)^{0.6}]$
Lee & Ryley	1967	Heat	0.23-1.13	Water	Superheated steam	64-250	anchored	$\bar{Nu} = 2+0.74Re^{0.5}Pr^{\frac{1}{3}}$
Toei, Okazaki & Kubota	1966	Heat	1.12-2.1	Water	Air-steam	0-120	anchored	$Nu = 2 + 0.65Re^{0.5}Pr^{\frac{1}{3}}$

CHAPTER III

EXPERIMENTAL SECTION.

The method consisted of photographically observing water drops as they fell down a vertical vessel containing pressurised superheated steam. The diameter and velocity were determined at six different observation points down the vertical axis. The superheated steam pressure was varied from 2 to 6 bar.

III.1. Photographic Technique.

For the photographic study of a freely falling drop, a large depth of field is necessary as the drop does not fall vertically but may drift at random from a vertical path even in a still atmosphere. Also, enlarged drop images were needed to study the behaviour of the drop in the pressurised superheated steam atmosphere. This was achieved by increasing the distance from the camera lens to the film. This distance increase was chosen so that, it was not too small to observe the change of shape and drift of the drop and not too large that the aperture was not too small so accurate image definition is ensured. In Fig.1., the photographic technique is shown.

Rear illumination from a 200-Watt tungsten-halogen lamp diffused by a temperature resistant ground glass screen was found to promote good definition.

III.2. Apparatus.

The flow diagram, Fig.2, shows the layout of the apparatus in nine parts:-

Diagram of Photographic Technique.

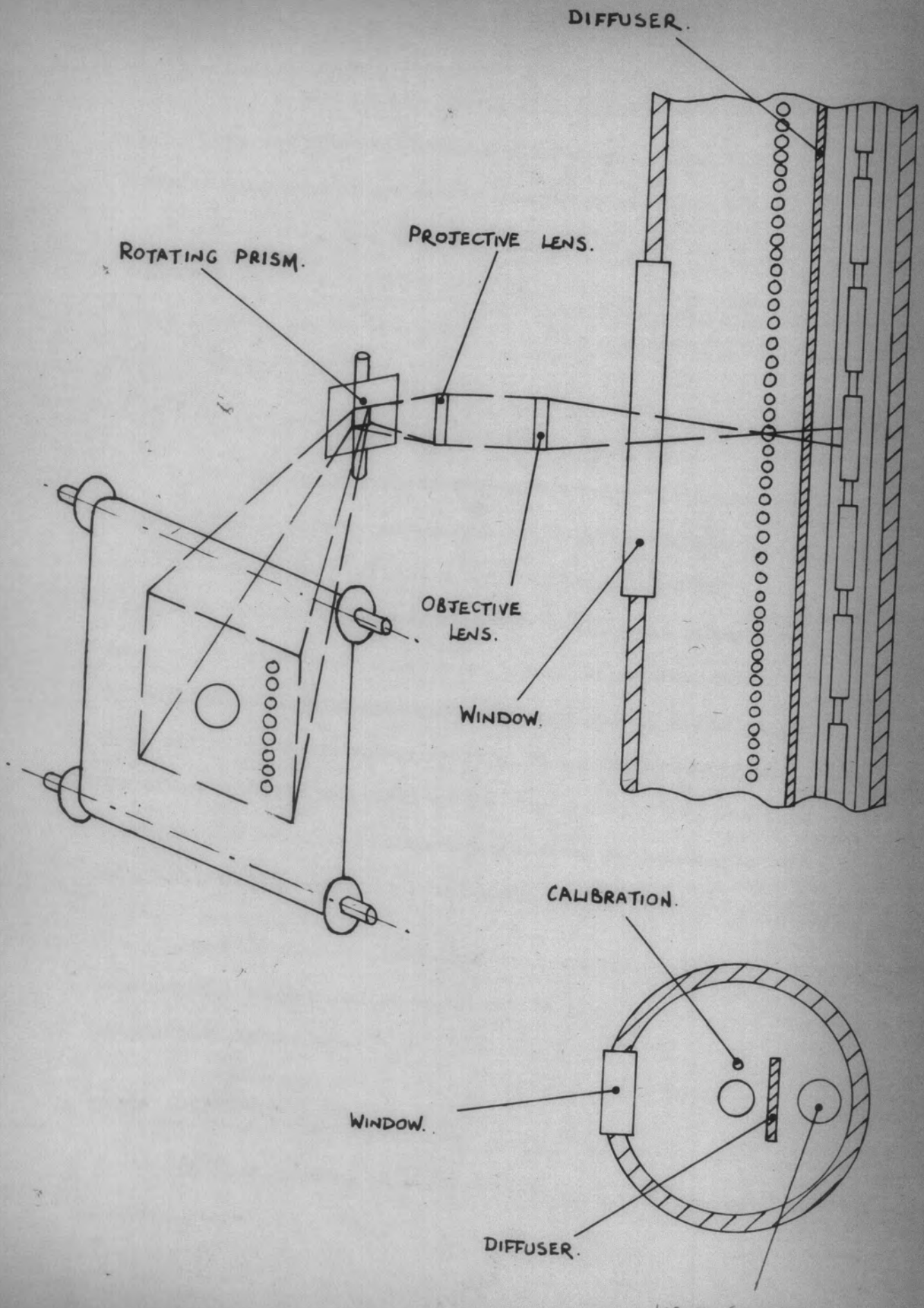

FIG. 1.

FIG. 1

1. Steam-generating system, consisting of feed tank, feed pump, boiler, separator, superheater and reducing valve.

2. Test section, consisting of pressure vessel, means of measuring temperature and pressure, apparatus for producing drops, and apparatus for recording the drop's behaviour in flight.

3. A condenser with cooling water and extraction pump.

III.3. Steam generating system.

Steam at pressures from 1 to 10 bars at a temperature of 200° C was required for the investigation. The feed water, processed to one part per million permanent hardness, was pumped into a Clayton steam generator, Model RO.110. The wet steam was passed through a separator, from which it emerged 97% dry, to an oil fired superheater in which its temperature was raised through a pressure reducing valve, set at the required pressure. The reducing valve was diaphragm operated, and had a downstream pressure tapping. This tapping sensed the downstream pressure and acted on the diaphragm for a fine controlled pressure. The steam now entering the testing section was superheated and pressure controlled. The used steam was condensed and drawn off with an extraction pump.

III.4. Test Section.

Measurement:

Experiments with a freely falling drop, 3 mm in diameter in air at room temperature showed a distance 350 mm was necessary for the drop to reach its terminal velocity. Consideration of the expected

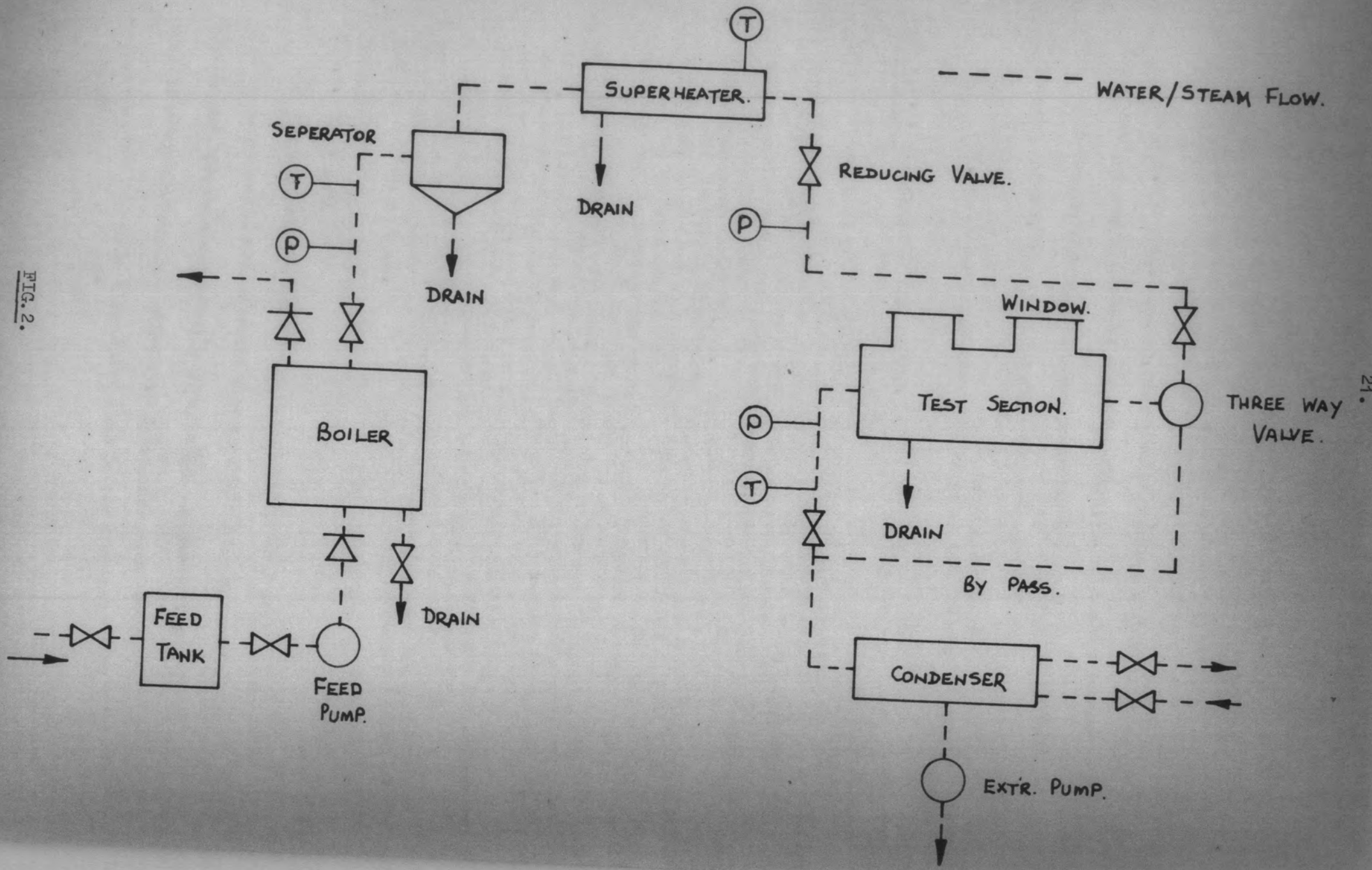
T
SUPERHEATER.
WATER/STEAM FLOW.
SEPERATOR
T
P
DRAIN
DRAIN
REDUCING VALVE.
P
WINDOW.
TEST SECTION.
P
T
THREE WAY VALVE.
DRAIN
BY PASS.
BOILER
DRAIN
FEED TANK
FEED PUMP.
CONDENSER
EXTR. PUMP.

FIG. 2.

evaporation rates, a distance of fall of 320 mm was thought to be necessary for the drop to reach its terminal velocity and therefore to be sufficient a distance for observation. The vessel, which was electrically heated externally, had six 360 mm x 50 mm windows, through which the drop could be observed. The internal temperature was measured by thermo-couples and closely controlled by means of a variable transformer in the circuit of the electric heater. The pressure inside the vessel was measured upstream of the steam outlet valve.

III.4.1. Pressure vessel.

The design of the pressure vessel is shown in Fig.3. The vessel is made of stainless steel tubing, 125 mm inside diameter x 13 mm wall thickness and 1225 mm long. Six windows are provided for (see Fig.3) to observe the drop's flight down the chamber axis. The windows are made of 12.5 mm thick, flat armour plate glass. Considering the testing pressure (P = 1.5 x 18 bar) the vessel was strengthened at its weakest points. In order to ensure that the vessel remained dry when steam was admitted, flexible, fibreglass heating elements were taped around the outside of the chamber. The elements were switched parallel and controlled by a 15 A, 250 V variable transformer. A voltmeter was connected to the variable transformer to give accurate voltage readings.

III.4.2. Temperature measurement.

The temperature distribution along the chamber axis was first measured in air. Since the walls were at a different temperature and heating the air in the chamber, a temperature difference was noticed along the wall, even after steady conditions had been reached. The radiation from the walls also contributed to the difference in temper-

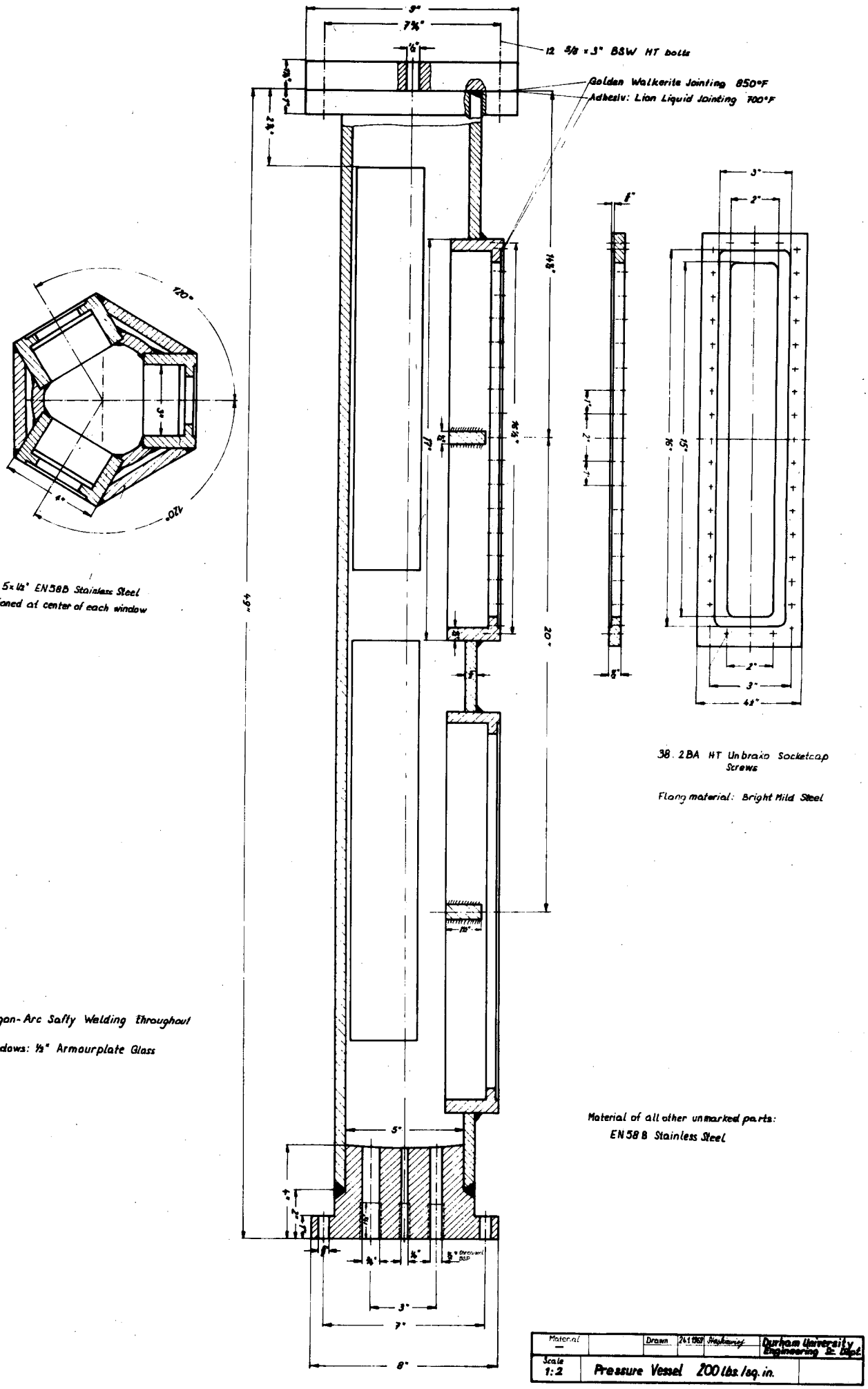
12 5/8 x 3" BSW HT bolts
Golden Walkerite Jointing 850°F
Adhesiv: Lion Liquid Jointing 700°F
120°
120°
1¾ x 5 x ½" EN58B Stainless Steel
Positioned at center of each window
38. 2BA HT Unbraxo Socketcap Screws
Flang material: Bright Mild Steel
Argon-Arc Safty Welding throughout
Windows: ½" Armourplate Glass
Material of all other unmarked parts:
EN58B Stainless Steel
Material
Drawn
Scale 1:2
Pressure Vessel 200 lbs/sq. in.
Durham University Engineering Dept.

FIG. 3.

ature measured along the chamber axis. In order to check the temperature profile along the chamber axis, a thermocouple was traversed down the path of the drop. (Fig.4.) Three thermocouples were positioned down the chamber. The top and bottom fixed at the wall surface and the third was suspended in the medium. The three readings were compared at regular intervals while the experiments were carried out. Since the chamber was only heated to ensure dryness, the temperature difference along the chamber wall became very small after having had the steam circulating for 15 minutes.

The thermocouples used were of 26 gauge copper wire, and fused together in a small flame. The measurements showed the temperature profile was uniform to within a 10°C tolerance.

III.4.3. Pressure Measurement.

The steam inlet is situated at the bottom of the vertical vessel to ensure no air lock could form. Along the delivery pipe, a pressure gauge is placed to observe the steam delivery pressure. A Budenberg Standard Test Gauge 0-300 psi is used to measure the pressure in the vessel during an experiment. The pressure readings were converted from psi into bar.

III.5. Drop producing system.

R. Hoyle and D. H. Matthews[1] carried out work on the effect of speed on the condensate layer on a cold cylinder rotating in a steam atmosphere. They studied the behaviour of drops (4.06 mm - 1.27 mm) as they were thrown off under the influence of centrifugal force. This study is primarily to observe the behavriouf of drops during their free flight and it was, therefore, of particular interest to study a drop diameter in the range of their work.

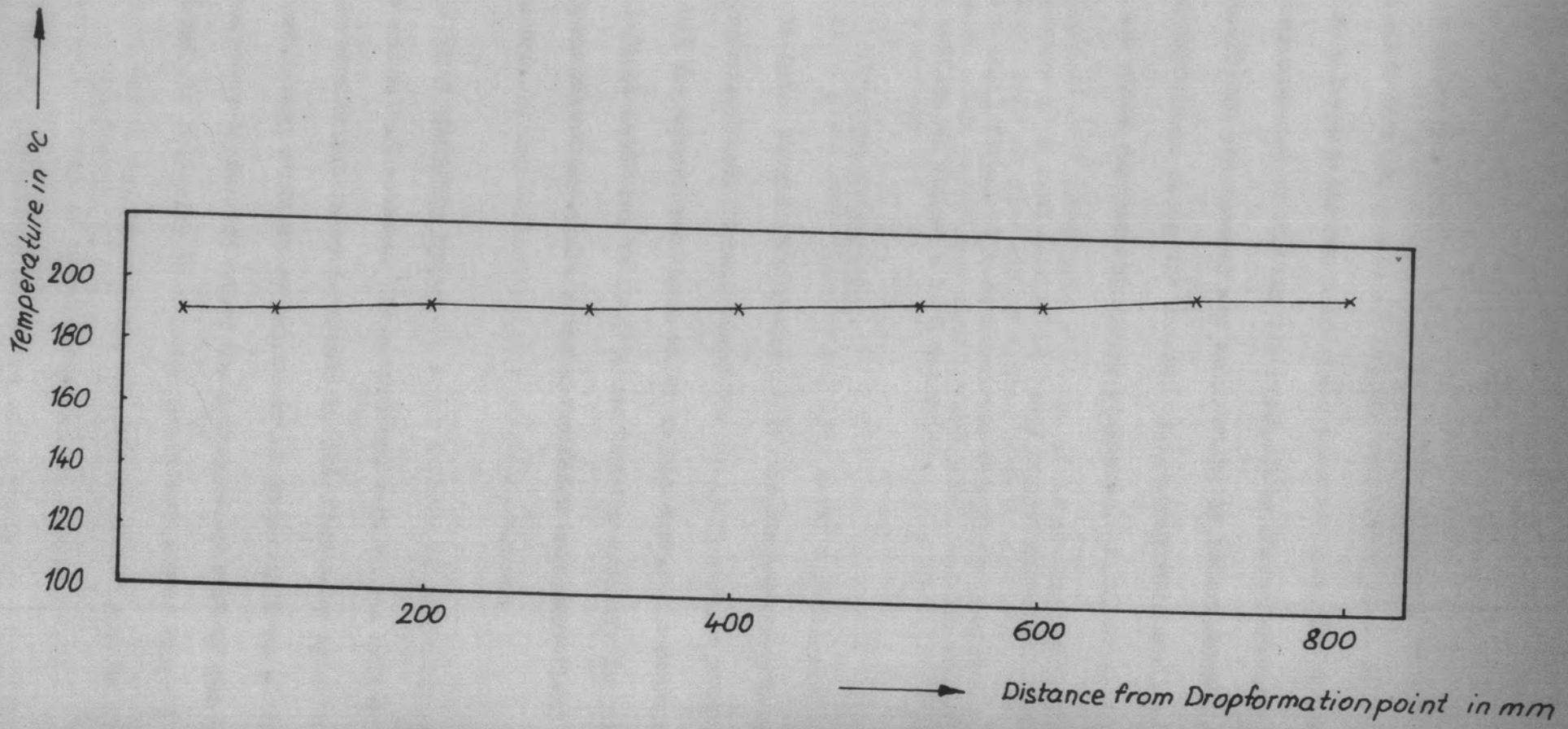

Temperature Distribution down Vesselaxis

Fig. 4

II.5.1. Methods of drop production.

Many investigators have built atomizers based on the principal of vibrating a fluid jet and thus disrupting it into a continuous droplet stream of constant diameter governed by the frequency of the disturbance. This was first investigated by Rayleigh[22] (1879). A model of such an atomizer was built with the information given by D. J. Ryley and M. R. Woods[23] and it was observed that the drops were spaced too close for individual investigation. J. M. Schneider and D. C. Hendricks[24] developed a method of separating individual drops. These drops were charged and by using electrostatic means deflected from the stream. This method was also investigated, and not followed for the following reasons:

a) A given drop diameter may only carry a particular electric charge. Should it evaporate to a diameter corresponding to its critical load, it would explode.

b) The drops would have to be highly charged in order to deflect them from their original path, and difficulty was encountered in establishing a sufficient electric field necessary for deflection in a steam atmosphere.

After considering these and other methods of producing drops, it was found most suitable to use a hypodermic tube as a heat exchanger and condensing superheated steam onto it. This gave the distinct advantage of having a closed cycle and only the latent heat of vapourisation was removed, thus reducing the heating-up period of the drop to a minimum.

III.5.2. Production of drops with constant diameter.

In Fig.5. the process occurring while producing single drops

FIG. 5.

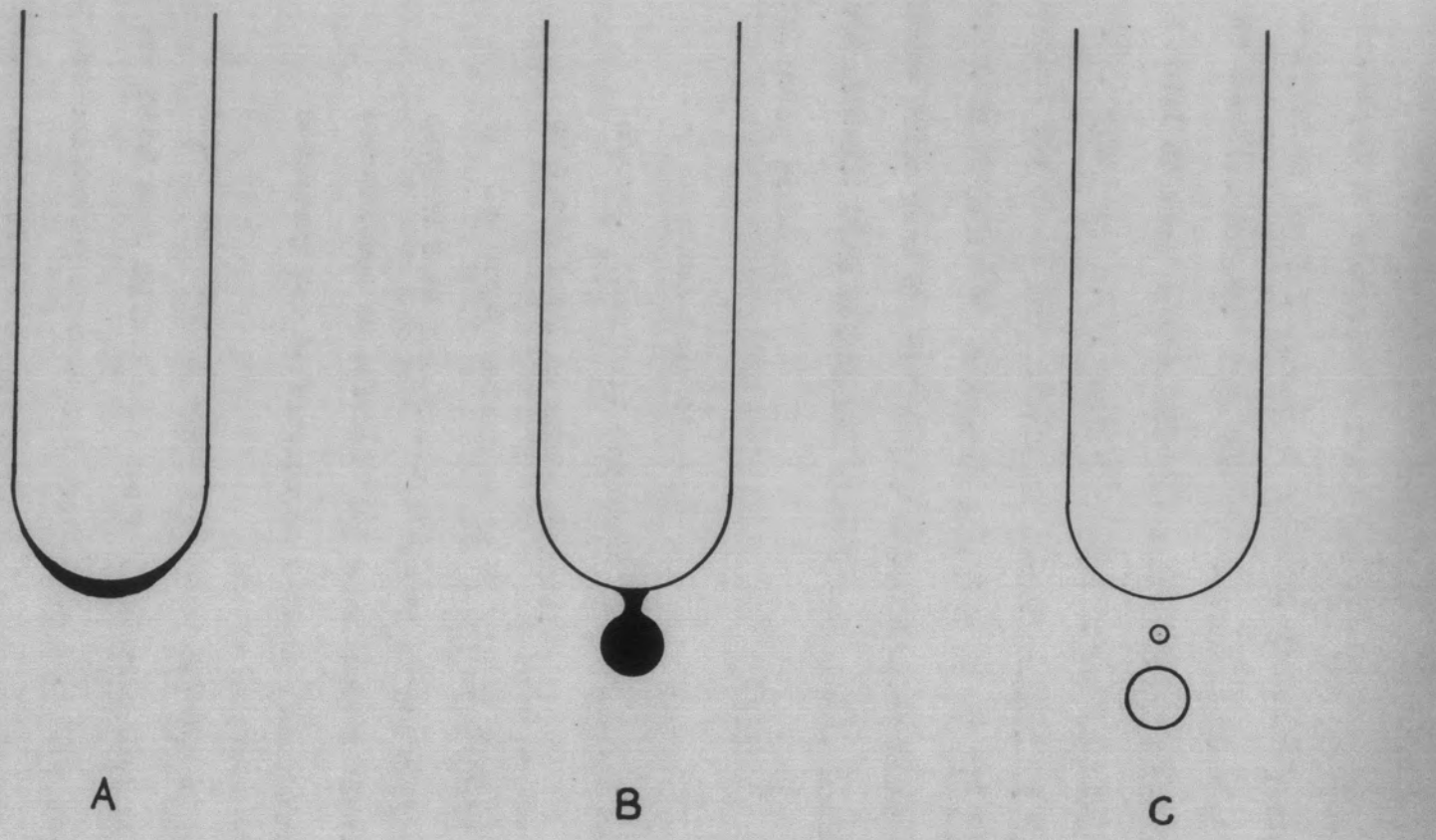

A

COLLECTION OF CONDENSATE.

B

FORMING OF NECK.

C

BREAKAWAY OF DROP AND COALLESCENCE OF NECK TO FORM DROPLET.

DROPFORMATION.

of constant diameter is shown. Nitrogen is passed through the 2 mm hypodermic tube acting as the transfer medium. Film condensation takes place, gravitational force acts on the film and draws it down to point A (Fig. 6.) This continues until the mass becomes so great as to overcome the surface tension force of the condensate, the drop forms a neck and breaks away. If care is taken to ensure constant steam and heat transfer conditions, that the drop forms a neck before lifting off, then there should be no measurable change of drop diameter. Fig.6. shows the typical formation of a drop. The neck was also observed to break away, to coalescend and form a droplet, 1/15 of the drop diameter studied. The consistency of the accuracy in the drop forming process was investigated and found to be satisfactory.

III.6. Photographic recording of a drop's flight.

A shadowgraphic method was used to record the size and position of the drop as it fell through the chamber. Rear illumination was used and a high-speed camera focused on the plane of the drop's fall. In order to illuminate evenly the field of view, a diffused point light source was used. The layout of the apparatus is shown in Fig.7.

The camera was positioned directly in front of the diffused point light source and the film exposed. The drop appeared on the negative as a white image on a dark background. During the drop's fall the framing rate and exposure time corresponded to the values necessary for synchronising with its terminal velocity. Originally, consideration was given to moving the camera further from the line of fall, so permitting a longer observation distance, but it was found that a magnification ratio greater than 2:1 was required for accurate drop-size measurements. The camera was, therefore, used near the line of fall and

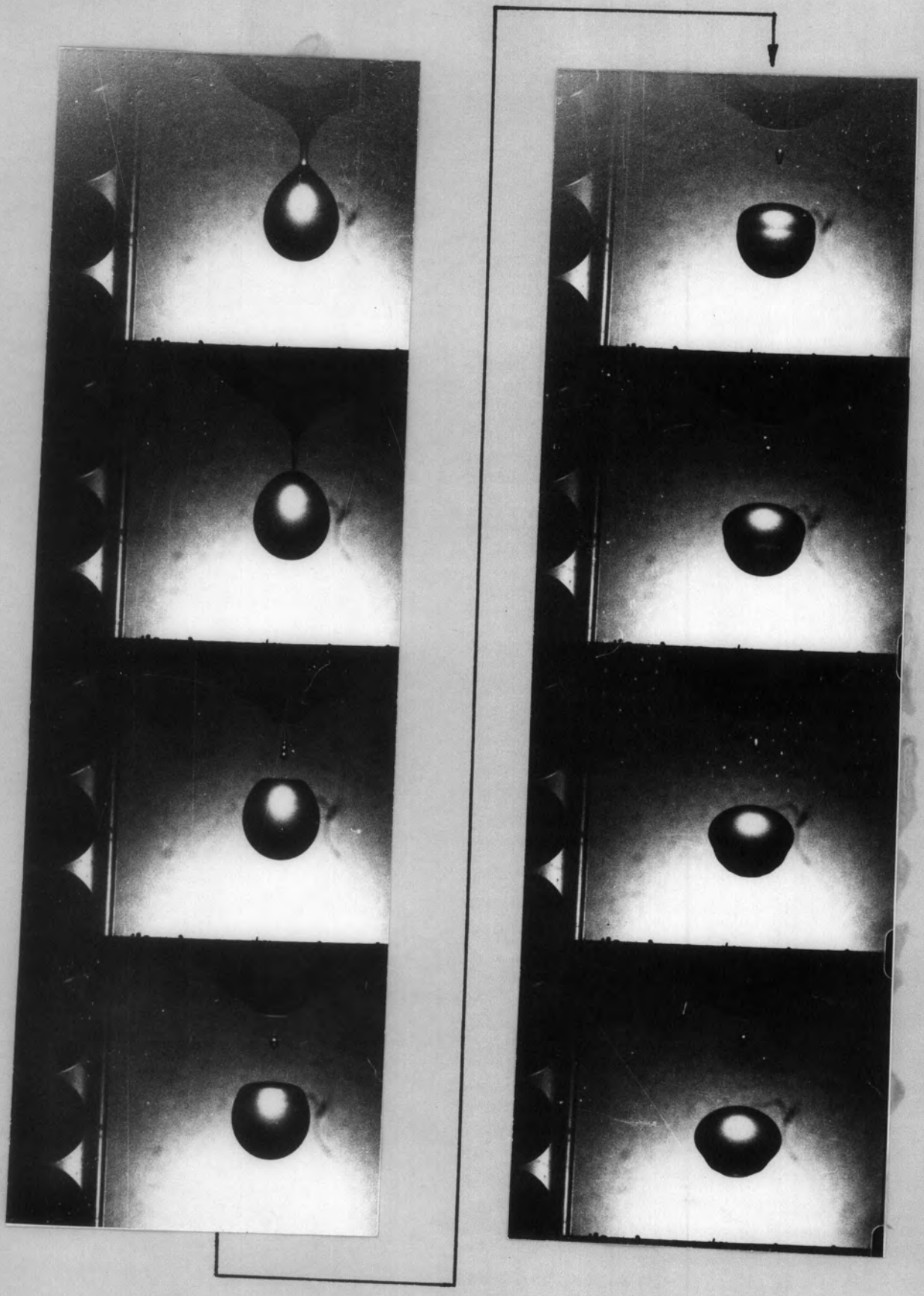

Drop Formation

Fig. 6

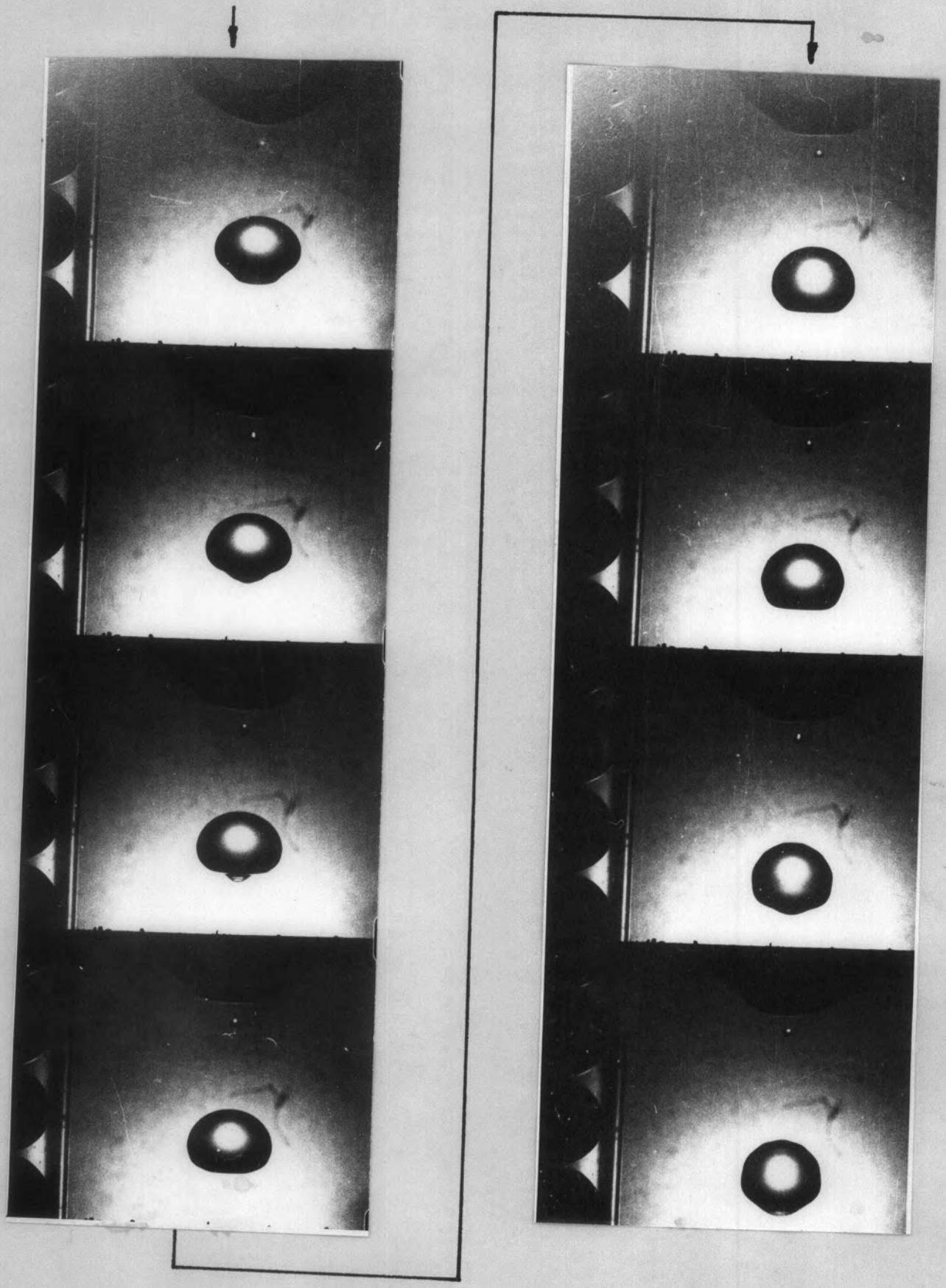

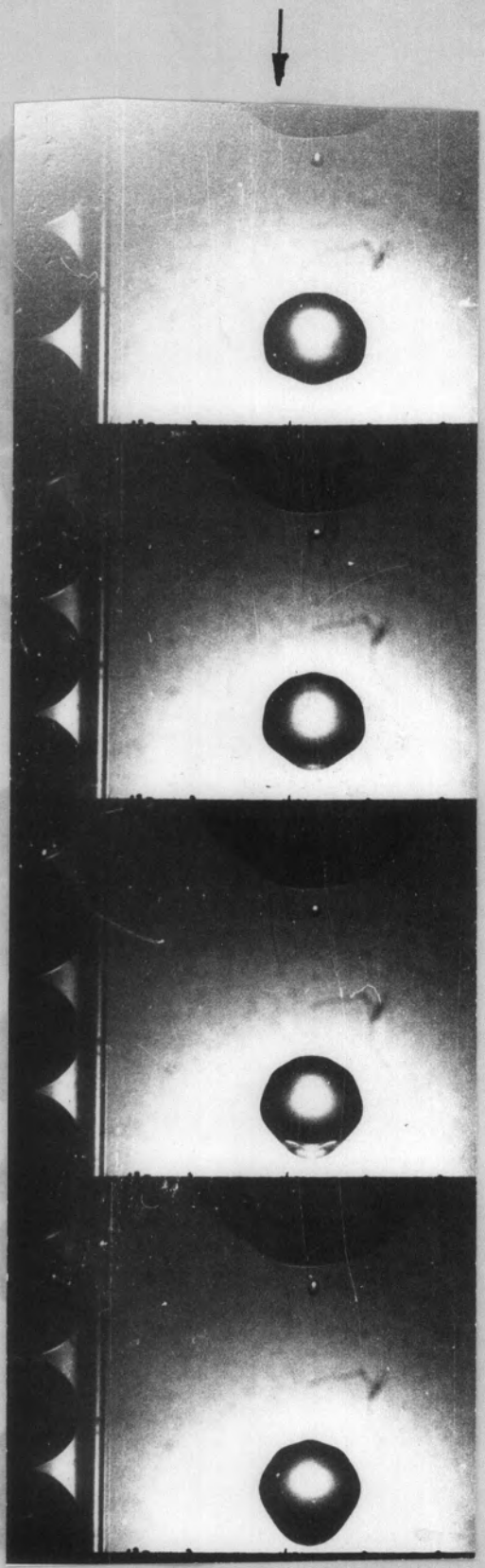

traversed down the outside of the chamber to record the drop at different positions on its line of fall.

III.6.1. Illumination System.

In order to use a shadowgraph method of recording and the chamber with its observation windows it was necessary to devise an illuminating system that could be exposed to a pressurised superheated steam atmosphere. In Fig.8, the system used is shown.

Twelve low voltage, 200 Watt Tungsten Halogen lamps were connected in series and powered by a mains volt supply. The light intensity could be carefully controlled by a variable transformer. The lamps were placed in a Pyrex glass tube and ventilated by loosely sleeving the connecting leads. It was difficult to establish a closed circuit between the lamps because of the freedom of movement necessary for thermal expansion. This was overcome by using balls from ball bearings as inter connecting links and by spring loading the two ends of the lamp.

III.7. Camera.

The camera used was a Heycam rotating-prism, high-speed camera and a 75 mm television camera lens. The lens was fitted on a metal extension tube, which permitted changes of image distance.

The 75 mm television camera lens formed a virtual image at the aperture mask. This image was then passed through two relay lenses and onto the film. The first relay lens is divided into the first-field lens and the second-field lens. The first-field lens collects the light passed through the aperture mask and passes it via a right-angle prism through the multifaced rotating prism, in a near-

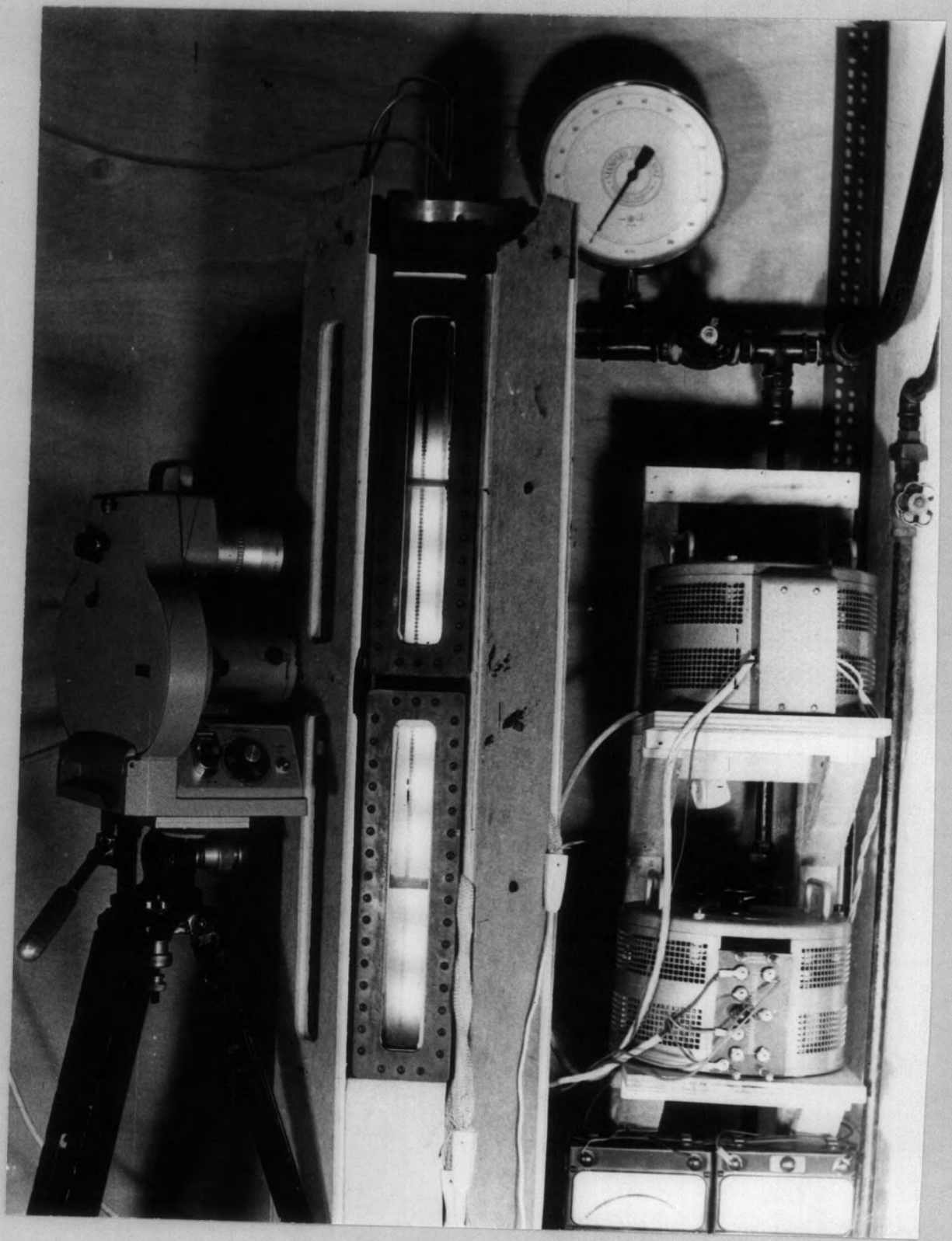

Apparatus

FIG. 7.

parallel beam, through the second-field lens and another right-angle prism. The light was then picked up by a relay lens and passed through a U-prism and the image was formed on the film.

The frame exposure may be varied by placing a sectored shutter-disc between the aperture mask and the first-field lens.

The camera was operated when a drop was seen to form a neck prior to its dropping off the hypodermic tube. This time interval, from formation to the observation point, was found to be sufficient for the camera to reach constant film speed. The photographs were obtained with 16 mm -X negative film and a 100 ft. reel permitted three different drops to be recorded. In order to achieve maximum definition, the films were developed for 8 minutes in D-19 developer.

To confirm that the camera was focused on the line of the drop's fall, a series of balls, in a glass tube, were suspended parallel to the drop's trajectory and photographed at various aperture settings. An aperture setting of f8 was found to give the best results and was used for all the experiments.

III.8. Procedure during a typical experiment.

Superheated steam at the required pressure was produced, by passing the testsection, but streaming through the pipes to ensure the removal of all condensate from the pipes, and heating them to a steady temperature. The temperature in the test section was checked to make sure it was safe to admit steam and then the test section was purged with steam until a steady temperature distribution was reached in it. In the meantime, the camera was focused, loaded with film, and the illumination system set at the required voltage. As the chamber reached

a steady temperature, it was locked and pressurised. Nitrogen passed through the drop producing system at a pre-set flow rate. As the condensate formed a drop at the end of the dropper, the camera was operated and the film exposed. Having recorded the drop (Fig.9.) the steam in the chamber was renewed and the next drop formed and recorded.

Six different positions were observed over a distance of 360 mm as the drop travelled at its terminal velocity. It should be emphasised at this point that the photographs so obtained are not of the same drop, but are different drops at the same position, produced under the same conditions.

III.8.1. Measurement carried out.

The measurement on film was carried out by also photographing ball bearings in the same plane as the drop. The shape of the drop changed from a prolate spheroid to an oblate spheroid. The major axis and minor axis were measured on the film, and grouped according to their direction with respect to the direction of fall. The equivalent diameter was determined as follows. Treating the drop as an oblate spheroid, it may be shown that its ratio volume/surface area (Shape factor), is:

$$(1) \quad \eta = \frac{V}{A} = 2ab \Big/ \left\{ 3b + \frac{3a^2}{\sqrt{a^2 - b^2}} \operatorname{Sin}^{-1} \frac{\sqrt{a^2 - b^2}}{a} \right\}$$

The equivalent spherical diameter is then taken as:

$$(2) \quad d_\eta = 6\eta$$

V = volume of oblate spheroid
A = Surface area of oblate spheroid
a = Major axis
b = Minor axis

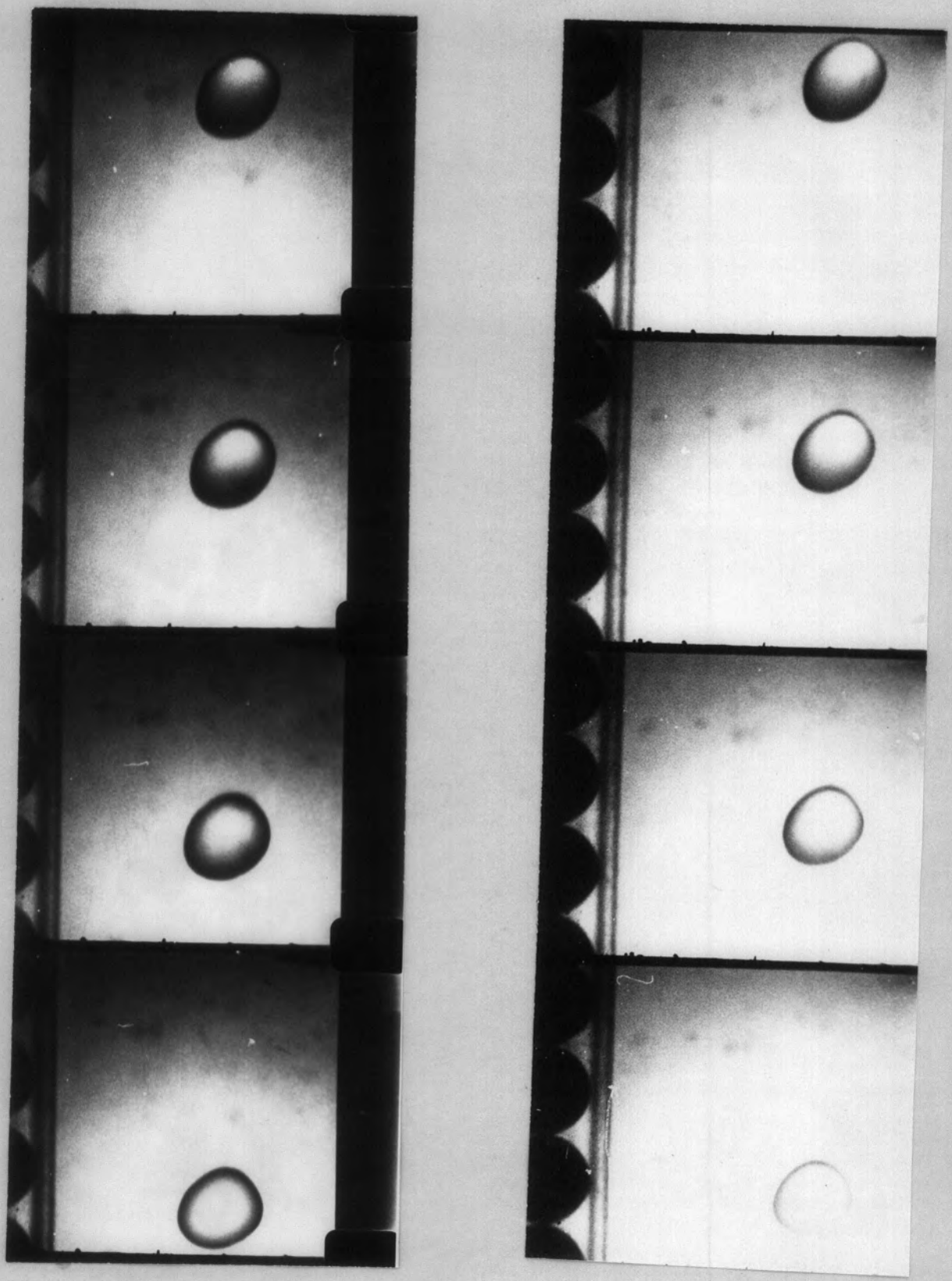

I II

FIG.9.

DROP POSITION

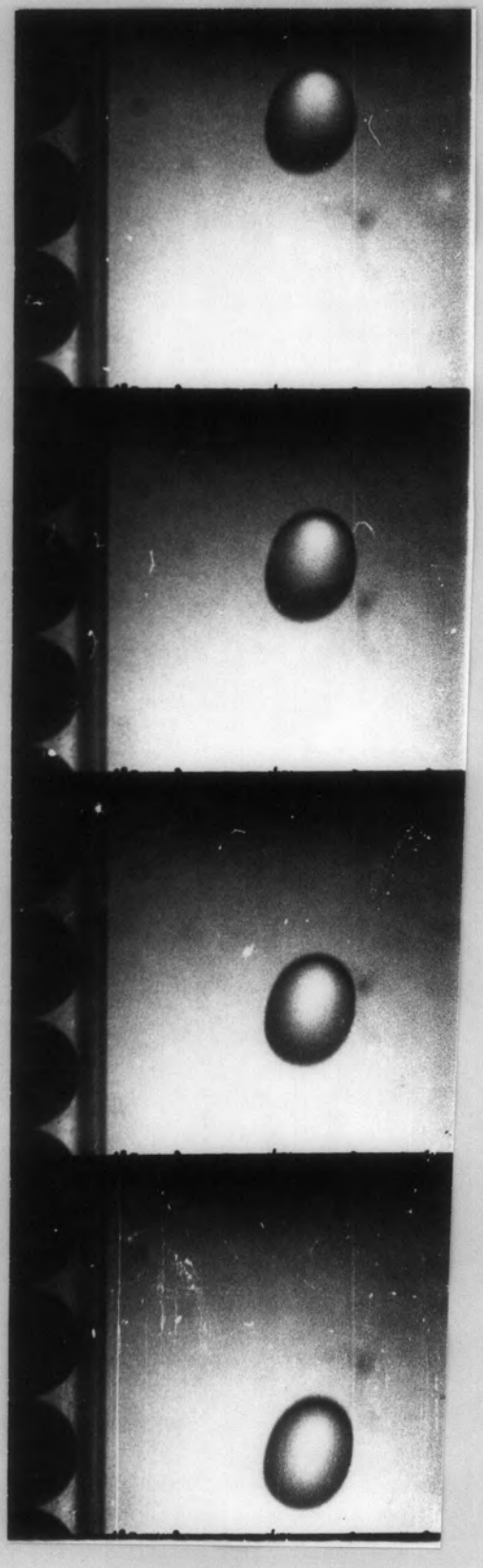

III

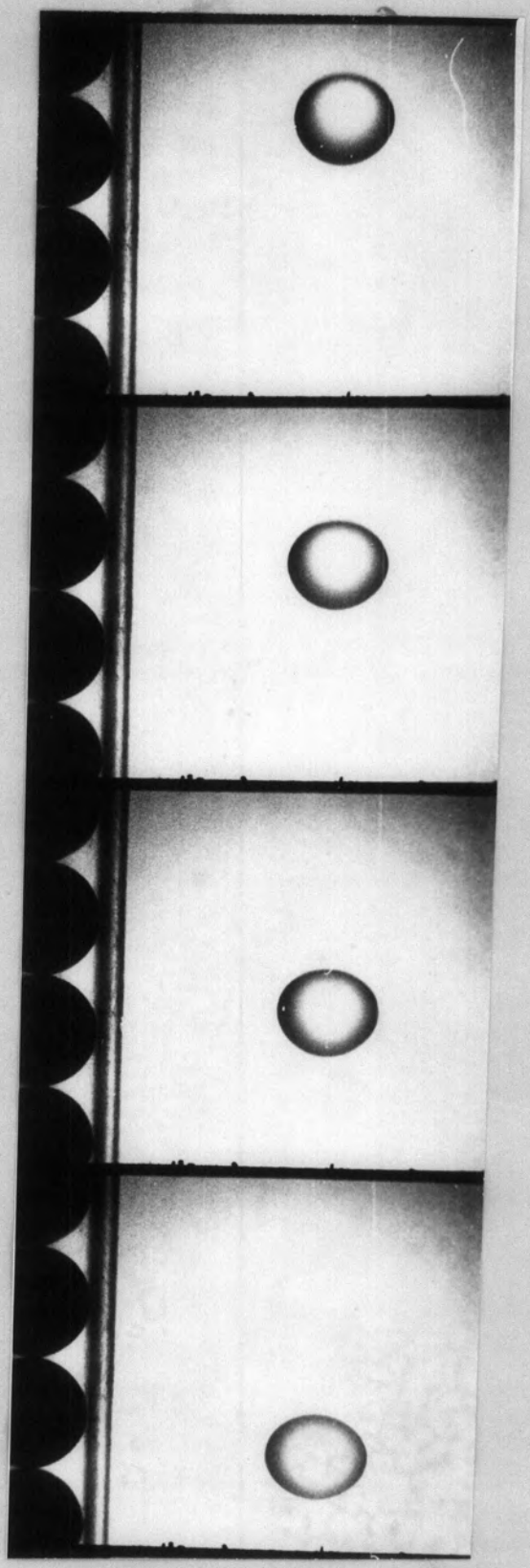

IV

DROP POSITION

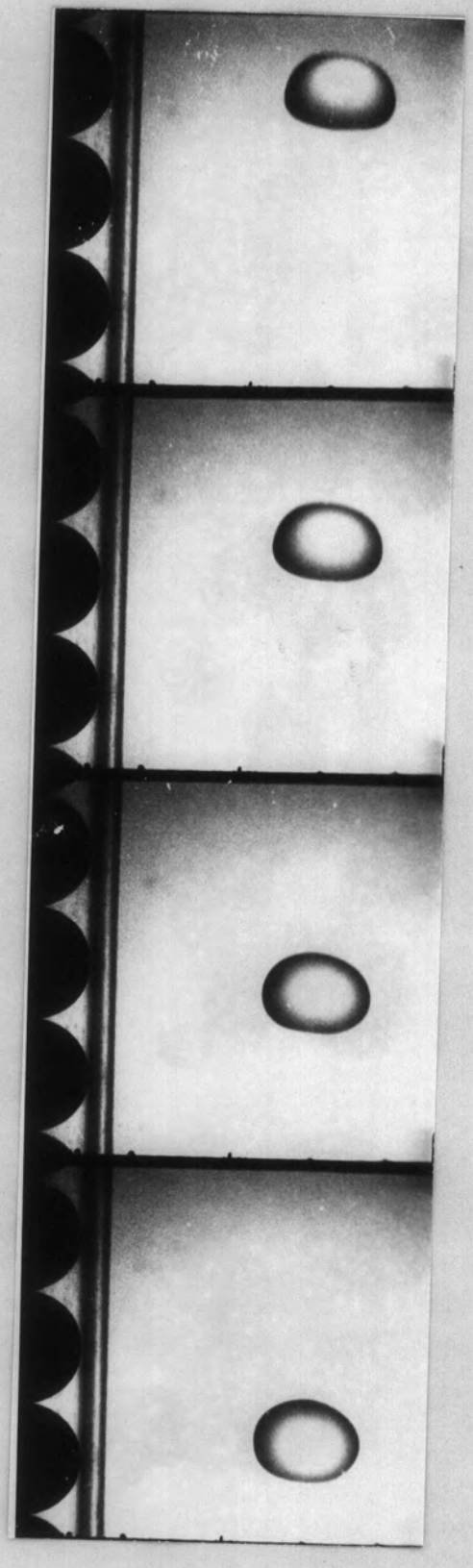

V

DROP POSITION

When the drop becomes a prolate spheroid, the shape factor may be expressed by using respective formulae for volume and surface area.

The velocity of each drop was determined by measuring the distance the drop travelled from frame to frame. Knowing the framed rate, the velocity can be determined.

III.9. Study of the source of error in the Experimental Technique.

The principal sources of error may occur in:

1) drop size measurement
2) drop not moving in a vertical plane
3) ± variation of camera speed
4) measurement of steam temperature.

In calculating the drag force, it is necessary to know the distance-time record of the moving drop accurately, as the velocity and acceleration values are required in the drag coefficient equation. The high speed camera employed requires only 0.2 sec. to reach the speed of 1000frames per second.

The pressure vessel was operated under constant pressure and temperature. To ensure no convection currents were present, after the admission of steam, drops were not produced until the temperature in the chamber was stable. Since the chamber walls were pre-heated the time required to reach a steady state was never more than ten minutes. Fresh steam was supplied after each drop formed.

III. 9.1. Drop Size Measurement.

Only drops which were in sharp focus during their flight have been reported in the results. The drop diameter was measured

on a travelling microscope. All pictures contained a series of ball bearings of equal diameter to determine the factor of magnification. It was found that the drop sizes could be measured to within 0.005 mm of their true size.

III. 9.2. Drop not moving in a vertical plane:

The magnification ratio was obtained by photographing a series of ball bearings of known diameter, positioned along the vertical axis of the pressure vessel from which it was found to be 2.21 : 1 (image size: true size). This value has been used in calculating distances and drop sizes from the film.

The distance from the vertical axis to the camera lens was 10 cm, and from the lens to the film ~ 22 cm.

The depth of field for a 4.7 mm drop was found to be 15 mm, therefore a drop of this size may fall down a plane ± 5 mm, and still remain in sharp focus. Hence, the magnification ratio may vary between 2.21 and 2.3; the maximum error so produced is approximately 2% (1.989%).

III. 9.3. Variation in Framing Rate:

In the camera, an electronic speed control is provided. This control operates off mains supply, 230 V 50 cycles/second. There are no rapid changes in the mains frequency and the maximum error of a period of 24 hours is 0.2 %.

III. 9.4. Errors in measurement of superheated steam temperature.

The superheated steam temperature could be measured to within about 5°C. The calculation of the Nusselt number includes a temperature difference term in the denominator between the temperature of the drop surface and the temperature of the superheated

steam surrounding the drop. A surface temperature of 140°C and a surrounding temperature of 200°C means a temperature difference of 60°C ± 5°C. ∴

The values for the physical properties of the superheated steam were taken at the measured temperature. A 5°C variation in the superheated steam measurement had little effect on the values of the physical properties.

Conclusion.

Experimental error caused by drop size measurement, drop movement and variation of framing rate is less than 5%. The error of temperature measurement is at maximum 5% and decreases as the temperature difference is increased.

III.10. Processes occuring during the drop's flight.

The drop parted from the drop producing system when its weight exceeded the restraining surface - tension force. As this state of balance approached its critical value, the drop was in creeping motion, elongating in shape, forming a neck and finally breaking away (Fig. 6). After breaking away, the drop was observed to be distorted. Such distortions will have had an effect on the surface area, and so on the heat and mass transfer. The drag coefficient is also a function of the shape of the drop and any distortion has an effect on the motion of the drop through the pressurised superheated steam. These distortions are of two main types; a distortion due to oscillations started by elongation as the drop breaks away, and distortion due to static causes. The oscillating

distortions promote internal circulation, promoting equal temperature distribution and so the heat and mass transfer. This was studied, and Fig.9. shows the drops as they change in diameter over a distance of 360 mm. It will be shown that $\frac{dD^2}{dt}$ has reached a steady value and all the heat transferred was used for evaporating the drop.

CHAPTER IV

THEORETICAL ANALYSIS

The evaporation of a freely falling water drop with high Reynolds number in a superheated steam atmosphere is a complex process, and as yet no complete theoretical analysis is available for this type of evaporation, although investigations have been made with low Reynold's numbers in an air atmosphere.(2.3.) In order to understand the nature of the evaporation of a freely falling drop it is first necessary to investigate the evaporative value of a stationary drop in a stationary atmosphere.

4.1. Evaporation of a stationary drop in a stagnant atmosphere.

This type of evaporation can be described by equations if the geometry of the evaporating drop and the physical properties of the boundary layer surrounding the drop are first simplified. The evaporation of a drop can be expressed in terms of mass or heat transfer. The mass transfer equations are inconvenient to use since the rate of diffusion of the vapour varies greatly with the change of concentration of vapour in the boundary layer covering the drop's surface, and neither the concentration distribution nor the thickness of the boundary layer are likely to be accurately known. Also, the partial pressure of the vapour has a large effect on vapourisation rates, as the rates change markedly with small changes of the drop surface temperature. The heat transfer equation is the more convenient method of the two since it is not affected by such difficulties.

The energy transferred by heat from the surrounding atmosphere provides the latent enthalpy of vapourisation of the water in the drop

and the heat energy necessary to superheat this vapour in the boundary layer. An important simplification has been made by dividing the drop and its surroundings into three zones. These zones are

1) the drop of radius r, a zone in which all the fluid is water at a temperature equal to, or lower than the evaporation temperature relevant to the ambient pressure.

2) the boundary layer of radial thickness, dr, a zone in which all the fluid is at evaporation temperature at the zone's inner surface, and at a temperature equal to that of the general steam atmosphere, at its outer surface.

3) An evaporation zone lying between these two, in which the fluid is continually evaporating and condensing, but in the present case, evaporating more than condensing. At points outside this zone nearer the drop's centre, the fluid is in the first zone at evaporation temperature or lower, and at points outside this zone further from the drop's centre the fluid is in the second zone at temperatures equal to or higher than the evaporation temperature.

Starting at the centre of the drop and moving outward, the temperature rises as one passes through the first zone until, at the boundary, the evaporation temperature is reached. Moving further outward through the evaporation zone the temperature remains the same, and, although the fluid is saturated water at the inner boundary and dry saturated steam at the outer, the change from one to the other is not made linearly. In this zone the vapour is wet and its degree of wetness is

decided by the motion of its molecules relative to the whole mass of fluid in the zone. Molecules with high kinetic energy will reach the inner boundary and others with low kinetic energy will reach the outer boundary. The radial thickness of the zone is assumed to be very small. In the boundary layer or outermost of the three zones, the temperature and specific volume have been assumed to increase linearly with the radial distance from the centre of the drop.

With regard to energy transfer from the general atmosphere inwards towards the drop it has been assumed to be by conduction through the boundary layer, by mass transfer through the evaporation zone, and by conduction through the drop. Energy transfer by radiation or convection through either the drop or the boundary layer have been assumed negligible.

Consider a stationary drop after the heating-up period - by which time the drop is saturated water throughout, and all conduction through the drop has ceased. As all the energy is transferred by conduction through the boundary layer of thickness δr, and as this energy, $K_m A_r \left(\frac{dT}{dr}\right)_r$, is equal to the latent energy necessary for evaporation plus the energy necessary to superheat the vapour as it diffuses through the boundary layer.

The energy balance for any boundary layer, radius r, which surrounds the drop, is given by:

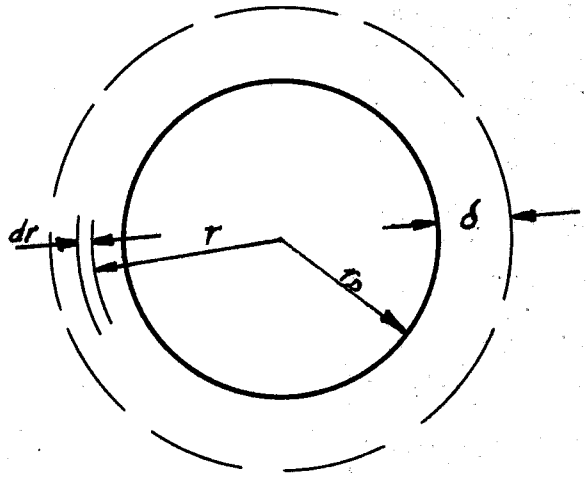

$$K_m \cdot A_r \left(\frac{dT}{dr}\right)_r = - \frac{dm}{dt}\left[L + c_p (T - T_E)\right] \qquad \text{V.1.}$$

K_m = mean thermal conductivity of the shell.

A_r = surface area at r.

r = radius from drop centre.

δ = boundary layer thickness.

L = latent enthalpy of drop.

c_p = specific heat at constant pressure.

T = temperature at radius r.

T_E = evaporation temperature.

m = evaporating mass.

t = time.

$\frac{dT}{dr}$ = temperature gradient at r.

For a high-temperature surrounding (air up to 1000°C), the solution of this energy balance is identical to the equation obtained by Godsave.(27) In this study the superheated steam temperature did not exceed 200°C, so the energy necessary to superheat the vapour as it diffuses through the boundary layer was very small compared to the latent energy necessary for evaporation and may be omitted from the energy balance. Equation V.1. then reads:

$$\frac{dr}{r^2} = - \frac{4 K_m \pi \, dT}{\frac{dm}{dt} . L} \qquad \text{V.1a.}$$

integrating from

$r = r + \delta$ to $r = r_D$ δ = boundary layer thickness.

where

$T = T_A$ to $T = T_S$ T_A = temperature of the superheated steam.

T_S = drop surface temperature.

$$\frac{1}{r_D} - \frac{1}{r_D + \delta} = - \frac{4 \pi . K_m (T_A - T_S)}{\frac{dm}{dt} . L}$$

or

$$\frac{dm}{dt} = \frac{4 \pi . K_m r_D (T_A - T_S) (r_D + \delta)}{L \left[(r_D + \delta) - r_D \right]}$$

For evaporation into a quiescent surrounding $r_D + \delta$ is large in comparison to r_D, therefore

$$\frac{r_D + \delta}{(r_D + \delta) - r_D} \longrightarrow 1$$

then $$\frac{dm}{dt} = \frac{4 \pi K_m r_D (T_A - T_S)}{L} \qquad \text{V.2.}$$

From this equation, which holds true for evaporation into low temperature surroundings, the mass vaporisation rate may be calculated. The effect of mass transfer on heat transfer may be expressed in terms of the Nusselt number. Nu_o being the Nusselt number for evaporation into a stationary superheated steam atmosphere.

From the heat balance at the drop surface:

$$A \cdot h (T_A - T_S) = - \frac{dm}{dt} . L \qquad \text{V.5.}$$

where h is the heat transfer coefficient at the drop surface

$$h = -\frac{dm}{dt}\,\frac{L}{A(T_A - T_S)}$$

$$\frac{h \cdot D}{k} = \frac{dm}{dt}\,\frac{L \cdot D}{K \cdot A(T_A - T_S)} = Nu_o \qquad \text{V.4.}$$

If heat transfer is simply by conduction and the expressions of V.2. and V.4. are combined, the theoretical value of $Nu_o = 2$ is obtained.

$$Nu_o = \frac{2 \cdot \pi \cdot k \cdot D \cdot (TA)\,T_S)}{L}\,\frac{L \cdot D}{k \cdot \pi D^2 (T_A - T_S)}$$

$$Nu_o = 2.$$

for $Re \longrightarrow 0$

4.2. Evaporation of an anchored drop with forced convection.

The dominant mechanism by which heat energy is transferred in forced convection is by the mixing of hot and cold fluid particles. It has been shown by Frössling,(7) Ranz and Marshall,(8) that experimental data for forced convective heat transfer can be correlated in the form of:

$$Nu = \phi\,(Re)\ \psi\ (Pr)$$

The exact relationship between the above dimensionless groups would involve a solution of the Navier-Stokes equation of motion to determine the velocity profiles in the boundary layer and the use of this solution to find the temperature profiles of the boundary layer itself. If an arbitrary velocity profile were assumed the exact solution to the heat flow equation could be obtained. However, the complexity of mass flow from the evaporative zone to the boundary layer does not permit the boundary layer condition of zero radial velocity. Since, in the case where vapour is emitted from the surface of the drop, it is accelerated from the surface in a tangenital direction as it effuses through the

boundary layer, a greater shearstress is therefore necessary within the boundary layer in order to sustain the given velocity profile than would be required if there were no mass transfer. The effect of the increase in shearstress is an increase of viscosity, which in turn increases the thickness of the boundary layer.

4.3. Evaporation of a freely falling water drop in a stationary superheated steam atmosphere.

If one now considers the case of a freely falling drop in a pressurised superheated steam atmosphere it is thought very unlikely that it will surround itself with the uniform film of vapour.

Take a drop oscillating and falling freely in its own vapour. For a solid spherical drop laminar boundary theory indicates that the heat transfer rate is largest at the stagnation point and decreases with distance along the surface as the boundary layer thickness increases. On the other hand, the heat transfer rate reaches a minimum near the film separation point. Beyond the separation point the heat transfer rate again increases because some turbulence will occur in the flow where the eddies of the wake sweep the surface. The heat transfer rate, however, will not be very effective since the eddies recirculate part of the surface.

Should the velocity of fall be large enough to permit transition from laminar to turbulent flow of the boundary layer without its separation, the heat transfer rate will be much higher, because of the turbulent effect on high and low energy level molecules intermixing in the superheated steam of the surrounding boundary layer.

The oscillating behaviour of the drop will also have an effect

on the heat transfer rate. The oscillations are mainly due to an unequal pressure distribution on the drop's surface and the evaporative behaviour can be described as follows:

As a drop oscillates the pressure will decrease at various points in the evaporation zone, which is postulated as being water on one side, at evaporation temperature, and saturated vapour on the other side at equal temperature. This decrease of pressure at any point in the evaporation zone will cause the saturation temperature to be lowered thus decreasing the enthalpy of the water. The excess heat energy which thereby becomes available is absorbed by the water. This volume of water becomes superheated and evaporates. The specific volume of this water-steam mixture increases rapidly and the energy which becomes available is used in accelerating the mixture away from the evaporation zone. As this mixture moves away it varies in temperature from the evaporation temperature relevant to the ambient pressure to the general steam atmosphere surrounding the drop.

It has been seen that the evaporation of a freely falling oscillating water drop in a pressurised superheated steam atmosphere is a very complex problem and is governed by a large number of variables. A combination of the three described evaporative cases takes place and the heat transfer rate is considerably increased.

4.4. Drag resistance on a moving spherical drop.

The resistance force of a freely falling drop is made up of pressure differences and frictional stresses arising from the atmosphere flowing around the drop (force required to accelerate being pressurised, superheated steam displaced). For a very slow flow with

Reynold's numbers less than circa 0.1, i.e. the condition of 'creeping flow', the evaluation of the drag force is given by Stoke's law, which is an analytical solution of the equations of motion and continuity.

With regard to the Reynold's number range in which this study was carried out, the calculation of the drag force is very difficult because of flow separation and the appearance of a wake behind the drop. The oscillations of the drop will also cause a fluctuation of the drag force. The drag coefficient relationship with the Reynolds number has been determined experimentally.

IV.4.1. Drag coefficient equation.

The following relationship is obtained for a drop falling under gravity[14]:

$$F' = m.a. = m.g. - wg - F_R' \qquad V.6.$$

g = acceleration due to gravity.

m = mass of the drop.

w = mass of the gas displaced by the drop.

m.g = gravitational force on the drop.

w.g. = boyant force on the drop.

F_R' = resisting force due to friction effects or force required to accelerate gas being displaced.

Newton developed an expression for the resisting force:

$$F_R' = (C_D') \; A \; \frac{P_A v^2}{2} \qquad V.7.$$

C_D' = drag coefficient.

P_A = gas density.

A = area of drop.

v = velocity of drop.

for a sphere:

$$F_R' = C_D \frac{\pi D^2 \rho_A v^2}{8}$$

C_D = drag coefficient.

If this value of F_R' is substituted in equation V.4.1., the steady-state maximum falling velocity may be calculated.

$$m \cdot \frac{dv}{dt} = m \cdot g - w \cdot g - F_R' \qquad \text{V.6.a.}$$

$$\frac{\pi D^3}{6} \rho_D \frac{dv}{dt} = \frac{\pi \cdot D^3}{6} (g \cdot \rho_D - g\rho_A) - C_D \frac{\pi D^2 \rho_A v^2}{8} \qquad \text{V.6.b.}$$

$$\frac{dv}{dt} = \frac{(\rho_D - \rho_A) \cdot g}{\rho_D} - \frac{3(C_D) \cdot \rho_A \cdot v^2}{4 \cdot D \rho_D} \qquad \text{V.9.}$$

At maximum velocity, v_m, $\frac{dv}{dt} = 0$.

$$\frac{(\rho_D - \rho_A) \cdot g}{\rho_D} = \frac{3(C_D) \rho_A \cdot v_m^2}{4 \cdot D \cdot \rho_D}$$

$$v_m^2 = \frac{4(\rho_D - \rho_A) \cdot D}{3(C_D) \rho_A} \qquad \text{V.10.}$$

$$v_m = \sqrt{\frac{4 (\rho_D - \rho_A) \cdot D}{3 (C_D) \rho_A}} \qquad \text{V.11.}$$

Equation V.10 is known as Newton's Lae. Solving for C_D:

$$C_D = \frac{4 (\rho_D - \rho_A) \cdot dg.}{3 v_m^2 \cdot \rho_A} \qquad \text{V.12.}$$

This relation applies when there is no mass transfer and the drop travels at terminal velocity Very few investigations have been made for the theoretical calculation of the drag coefficient of an evaporating sphere. Ingebo [13] and Eisenklam[25] have investigated the effect of evaporation on the drag coefficient. Eisenklam used the slow viscous-flow theory to correlate drag coefficient relationships from the pressure forces and viscous forces in the direction of flow, together with the effect of vapour coming off. This theory is based on steady flow and is valid only when the velocity variation of the drop is not very high.

CHAPTER V.

EXPERIMENTAL RESULTS

The main object of this work was to study the heat transfer to single water drops falling freely through a superheated steam atmosphere. Experiments have been carried out in superheated steam varying from 1 to 6 bar in pressure. The drop diameter at the beginning of the fall was approximately 4.7 mm and the superheated steam temperature was kept constant at 200°C. The experimental conditions were chosen so that a range of mass transfer intensities could be investigated. From the photographic record, the drop diameter and velocity of fall were obtained as a function of distance travelled. These results are tabulated in Appendix I.

V.1. Distance and Drop Size Records.

The construction of the pressure vessel allowed for the drop to be observed as it formed, and its flight over a distance of 800 mm. From observation it was found that the evaporation of the drop had reached a steady rate and terminal velocity had always been reached in the last 300 mm of the drop's fall. For this reason photographs of the drop were only taken in its last 300 mm of fall. The observation points, measured from the drop formation point were 470 mm, 530 mm, 590 mm, 650 mm, 710 mm, 770 mm. These points were marked on the camera stand and the camera was operated at a constant framing rate and shutter speed. The high framing rate (1000f.p.s.) and shutter speed (i.e. time of exposure 1/10,000 second) made it possible to obtain very accurate pictures of a drop over a distance of 20 mm at each observation point. The distance between the successive drop images were measured on the

film using a travelling microscope; knowing the magnification ratio and the framing rate of the camera, actual drop diameters and velocity of fall could be determined. The drop had spheroidal shape and was observed to oscillate and rotate. The major and minor axis was therefore measured and an equivalent spherical diameter calculated according to the position of the major axis in relation to the direction of fall.

In Fig. V. 1, 2, 3 and 4, drop diameter position relationships are shown for pressures 2, 4, 5 and 6 bar. Bearing in mind that the drops are initially of equal diameter, it can be seen that with an increase in pressure, the drop diameter decreases more rapidly. It is thought that this increase in evaporation is mainly due to the increasing pressure decreasing the temperature difference between drop surface and the surrounding atmosphere, so bringing the drop into regions to which high heat transfer coefficients are attached. (See Discussion). Maximum, minimum and mean values for all recorded equivalent spherical diameters are plotted.

In Fig. 5, 6, 7 and 8, Velocity-position relationships are shown. Maximum, minimum and mean values are plotted, and it can be seen that the velocity of fall oscillates and decreases with an increase in pressure. The oscillatory nature of the velocity is due to the change in shape of the drop. Sometimes the drop has a very good aerodynamic shape, thus the drag force is decreased and the resulting free fall velocity is higher than the velocity of a poor aerodynamic shape, due to an increase of the drag force. The decrease of terminal velocity with an increase in pressure is also due to the boyant force acting on the drop and on the evaporative rate of the drop. The boyant force

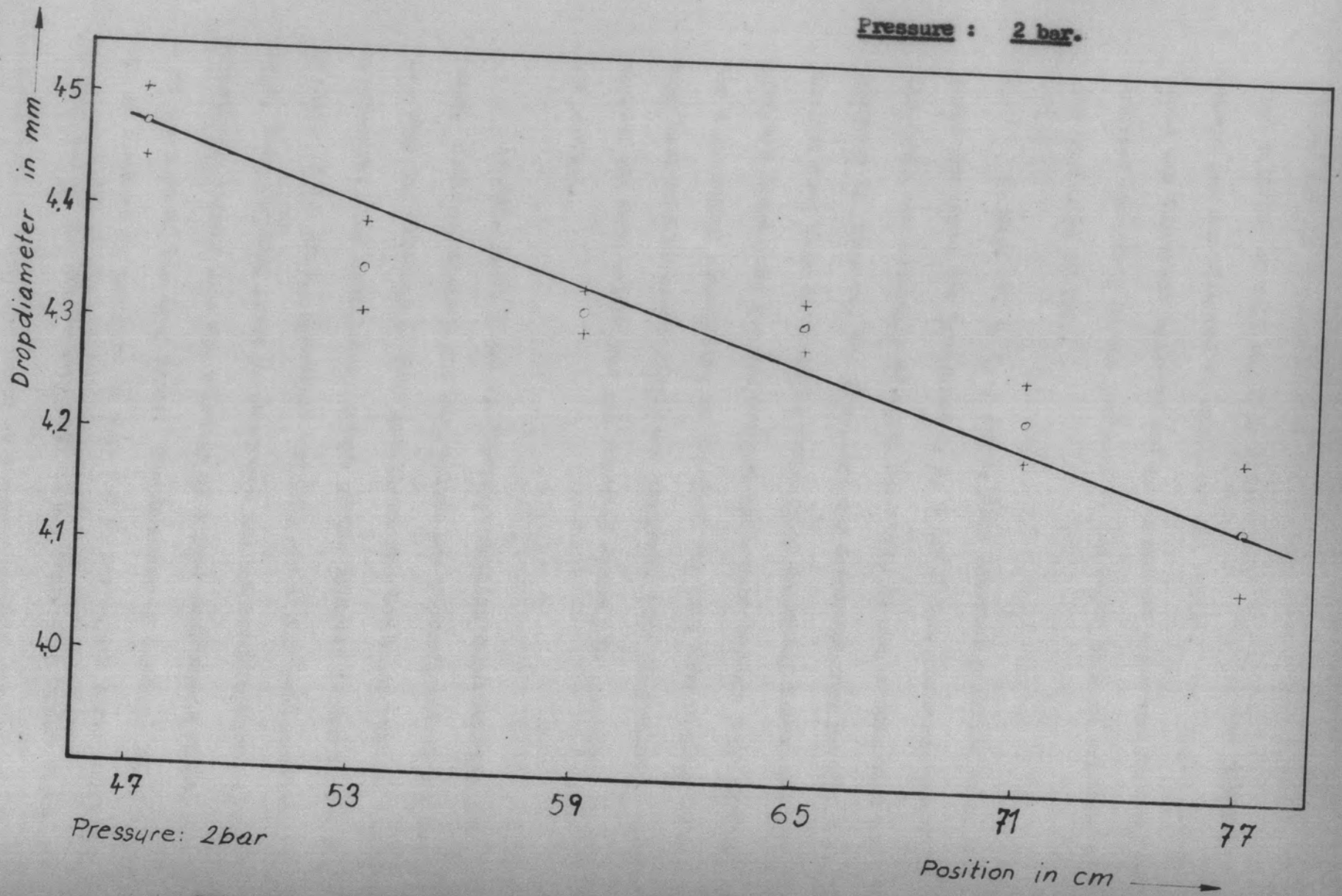

FIG. V.1. Drop Diameter - Position Relationship.

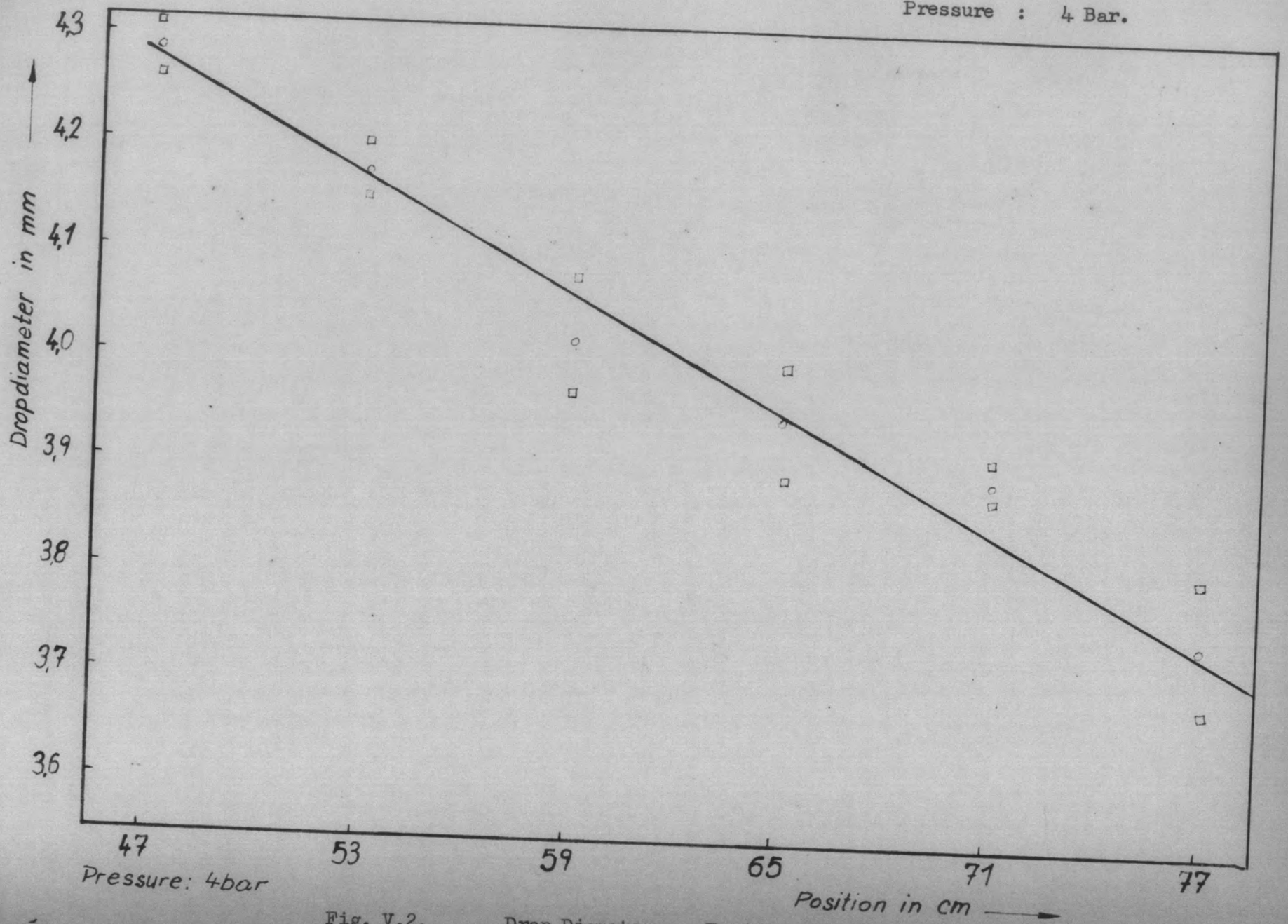

Fig. V.2. Drop Diameter - Position Relationship.

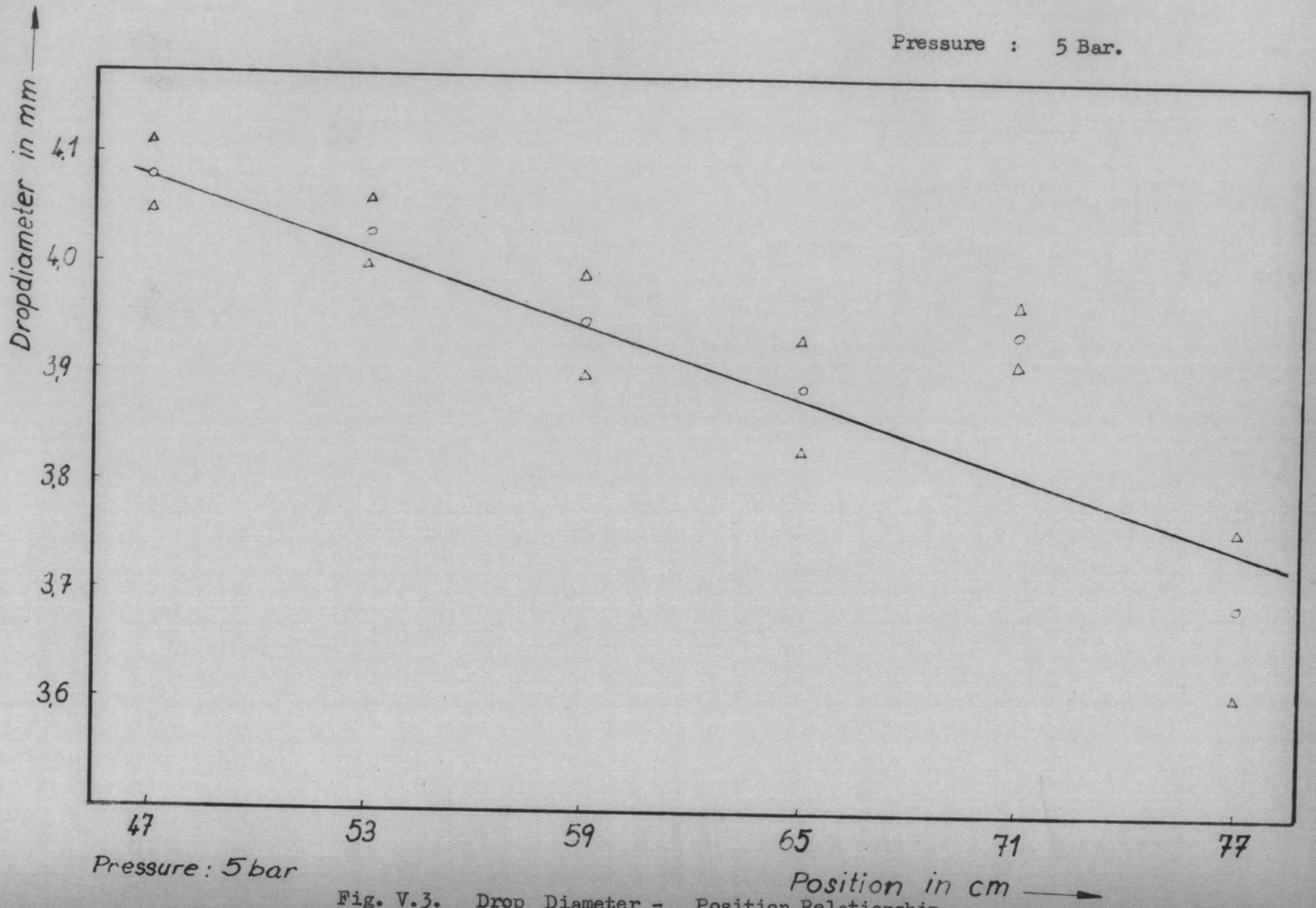

Fig. V.3. Drop Diameter - Position Relationship.

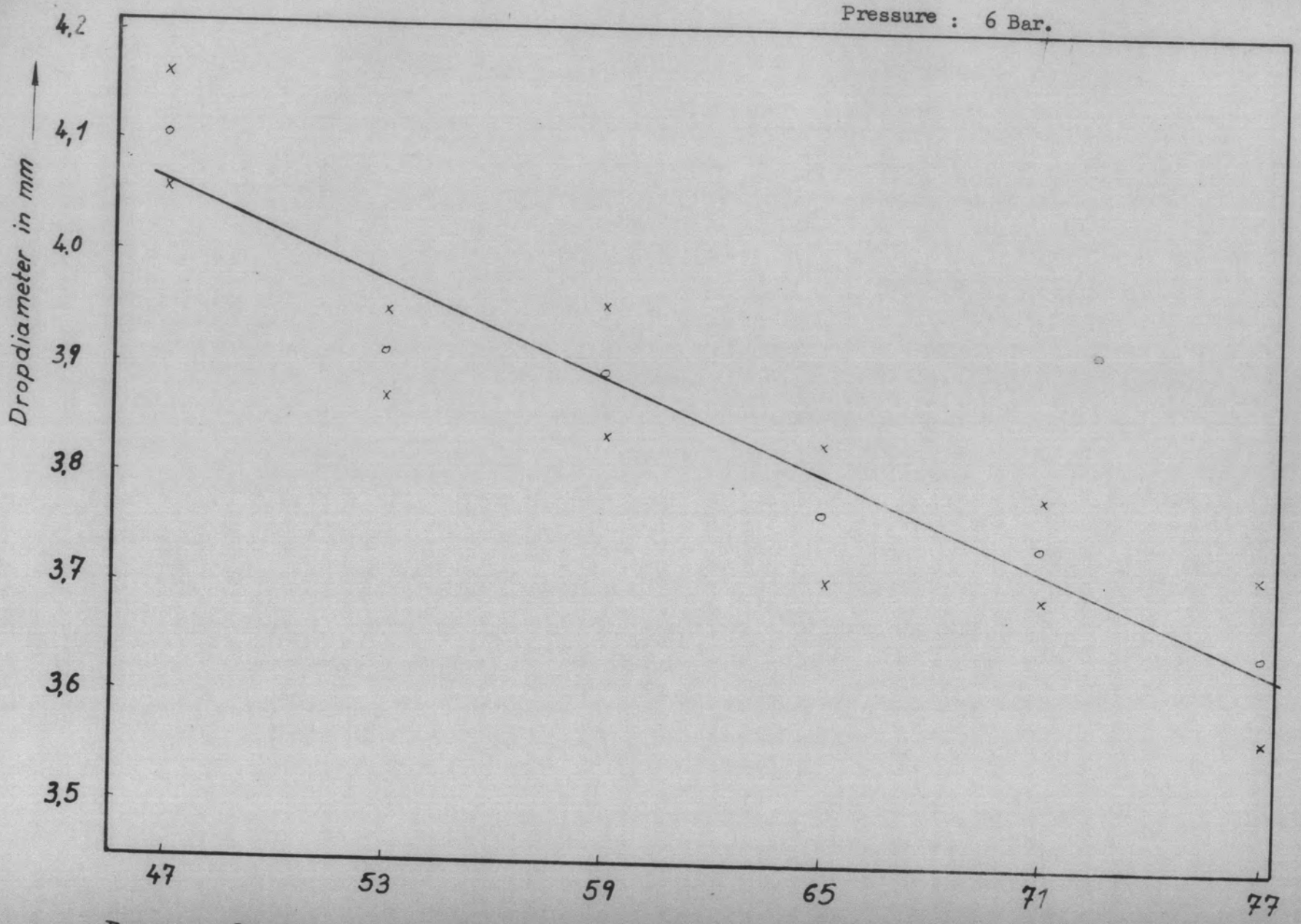

Fig. V.4. Drop Diameter - Position Relationship.

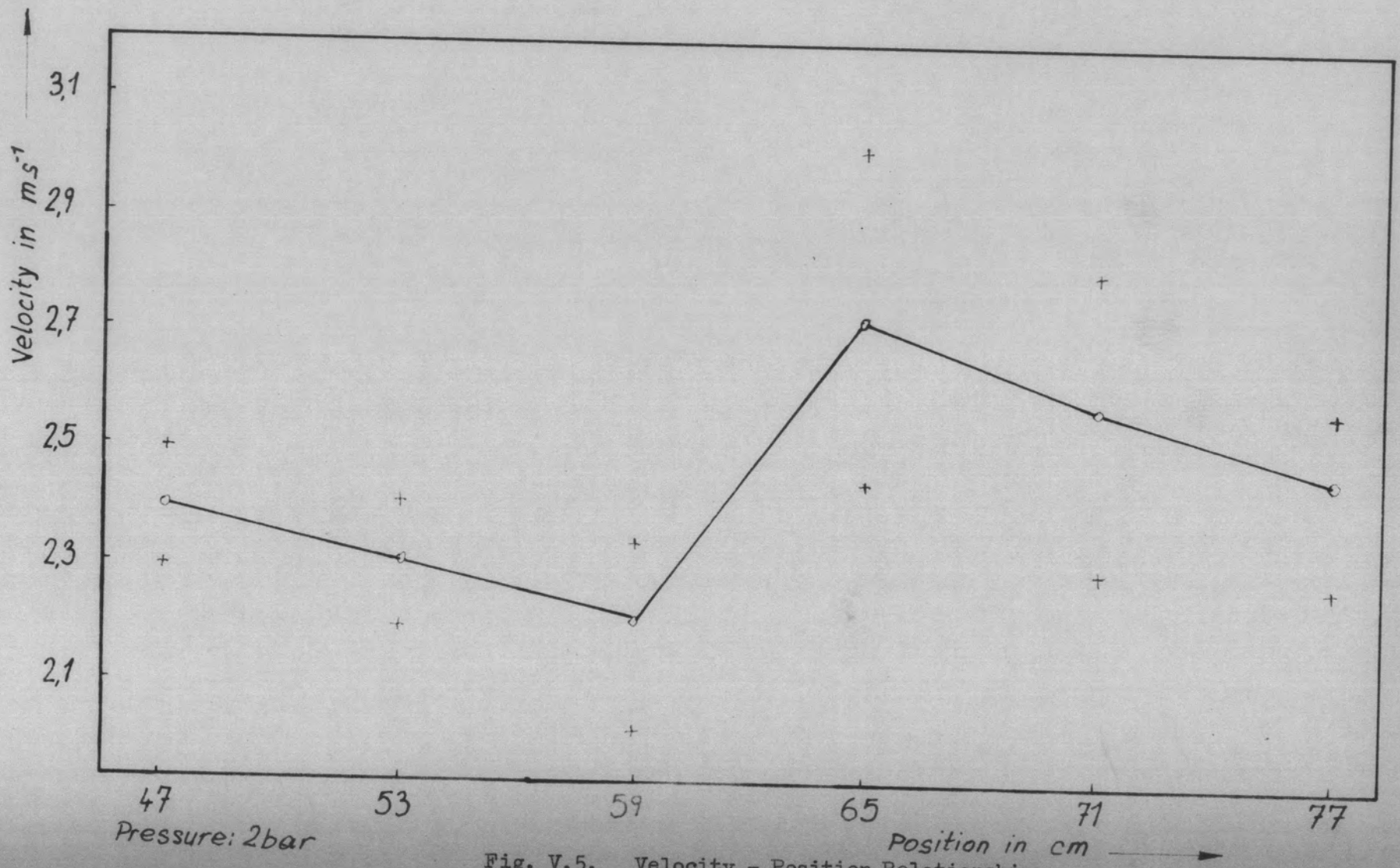

Fig. V.5. Velocity - Position Relationships.

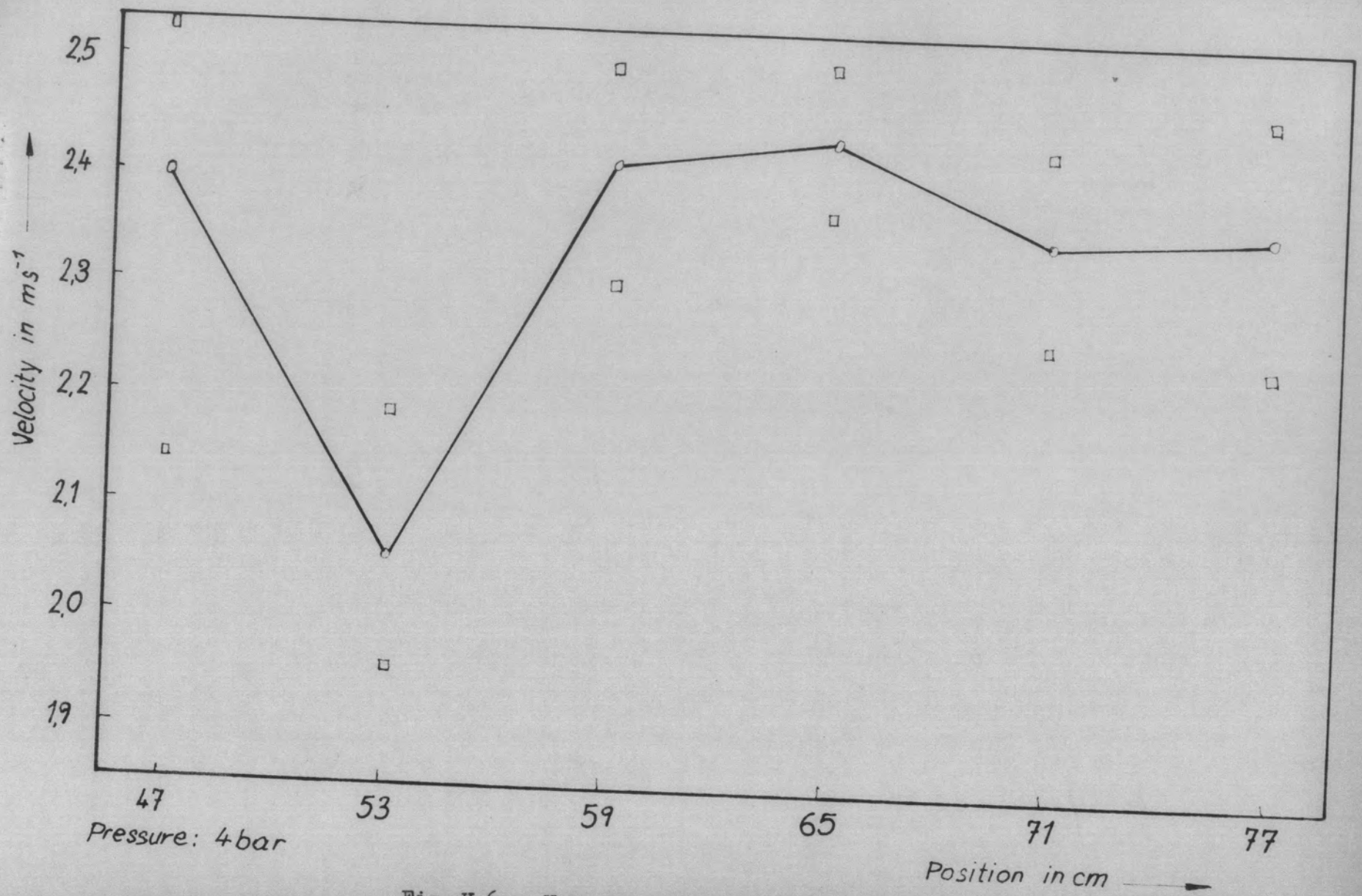

Fig. V.6. Velocity - Position Relationships.

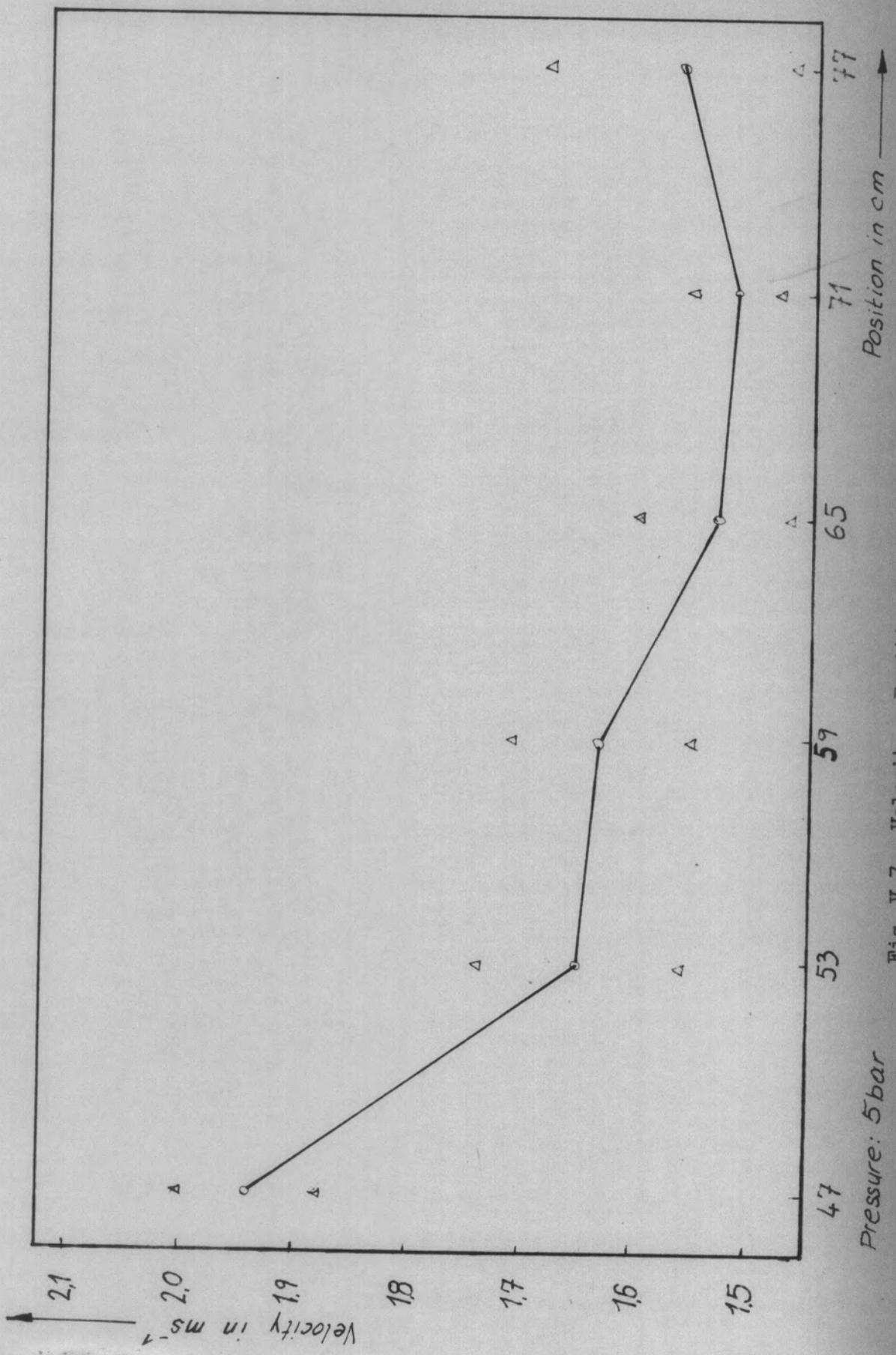

Fig. V.7. Velocity - Position Relationships.

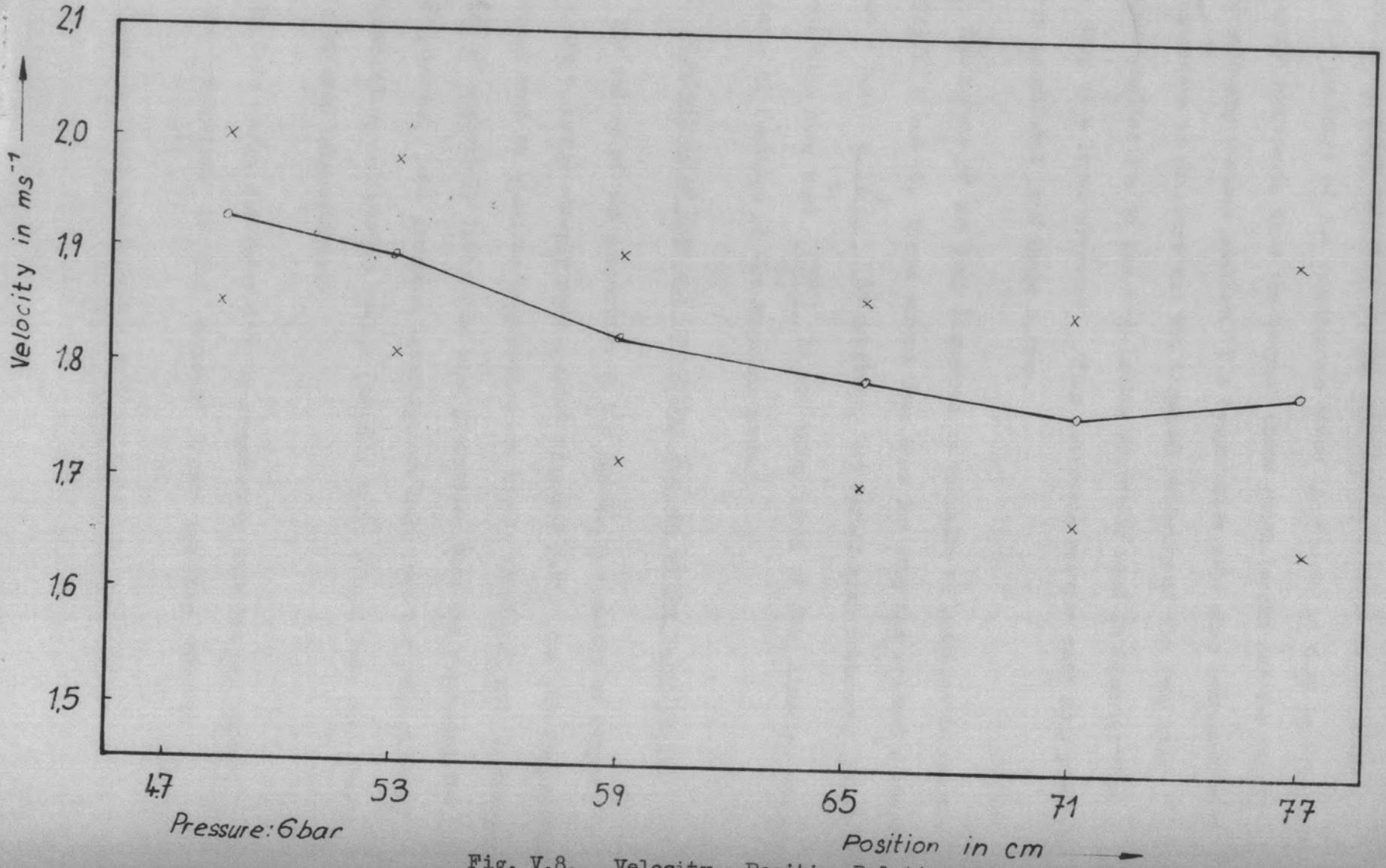

Fig. V.8. Velocity - Position Relationship.

results from displacement of superheated steam by the drop multiplied by gravitational acceleration $\left(\frac{\pi D^3}{6} \rho_{\text{steam}}. g.\right)$ and acts in opposite direction to the gravitational force on the drop. As the pressure of the superheated steam increases, so also is its density increased, thus the buoyant force grows larger and the resulting velocity becomes smaller. The evaporative rate also increases with an increase in pressure and the terminal velocity of the drop will become smaller due to the drop having decreased more in diameter than the drop at a lower pressure. Time intervals between each drop position where calculated from these curves.

The square of the drop diameters in relation to position is shown in Fig.V. 9 and 10. These curves show that the drop has reached a steady value - i.e. $\frac{\Delta(D^2)}{\Delta t.}$ is constant, but varies with pressure. These curves also show that $\frac{\Delta D^2}{\Delta t}$ is not independent of drop diameter and is, in fact, of function of the Reynolds number.

V.2. Evaluation of Physical Properties for use in the calculations.

The values of the properties in the immediate vicinity of evaporating drops change steeply over a short transfer path. The physical models generally used to simulate evaporation are highly idealised and, therefore, the use of accurately integrated mean properties does not represent the actual process. Some previous investigators have used the properties of the surrounding undisturbed medium (usually air), others have used values of air at mean temperatures.

In this study, the water drop is evaporating into its own vapour, and the conditions in the boundary layer are very complex

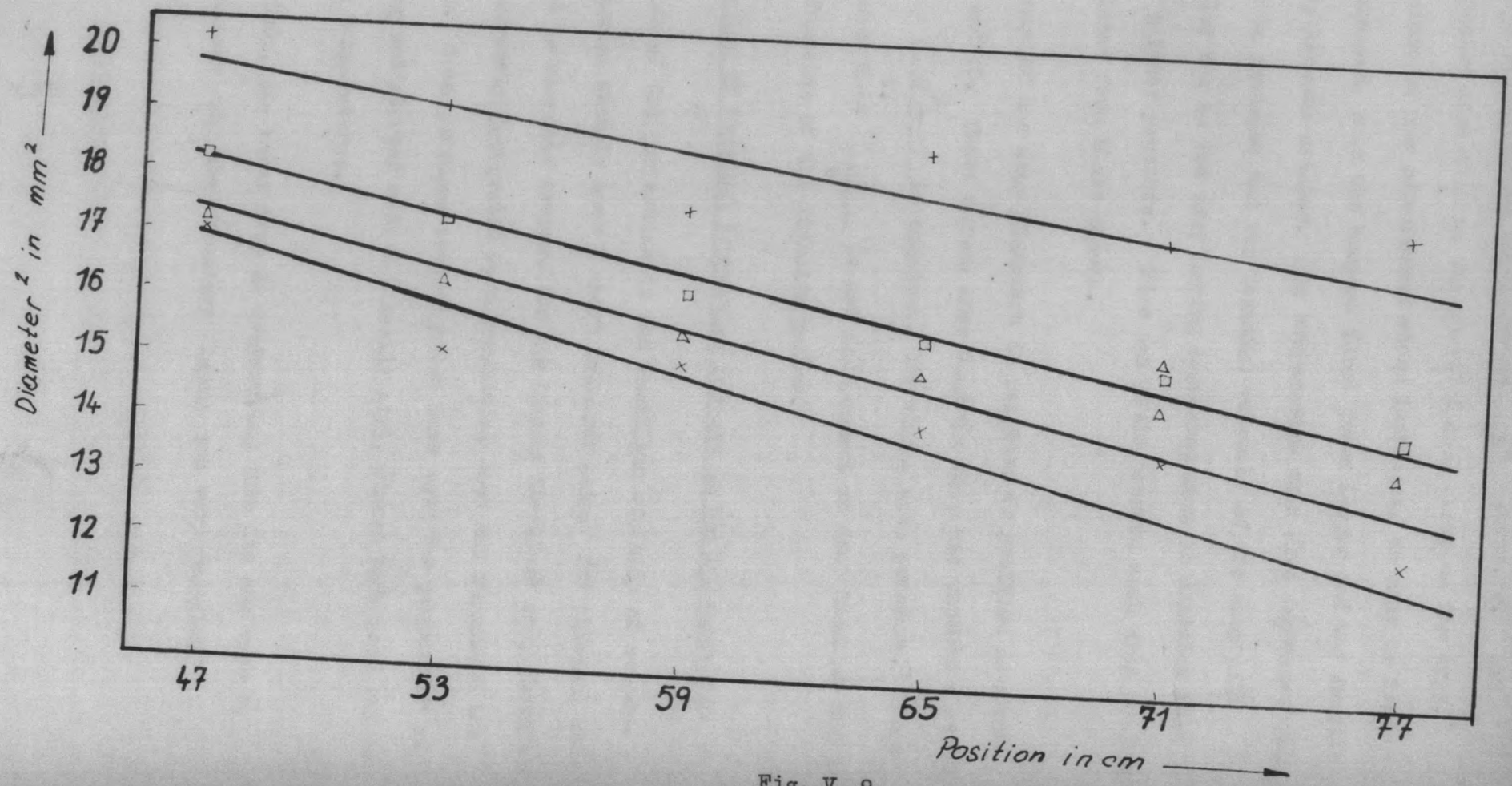

Fig. V. 9.

Square of Drop Diameter vPosition Relationship.

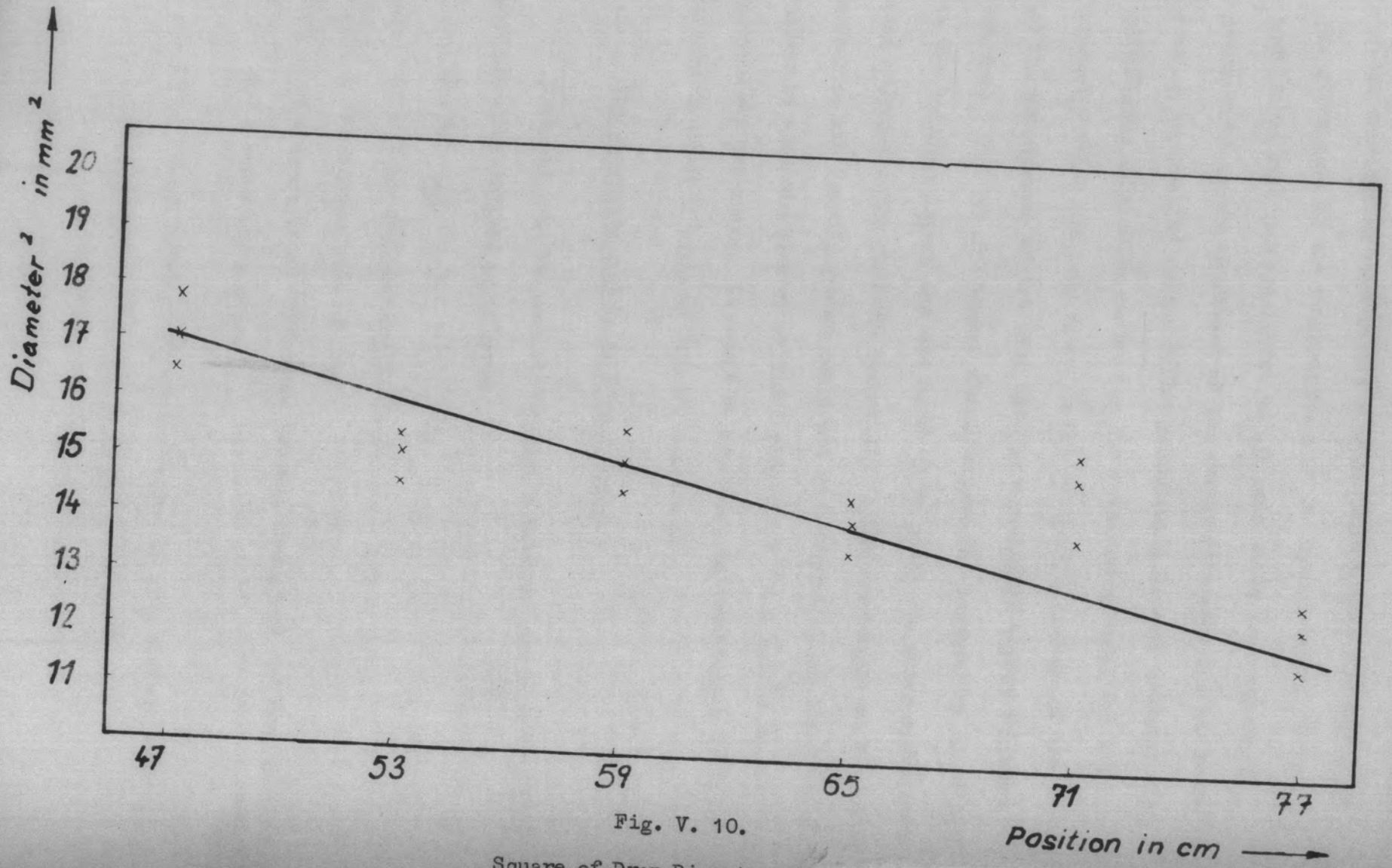

Fig. V. 10.

Square of Drop Diameter v Position Relationship.

due to simultaneous heat and mass transfer. There is no information justifying the use of mean values based on conditions of the surrounding superheated vapour. However, as the vapour at the outer part of the evaporative zone is dry saturated, it is considered more representative to use arithmetic mean values of steam based on the condition of the evaporative zone and the surrounding superheated vapour whilst calculating Nusselt numbers. In calculating a Reynolds number for the evaporating drop, the kinetic viscosity value has been taken as the arithmetic average of the vapour at the temperature of the drop and the superheated vapour surrounding the drop. The Prandtl Number characterises the temperature distribution in the boundary layer, and was found to be close to unity again using mean values for the physical properties. The dependence of the Nusselt number on the Prandtl number could not be obtained, since the Prandtl number is a combination of physical properties whose values do not vary appreciably for steam. It would be necessary to investigate different liquids to cover a range of Prandtl numbers .

V.3. The Evaporation Rate of Liquid Drops.

From the heat balance at the drop's surface, the heat transfer coefficient is defined as follows:

$$h \cdot A \cdot \Delta T = -\frac{dm}{dt} \cdot L \qquad \text{V.1.}$$

where h = heat transfer coefficient.

A = surface area of drop

ΔT = temperature difference between atmosphere and drop surface.

$\frac{dm}{dt}$ = evaporating rate.

L = Latent enthalpy of vapourization at drop surface temperature.

Ranz and Marshall showed that the evaporating rate can be expressed in terms of the Nusselt number, as follows:

$$Nu = \frac{h.D}{k} = \frac{1}{4} \cdot \frac{P_L \cdot L}{k. \Delta T} \cdot \frac{d(D^2)}{dt.}$$

where D = drop diameter.

P_L = density of drop at liquid temperature.

k = thermal conductivity.

Values for $\frac{d(D^2)}{dt}$ and corresponding velocities were obtained from measuring the drop diameter and distance travelled on the film. Since the drop was formed by condensing steam onto a hypodermic tube (III.5.), thus only removing little more than the latent enthalpy, it was assumed that the heating up period was well completed by the time the drop had reached the first observation point.

The variation in Nusselt number and Reynolds number are shown in Fig. V.11. for evaporating water drops into pressurised superheated steam. These figures show that the Nusselt number decreased as the pressure decreased. Physical properties used in the calculation are based on mean conditions in the boundary layer.

The Prandtl number has been omitted in these correlations as the value of the Prandtl number is relatively independent of temperature. The values of the Prandtl number in this investigation varied from 0.989 - 1.112, which raised to the power, $\frac{1}{3}$, are close to unity.

In calculating the Nusselt number, the temperature difference was the difference in temperature of the boiling point of the water and the surrounding pressurised superheated steam.

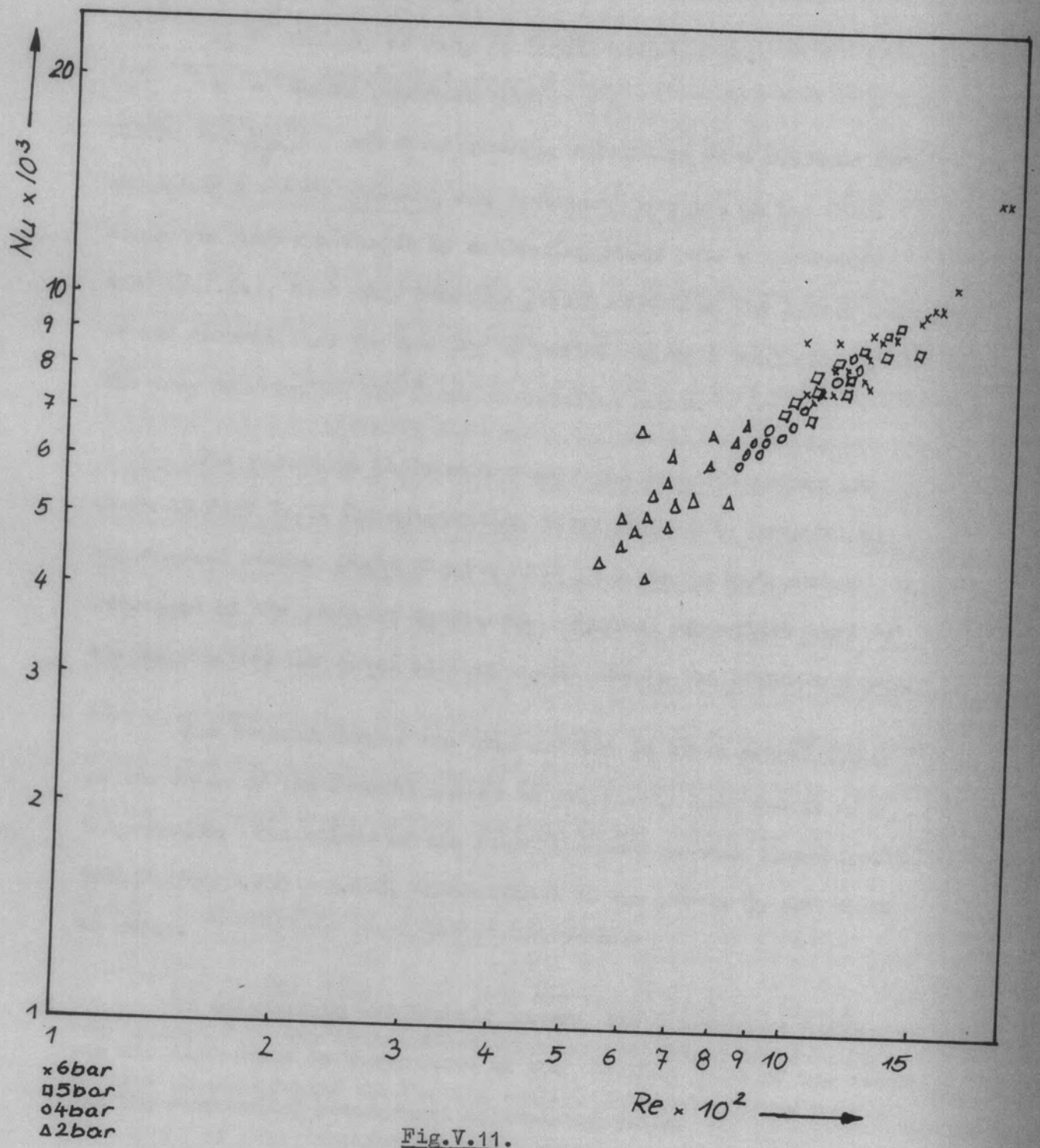

Fig.V.11.

Nusselt Number v. Reynolds Number (Mean Properties) for Evaporating Drops.

V.4. Results of the Drag Coefficient of Water Drops.

As shown in Section IV.4., the drag coefficient may be calculated from Equation IV.4.1.

The value for the superheated steam density, ρ_s, may be taken as that of the undisturbed medium, or as the mean value of the surrounding superheated steam and the saturated steam at the evaporative zone.

V.4.1. Drag coefficient for non evaporating water drops.

The drag coefficients of liquid drops in air under normal atmospheric conditions are known to be close to the standard curve which applies for a smooth solid sphere. If the drop size is greater than about 1.5 mm diameter then circulation within the drop and deformation may occur which affect the drag force. As a test of the experimental system, drag force measurements were carried out with water drops 1.5 mm diameter falling through air at 20°C. It was found that the drag coefficient values fall close to, but with a very small tendency to lie below the standard curve. (Taken from refs. 28, 29.) It may be assumed that the very small evaporation rate occuring from water drops falling through air at 20°C has caused the small reduction in the drag coefficient values compared to the values for solid spheres.

V.4.2. Drag coefficient of evaporating drops.

Drag coefficient values were determined from the time it was assumed that the drop had attained a steady state temperature - as used in calculating the Nusselt number. The velocity of fall was determined at every observation point which applied over the small time interval necessary for the drop to reach the next observation

point, a distance of 60 mm down the chamber.

In Fig. V.12, calculated drag coefficient values are plotted against corresponding Reynolds number. Curves with the sphericity $\psi \left(\frac{\text{Volume}}{\text{Surface area}}\right)$ as parameter (taken from Ref.15) have also been included to show the effect of sphericity on the drag coefficient.

The curve labelled ψ = 1 applies to smooth solid spheres and it is seen that all the drag coefficient values lie above this standard curve. This is due to the drop changing its sphericity continuously from approximately 0.7 to 0.9. As the pressure increased, the drop was closer to a spherical shape (ψ = 0.8 - 0.9) than at the lower pressure. The drag coefficient is reduced with an increase in pressure and it is thought that consequent increase of the evaporative rate lowered the drag coefficient. However, due to the oscillation exact evaluation of the effect of evaporation on the drag coefficient could not be made.

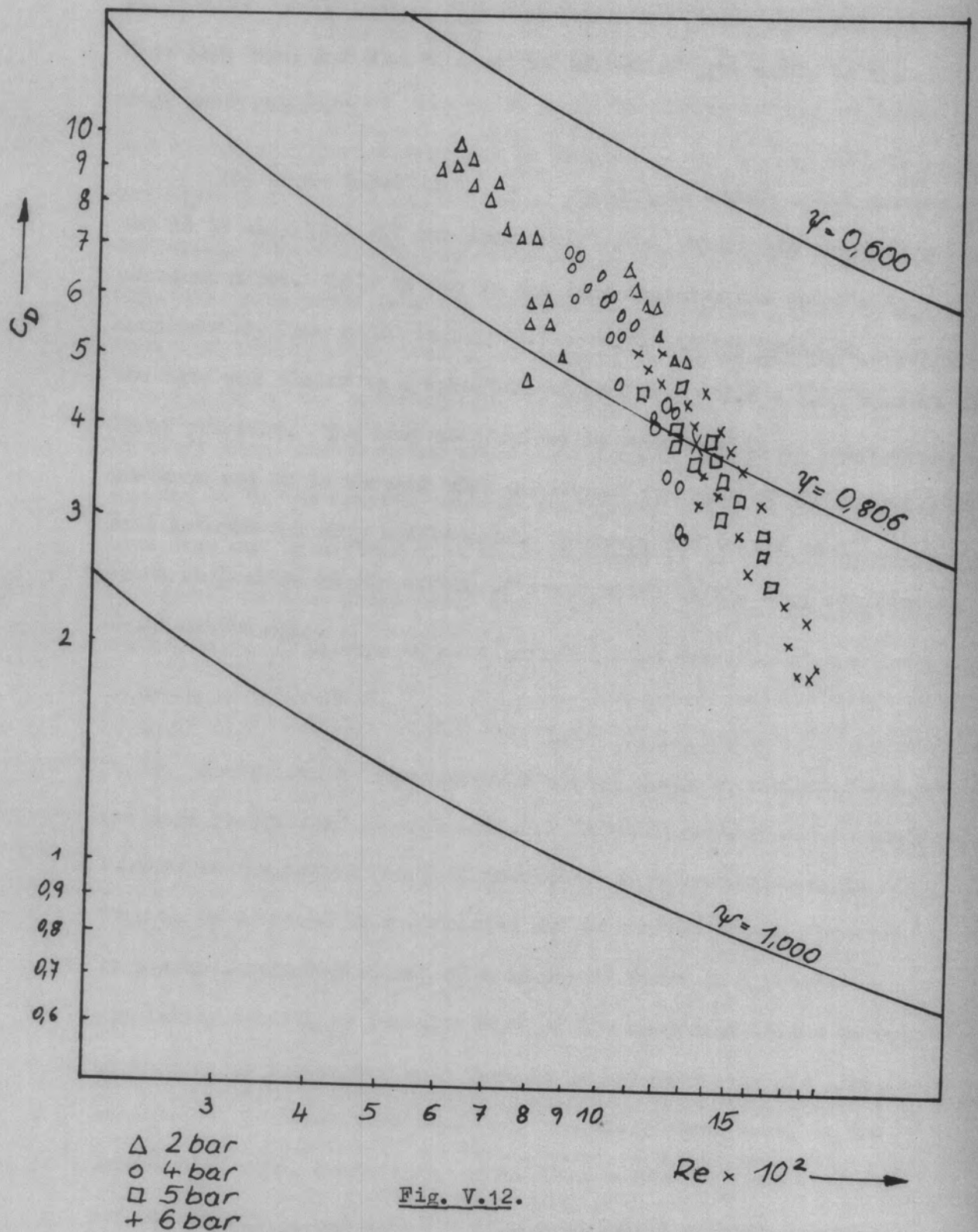

Fig. V.12.

Drag Coefficient v. Reynolds Number for Evaporating Drops.

CHAPTER VI.

DISCUSSION OF RESULTS.

The second law of Thermodynamics states that heat is an action dependent on energy transfer from one body to another at a lower temperature with which it is in direct thermal contact, and accordingly heat energy may be defined as the energy that is so transferred by either conduction or radiation. In the case of radiation, some complex considerations of the nature of electro-magnetic waves comes into the discussion. It is sufficient to say here that radiation is seen to be subject to the second law when the temperature of the emitting body is thought of with relation to absolute zero, and that therefore radiation is heat. When two bodies are not in direct thermal contact, energy may still be transferred by heat from one to a fluid with which the body is in thermal contact, and be carried by that fluid until the fluid is in thermal contact with the second body. This type of heat includes mass transfer of the fluid and is known as convection.

Energy can be transferred from one fluid to another fluid at the same temperature by mass transfer in which no heat - i.e. action subject to the second law - is involved. A well-known example of this is to be found in evaporation and in condensation. Whenever there is a concentration gradient of a component there is a potential available, tending to transfer mass of the component in the direction of decreasing concentration. This is called diffusion and like convection, includes mass transfer. In the present case, in the evaporative zone, conduction, radiation, convection, and diffusion are all operating and when the term coefficient of heat transfer between drop and the steam atmosphere is used it is to be understood

that energy transfer by any or all of these actions may be included.

The results presented in Chapter V. have shown that the evaporative rate of a freely falling drop in a superheated steam atmosphere is increased relative to that of an anchored drop in a moving superheated steam atmosphere. This is attributed to the dynamics of the drops investigated.

Consider a drop (Fig.VI. 1A) without a boundary layer, falling at terminal velocity in a frictionless atmosphere. The individual velocities distributed evenly on the drop surface are equal to the velocity in the drop centre. Should this drop be of a diameter where it may begin to oscillate, then the velocity distribution on the drop surface will become irregular. Fig. VI. 1.B. shows a drop oscillating in a horizontal direction. The resulting velocity on the surface consists of the terminal velocity component, plus the velocity component induced by oscillation. For this direction of oscillation the resulting velocity is larger than the terminal velocity acting in the drop centre. In the case when the drop oscillates in the direction as the terminal velocity (Fig. VI. 1.C) the resulting velocity on the front half of the drop will be increased and on the rear half it will be reduced. The net increase of the velocity will be zero and the drop falls at its terminal velocity.

Consider now a spherical drop, surrounded by a uniform boundary layer, being accelerated in a superheated steam atmosphere. In Fig. VI. 2. A. the development of stream-lines for an intermediate instant of the drop's acceleration period are shown. (19) The thickness

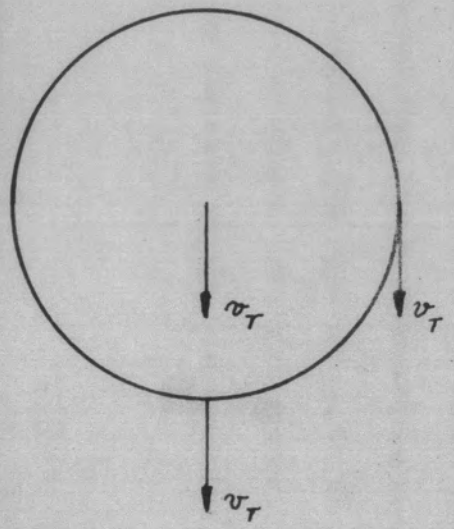

A

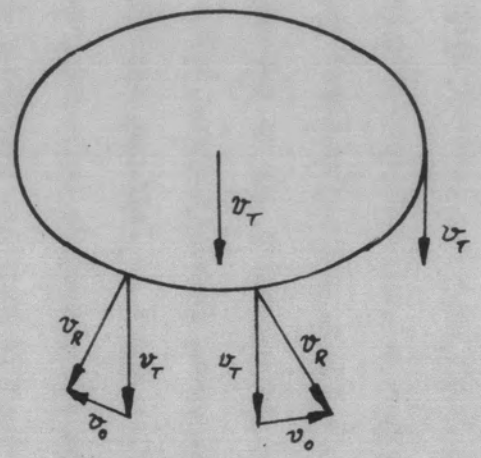

direction of oscillation

B

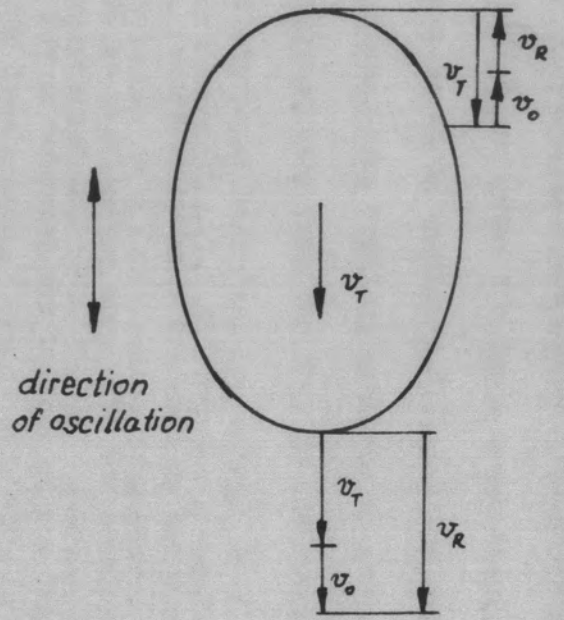

D.

FIG. VI.1.

of the boundary layer has been exaggerated for the sake of clarity. A potential frictionless flow pattern exists during the first instant after the drops break away. Separation then takes place as shown in Fig.VI.2.A, and the point of separation moves upstream. The vortices continue to grow, become unstable and are carried away from the drop by the external flow. This continual mixing of high- and low-energy level molecules in the vortices, promotes the heat transfer to the drop. In Fig. VI.2.B and Fig. VI.3, an oscillating drop with the development of stream-lines is shown for an intermediate instant of the drop's flight. The periodic boundary layer flow may be described as follows.(19)

The high-energy level water molecules of the superheated steam atmosphere flow towards the drop from above and below. Some of these molecules penetrate the drop's evaporative zone and give off their energy to the water molecules at a lower-energy level. The molecules then transfer in the direction of decreasing concentration (boundary layer). The boundary layer moves away from the evaporative zone in both directions parallel to the oscillatory motion of the drop. Rotation of the drop was also observed; the speed of rotation, however, was very small and resulting centrifugal forces were negligible.

It can be seen that vigorous mixing of the boundary layer is caused. Due to the subsequent mixing of high- and low-energy level molecules, the rate of heat energy transfer to the evaporative zone is much higher than for an anchored drop. It has been shown that the relative velocity of the boundary layer is also increased, causing the boundary layer thickness (constant viscosity) to decrease, consequently causing an increase in the heat transfer. Since the shape of the

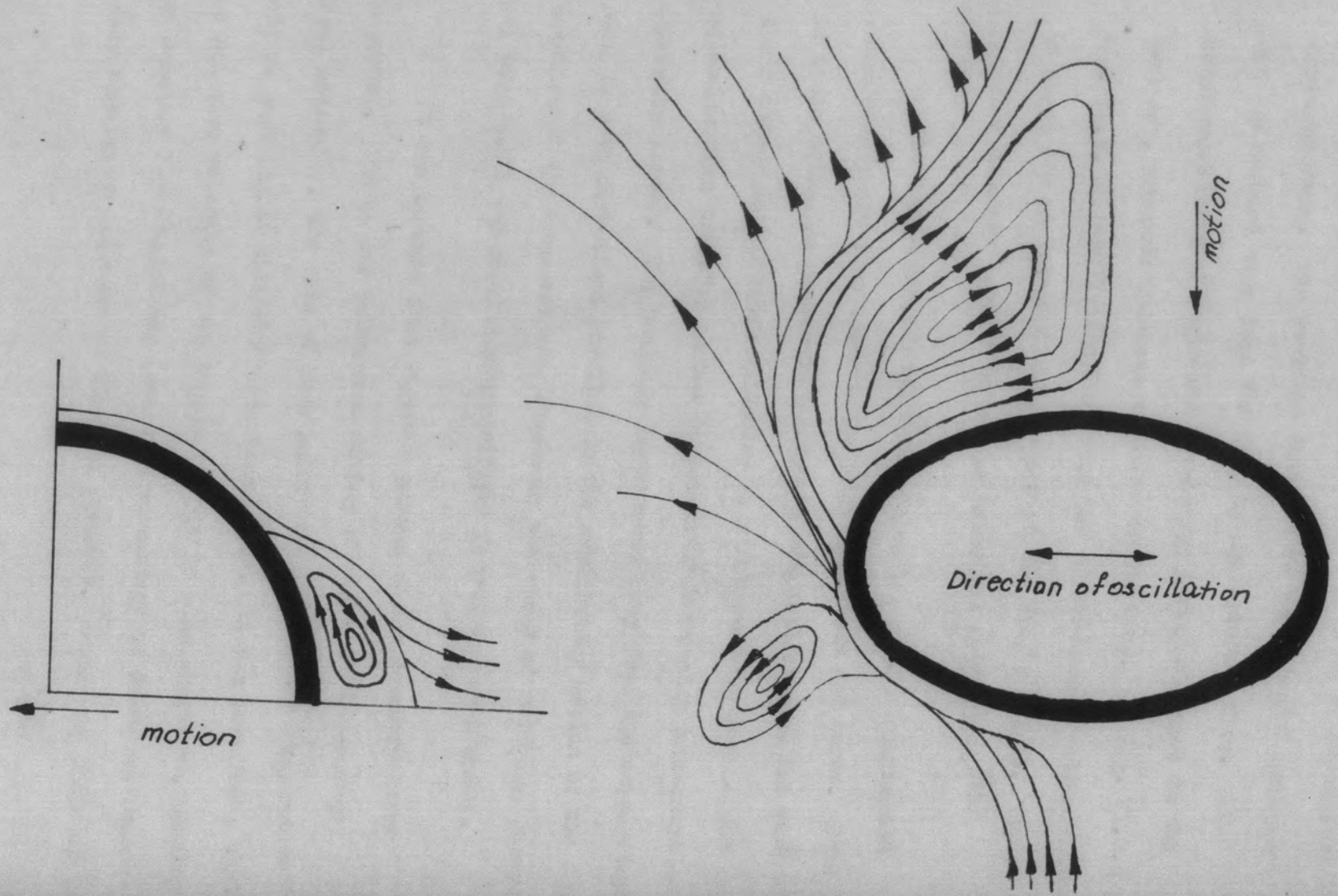

FIG. VI.2.

Streamline Development

77.

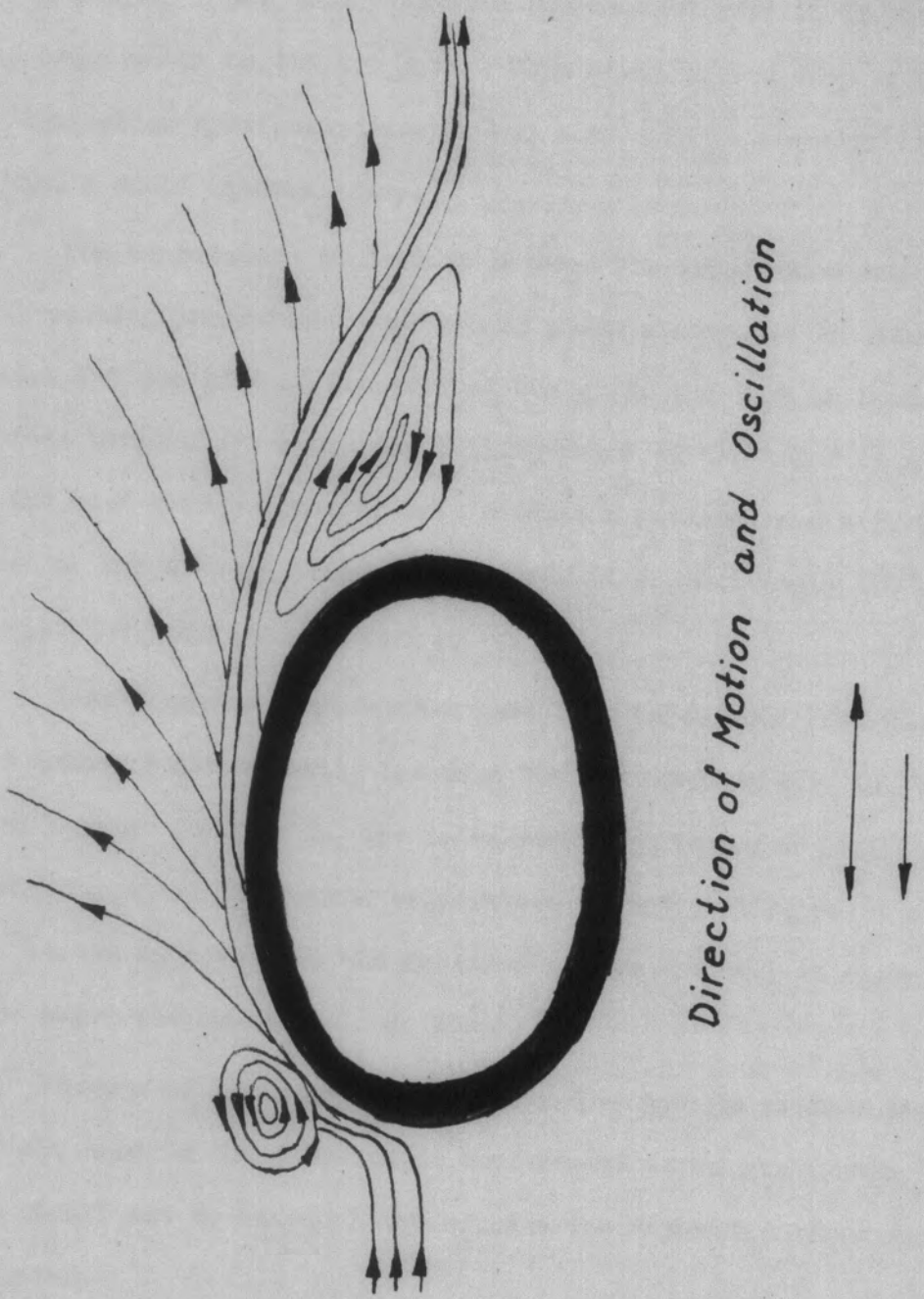

FIG. VI.3.

Streamline Development

drop is not spherical, but changes periodically from an oblate to a prolate spheroid, the available surface for heat energy transfer is much larger than the area of a sphere of equal volume.

Topps[17] has shown that the evaporative rate is proportional to the drop radius to the 4.6 power. This means that a drop with a large equivalent spherical diameter has a greater heat-energy transfer rate than a small diameter drop.[9]

The temperature difference between the evaporative zone and the surrounding pressurised superheated steam atmosphere is also very important for the rate of transfer of energy in the form of heat. When the excess temperature above the boiling point of the water is approximately 35°C, the heat energy transfer rate reaches a maximum, and a further increase of temperature causes a decrease, at approximately 100°C it rises again with the increase of temperature.

Heat transfer coefficients have been calculated from the Nusselt number obtained using the mean thermal conductivity in the boundary layer. In Fig.VI.4, the calculated heat transfer coefficients are plotted against the excess temperature of the boiling point of the water. It can be seen that the obtained values are well in agreement with the curve presented by A. J. Ede.[18]

Because of the many effects which interact to produce the results obtained in the pressurised superheated steam atmosphere, the results should not be extrapolated outside the Reynolds number range investigated.

VI.1. Physical Properties used in the calculation.

Results have been presented in the previous chapter based on

Heat Transfer Coefficient v. Excess Temperature.

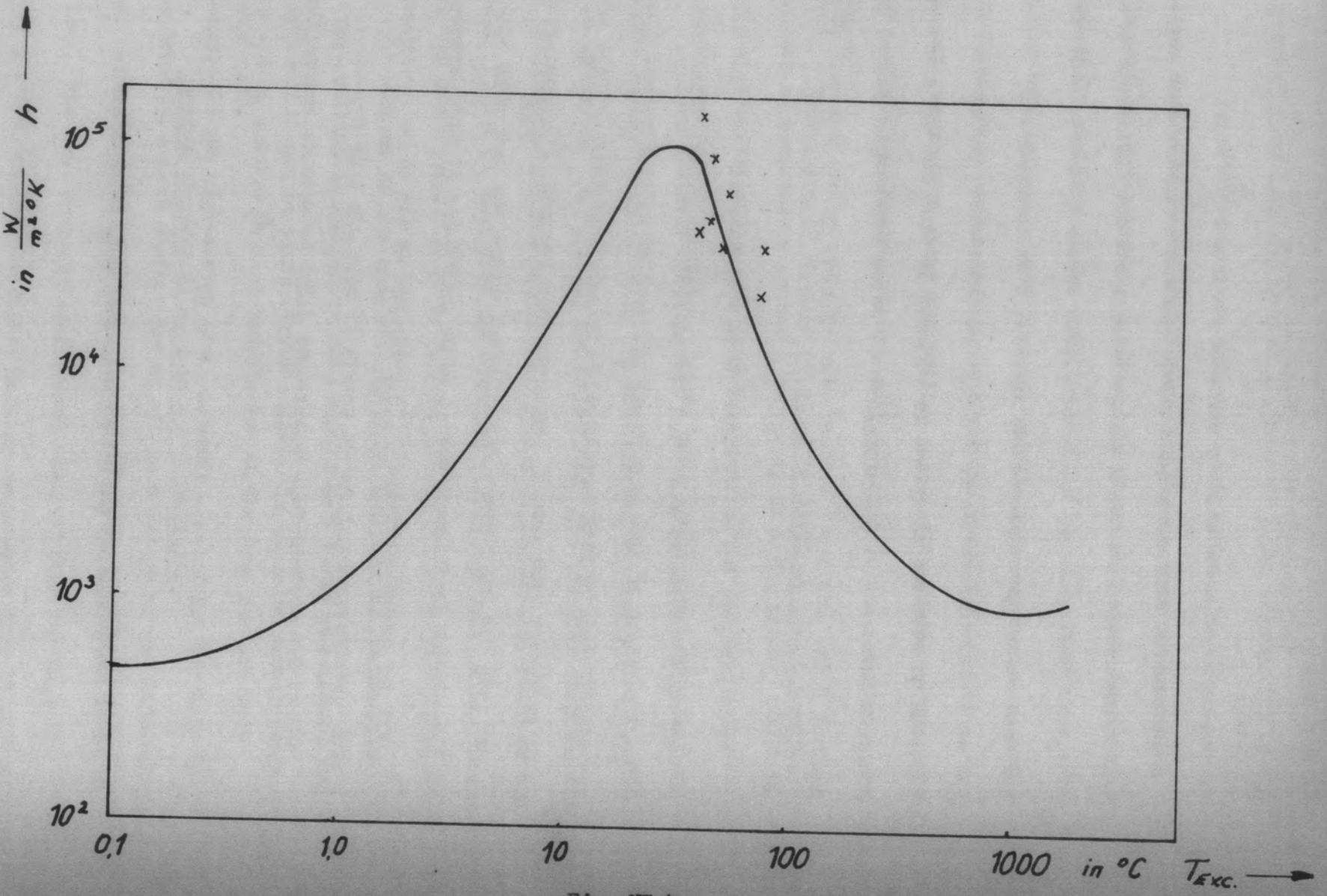

Fig. VI.4.

mean conditions of the boundary layer and on the properties of the water based on mean boundary layer temperature.

In order to compare obtained results, values for the water evaluated at the mean boundary layer temperature were used. In heat energy transfer with change in phase, conditions in the immediate vicinity of the drop (within the boundary layer) are taken into account. Heat transfer coefficients may be calculated using the mean conditions in the boundary layer, and related to the excess temperature above the boiling point of the water in the pressurised superheated steam atmosphere.

VI.2. Comparison of Results obtained by previous investigators.

Many investigations have been made in the evaporation of drops under forced convective forces using model drops or relatively small anchored drops in a moving atmosphere, and it has been found that $\frac{d(D^2)}{dt}$ decreased linearly with time. In this study it has been shown how $\frac{d(D^2)}{dt}$ changed with pressure. During drop formation only little more than the latent enthalpy was removed and the drop was observed after it had fallen 50 cm in the pressurised superheated steam atmosphere; there was no maximum $\frac{d(D^2)}{dt}$ observed during the observations. It is thought that the drop is almost at boiling temperature. The oscillations promote an equal temperature distribution within the drop and it attains boiling temperature at the drop surface very quickly. If the high-energy level molecule penetrating the drop is considered as a hard surface giving off heat energy to the surrounding water molecules at boiling point, the drop may be considered to be boiling. The heat transfer coefficient obtained from the Nusselt number plotted against the excess boiling temperature (Fig.VI.4.) is

well in agreement with the fitted boiling heat transfer coefficient curve. This suggests that the drop surface has attained boiling temperature and a maximum $\frac{d(D^2)}{dt}$ will not be observed.

The work of Lee and Ryley[9] for an anchored drop 1 mm diameter in a superheated steam atmosphere (143°C), showed a higher evaporative rate to the work of Ranz and Marshall[8] for equal size drops in an airstream of 220°C. Lee and Ryley[9] stated their case differed, in as much that it treated a drop evaporating into an atmosphere composed entirely of its own vapour. They had evidence that the anchored drop oscillated slightly under certain circumstances. They did not know how this influenced the evaporation. In this study, however, it has been shown that the oscillation and the larger surface area increased the evaporative rate. Due to the difference in the drop dynamics in this study, the values obtained by Lee and Ryley[9] could not be extrapolated to the Reynolds number range of this study. (Fig. V.6)

Rasbach and Stark[12] studied the evaporation in a bunsen flame of anchored water drops suspended on quartz fibres. It was found that in the range of sizes investigated, 1.3 - 2.3 mm, the heat energy transfer agreed well with the Ranz and Marshall[8] law, if the calculated value of heat energy transfer were multiplied by a constant factor of 0.63. Values for $\frac{d(D^2)}{dt}$ extrapolated to zero fibre thickness were $25 \frac{mm^2}{s}$ and a typical result in this study was $30 \frac{mm^2}{s}$. It is seen that the values obtained in this study are in agreement with the results obtained by Rasbach and Stark[12], even though their work was carried out with much higher temperature differences.

Comparison of Results

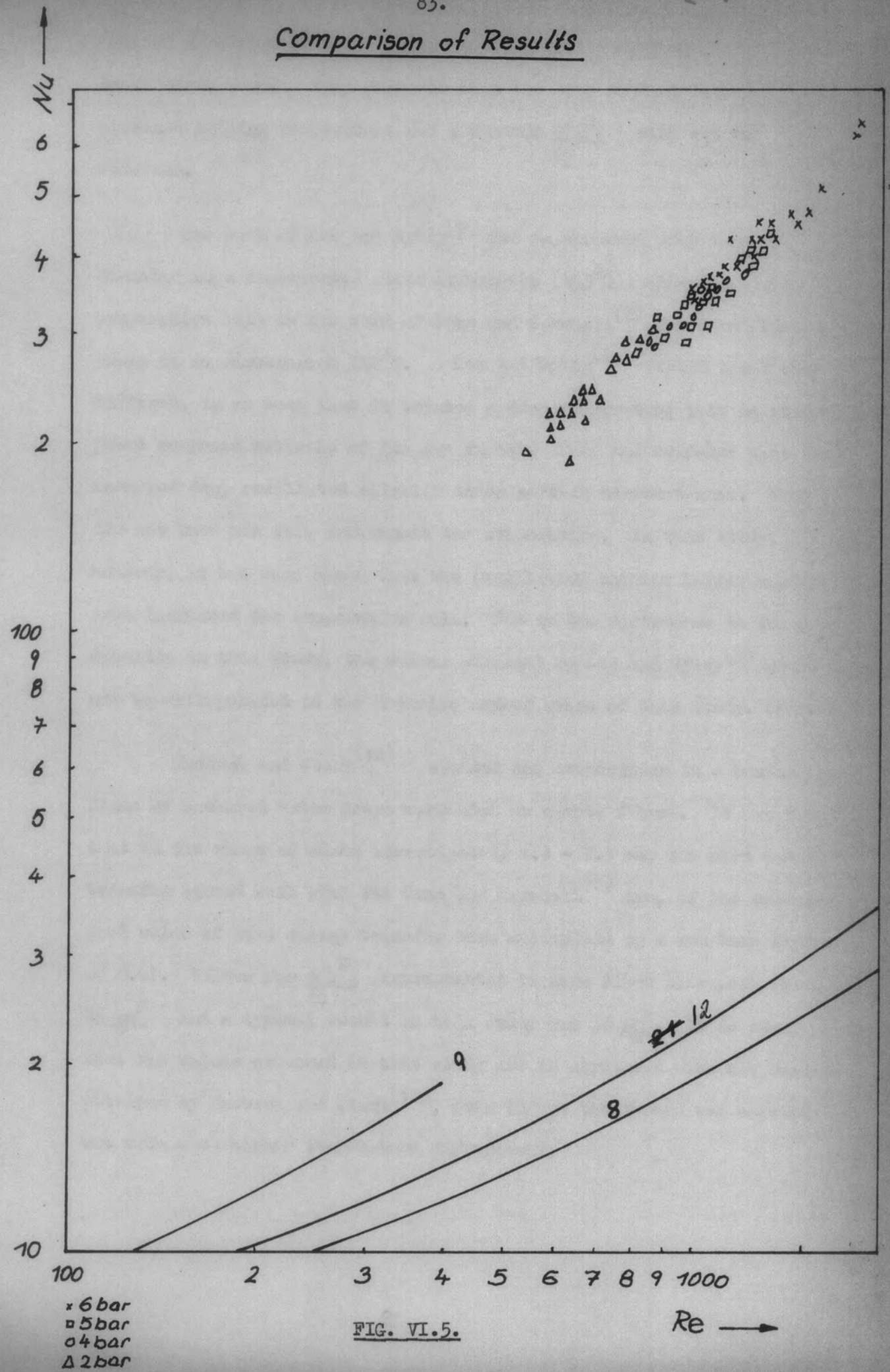

FIG. VI.5.

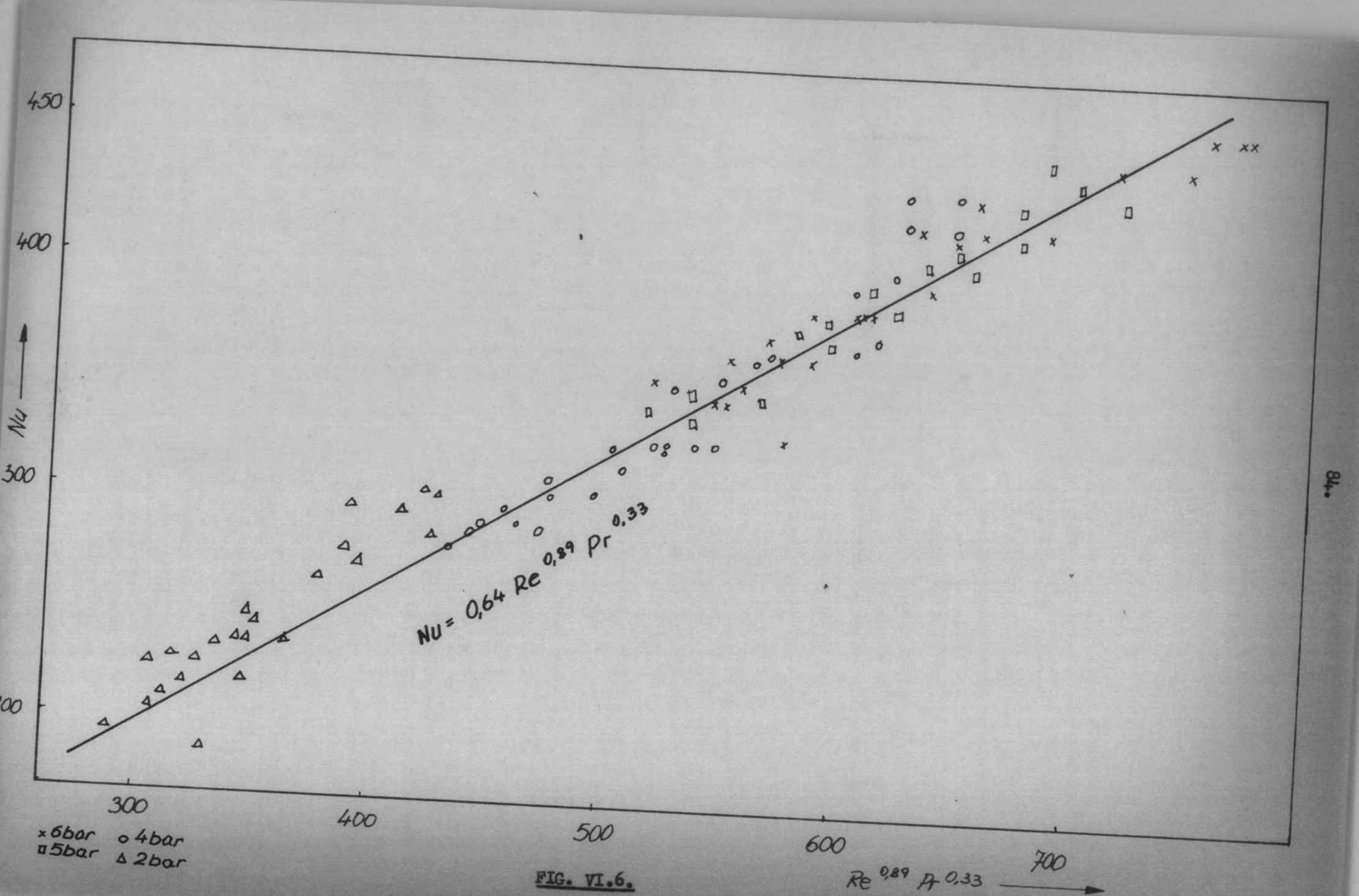
450
400
Nu
300
200
300
400
500
600
700
Re 0,89 Pr 0,33
NU = 0,64 Re 0,89 Pr 0,33
x 6bar o 4bar
□ 5bar △ 2bar

FIG. VI.6.

Nusselt Number v. dimensionless Temperature

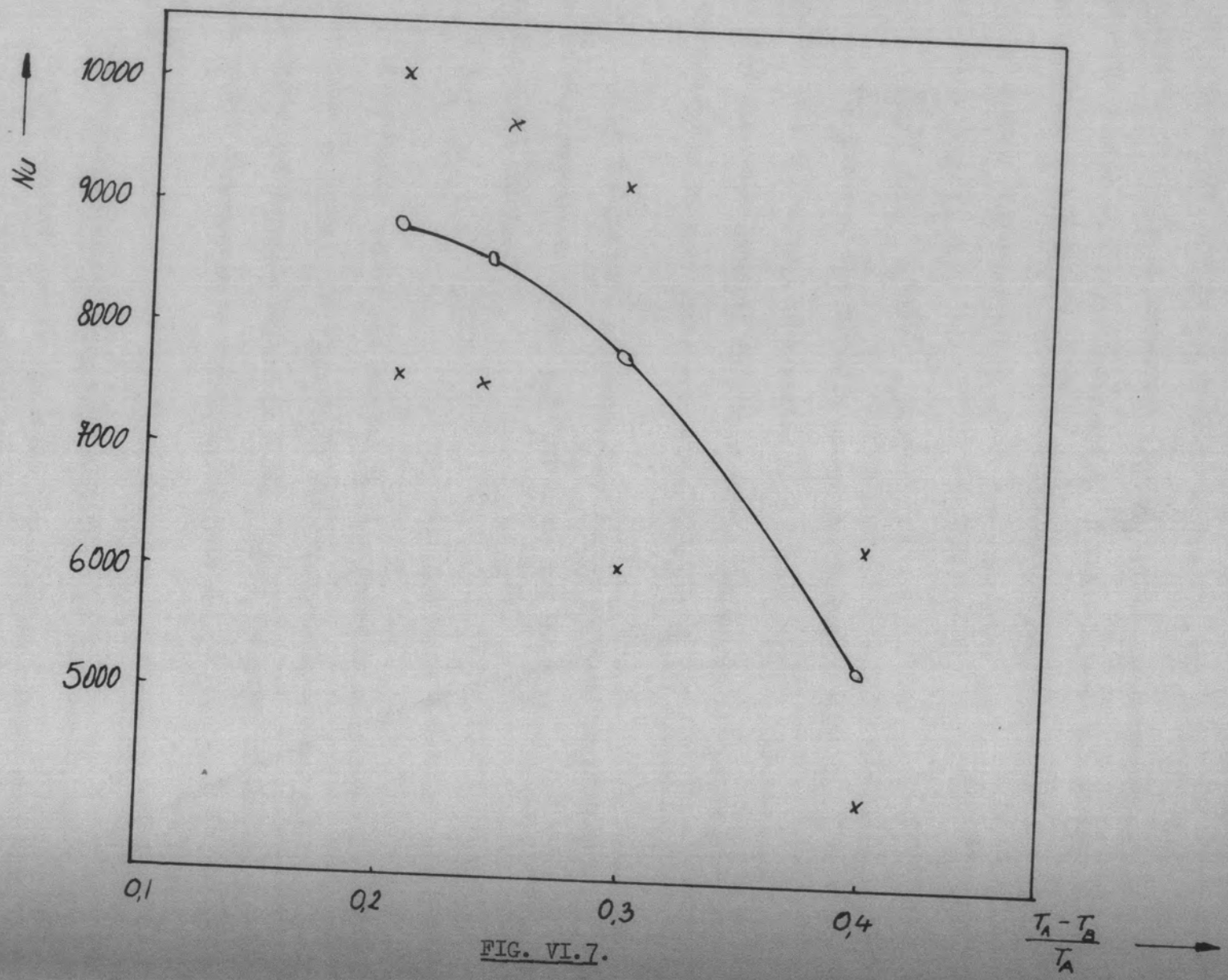

FIG. VI.7.

VI.3. Correlating of Results for Evaporating Drops.

The Nusselt number for evaporating drops has been calculated using physical property values of water evaluated at boundary layer temperature, and it was found to increase as the pressure increased. The Nusselt number was plotted against its corresponding Reynolds number on a logarithmic scale. A least squares fit method was employed to determine the most representative expression for all points, and the following was obtained for a Reynolds number range of 600 - 1600 (Fig. VI.6.)

$$\bar{N}u_m = 0.64 \quad RE^{0.89} \quad Pr^{0.33} \qquad \text{VI.3.1.}$$

The power of the Reynolds number for turbulent heat energy transfer in a cylindrical tube varies from 0.8 - 0.87[20]. It can be seen that the power obtained in this study is comparable if the drop is considered to be a cylinder with a length equal to its diameter.

It is thought more representative to use physical properties based on mean condition in the boundary layer and the following correlation was obtained:

$$\bar{N}u_m = 4.2 \quad Re^{0.8} \qquad \text{VI.3.2.}$$

The Prandtl number was omitted in this correlation, since it was very close to unity. In Figl VI.8. the relationship between the Nusselt number and Reynolds number is shown. Again the power of the Reynolds number corresponds to the turbulent heat energy transfer inside tubes.

The Nusselt number, using mean conditions in the boundary layer, was also plotted against another dimension-less quantity (Fig.VI.7.) equal to the ratio of $\frac{\text{excess boiling temperature}}{\text{boiling temperature}}$ and it was again seen how the Nusselt number decreased with the increase in temperature difference under the condition of this study.

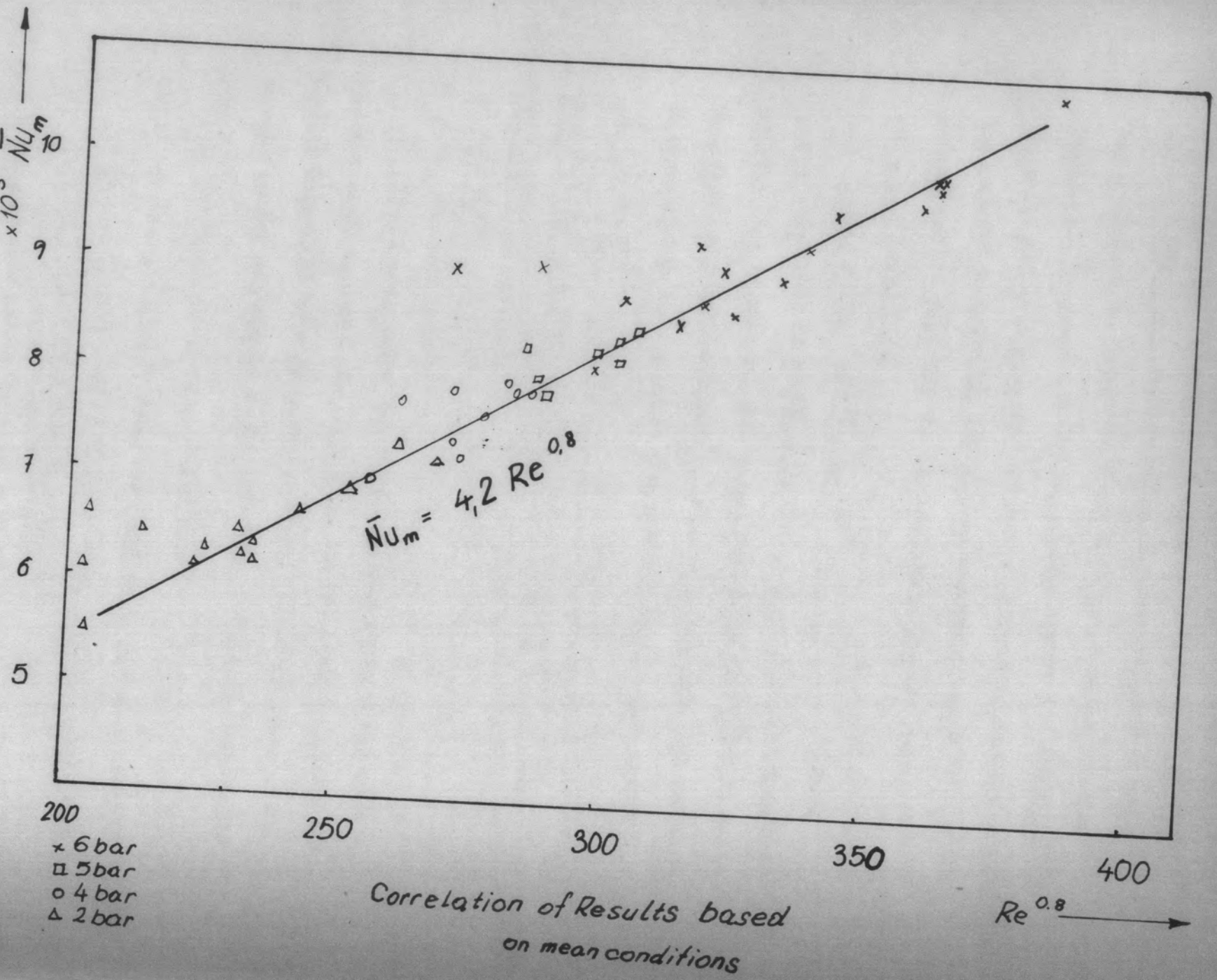
$\bar{Nu}_m$
$\times 10^3$
10
9
8
7
6
5
$\bar{Nu}_m = 4{,}2\ Re^{0{,}8}$
200
250
300
350
400
$Re^{0.8}$
× 6 bar
□ 5 bar
○ 4 bar
△ 2 bar
Correlation of Results based
on mean conditions

Fig. VI.8

VI.5. Drag coefficient of Evaporating Drops.

Due to the drop oscillating, it is very difficult to say how the evaporation affected the coefficient of drag. However, it was seen that the coefficient of drag decreased with an increase in pressure. The pressure increase brought about an increase in the evaporative rate. Therefore, it can be said that the drag coefficient is reduced as the evaporative rate is increased. Ingebo[19] and Eisenklam[25] showed that the coefficient of drag for small drops in free flight is greatly reduced when evaporation is taking place. In addition, the rotation of the drop causes the coefficient of drag to decrease.[16] The physical reason for this behaviour is connected with centrifugal forces acting on the steam molecules rotating with the drop in its boundary layer. In Fig.V.12, calculated coefficient of drag values are plotted against the Reynolds number. Curves for different sphericities are included, and it can be seen that the coefficient of drag lies above the standard curve for a sphere. It has been shown that the drop oscillates, and it is therefore very difficult to say whether the coefficient of drag falls below the line of equivalent sphericity.

The results have shown that the heat energy transfer for an oscillating freely falling drop in a pressurised superheated steam atmosphere is above the relatively small anchored drop studied by Lee and Ryley[9] and Toei[30]. It has been found that the dynamics and excess boiling temperature and drop size are the main reason for this difference.

The experimental technique of this study could be used to investigate the dynamics of different size drops and different temperature differences, to give more information of drops evaporating into an atmosphere composed entirely of its own vapour.

CHAPTER VII

CONCLUSIONS.

1. An experimental technique was developed that allowed the study of freely falling, oscillating water drops evaporating into a pressurised superheated steam atmosphere.

2. The values of $\frac{d(D^2)}{dt}$ were found to increase as the pressure was increased. The obtained values are in disagreement with the values obtained by investigators using anchored drops in an unpressurised, high and low temperature atmosphere (usually air). It was shown that this fact could be attributed to the dynamics of the freely falling drop.

3. The Nusselt number for evaporating drops were found to increase as the pressure of the superheated steam increased.

4. Heat transfer coefficients were calculated from the obtained Nusselt number, and found to agree with known boiling heat transfer coefficients.

5. The drag coefficients for evaporating drops were calculated. The effect of evaporation on the drag coefficient could not be investigated due to the drop's oscillating behaviour.

6. It has been considered more representative to base the values of the physical properties on mean condition of the boundary layer and the surrounding superheated steam.

7. The results of the evaporation rate have been correlated by the equation:

$$\overline{Nu}_m = 4.2 \quad Re_m^{0.8}$$

for the Reynolds number range of 600 to 1000. The Prandtl number was omitted, since it was close to unity.

APPENDIX I.

TABLES OF RESULTS.

Pressure : 2 bar.

Major axis. a. in mm.	Minor axis. b. in mm.	Volume. in mm^3	Surface area in mm^2	Velocity in m/s.	Diameter in mm.
Position I.					
2.63	2.119	49.466	66.435	2.30	4.518
2.513	2.098	46.351	63.789	2.28	4.431
2.432	2.053	45.203	65.823	2.31	4.443
2.553	2.102	47.352	64.352		4.492
Poaition II.					
2.395	1.823	43.818	61.320	2.17	4.39
2.385	1.823	43.453	60.972	2.19	4.37
2.385	1.823	43.453	60.972	3.21	4.32
2.362	1.823	43.462	60.985		4.33
2.385	1.812	43.191	60.723	2.19	4.28
2.353	1.780	41.297	58.94	2.17	4.25
2.321	1.823	41.152	52.802	2.42	4.23
2.300	1.855	41.120	58.771		4.22
2.374	1.855	43.809	61.310	2.04	4.28
2.395	1.812	43.554	61.072	2.36	4.34
2.395	1.802	43.314	60.842	1.190	4.33
2.374	1.802	42.557	60.137	1.85	4.27
2.374	1.833	43.289	60.823		4.31
Position III.					
2.534	2.012	42.966	60.347	2.254	
2.449	2.055	43.322	60.670	2.040	4.306
2.417	2.098	44.577	61.839	2.342	4.334
2.343	2.108	43.605	60.942	2.289	1.383
2.481	2.044	43.410	60.760		4.359
2.449	2.055	43.322	60.673	2.360	4.302
2.417	2.066	43.211	60.572	2.235	4.334
2.332	2.161	45.609	62.825	2.307	4.335
2.492	2.066	44.55	61.832		4.729
2.439	2.076	44.023	61.333	2.502	4.372
2.374	2.117	44.650	61.924	2.626	
2.278	2.163	44.639	61.914	2.644	4.361
Position IV.					
2.23	2.16	43.721	61.112	2.49	4.365
2.26	2.15	43.815	61.282	2.49	4.370
2.36	2.13	45.210	62.310		4.400
2.26	2.15	43.790	61.200	3.03	4.370
2.28	2.13	43.289	60.823	2.58	4.354
2.25	2.10	41.920	52,203		4.924
2.21	2.12	41.937	59.242	2.94	4.298
2.24	2.09	41.320	58.661	2.81	4.274
2.25	2.07	40.923	58.090		4.251

Pressure : 2 bar.

Major axis. a. in mm.	Minor axis b. in mm.	Volume in mm^3	Surface area in mm^2	Velocity in m/s.	Diameter. in mm.
Position V.					
2.276	2.019	38.861	55.978	2.923	4.192
2.212	2.083	40.193	57.732	2.930	4.248
2.319	1.986	38.312	55.973		4.165
2.276	2.040	39.669	57.241	3.132	4.223
2.330	1.997	38.922	56.542	2.953	4.187
2.352	1.833	33.101	51.082	3.15	3.942
2.298	2.062	40.918	58.421	2.577	4.267
2.288	2.040	39.008	56.627	2.326	4.229
2.352	1.965	38.040	55.770	2.543	4.150
Position VI					
2.686	1.974	43.835	61.159	2.423	4.306
2.729	1.842	38.776	56.40	2.315	4.094
2.697	1.974	43.835	61.152	2.291	4.310
2.708	1.842	38.776	56.40		4.087

Pressure : 4 bar.

Major axis. a. in mm.	Minor axis.b. in mm.	Volume in mm^3	Surface area in mm^2	Velocity in m/s.	Diameter in mm.
Position I.					
2.358	2.048	41.428	58.100	2.560	4.278
2.336	2.048	41.041	57.710	2.525	4.267
2.336	2.081	42.375	58.912		4.315
2.315	2.087	41.537	59.207	2.222	4.325
2.304	2.037	40.046	56.755	2.047	4.234
2.315	2.048	40.672	57.344	2.186	4.256
2.347	2.037	40.793	57.507		4.256
Position II					
2.293	2.018		55.882	2.130	4.200
2.335	1.976	39.114	55.107	2.219	4.158
2.399	1.944	38.190	55.053	2.130	4.139
2.431	1.944	37.976	55.595	2.	4.153
2.314	1.987	38.483	55.139	2.124	4.164
2.399	1.966	38.269	55.842	2.188	4.173
2.399	1.976	38.841	56.202		4.189
Position III					
2.215	1.950	35.280	52.167	2.031	4.058
2.215	1.950	35.280	52.167	1.943	4.058
2.204	1.911	33.715	50.648	2.190	3.994
2.204	1.992	36.634	53.438	1.960	4.113
2.194	2.024	37.648	54.385		4.154
2.236	1.918	34.455	51.415	2.501	4.021
2.204	1.908	33.609	50.546	2.480	3.990
2.173	1.897	32.755	49.667	2.713	3.957
2.204	1.886	32.839	49.800	2.332	3.956
2.151	1.918	33.146	50.015		3.976
Position IV.					
2.337	1.882	34.673	51.835	2.764	4.013
2.272	1.819	31.489	48.633	2.871	3.885
2.337	1.863	33.976	51.77		3.983
Position V.					
2.287	1.906	34.802	51.844	1.98	4.028
2.255	1.830	31.633	48.733	1.98	3.895
2.320	1.819	32.155	49.396	1.95	3.906
2.309	1.830	32.390	49.594	1.90	3.919
2.309	1.819	32.002	49.221	2.11	3.901
2.331	1.797	31.530	48.823		3.875
Position VI					
2.369	1.773	31.194	48.605	2.997	3.851
2.369	1.775	30.564	47.996	2.907	3.821
2.121	1.733	26.683	43.485		3.682

Pressure : 5 bar.

Major axis.a. in mm.	Minor axis.b. in mm.	Volume in mm^3	Surface area in mm^2	Velocity in m/s	Diameter in mm.
Position I					
2.230	1.914	34.220	51.179	2.09	4.012
2.385	1.957	38.261	55.281	1.88	4.153
2.417	1.904	36.703	53.930		4.083
2.407	1.947	38.221	55.296	1.56	4.147
2.385	1.904	36.217	53.398	1.70	4.069
2.422	1.882	35.934	53.233		4.050
2.240	2.000	37.532	54.332	1.72	4.145
2.280	1.970	37.064	53.959	1.74	4.121
2.330	1.920	35.979	35.045		4.070
Position II					
2.310	1.925	35.856	52.887	1.69	4.068
2.332	1.893	35.004	52.136	1.61	4.028
2.332	1.893	35.004	52.136	1.65	4.028
2.342	1.882	34.747	51.917		4.016
2.481	1.893	37.241	54.602	1.566	4.092
2.477	1.782	36.272	53.686	1.630	4.054
2.514	1.850	36.041	53.606	1.694	4.034
2.481	1.882	36.809	54.208		4.074
2.481	1.904	37.675	54.997	14.70	4.110
2.492	1.882	36.972	54.390	16.04	4.079
2.542	1.867	36.616	54.164	1.540	4.056
Position III.					
2.171	1.890	32.484	49.399	1.42	3.946
2.112	1.872	32.030	48.973	1.55	3.924
2.274	1.850	31.740	48.750		3.907
2.293	1.882	34.020	51.115	1.72	3.493
2.396	1.850	34.349	51.684	1.72	3.988
2.396	1.840	33.979	51.336	1.73	3.971
2.385	1.860	34.562	51.854		3.499
Position IV					
2.160	1.893	32.422	49.321	1.60	3.944
2.138	1.914	32.655	49.503	1.60	3.958
2.086	1.947	33.123	49.920		3.981
2.203	1.743	28.035	45.048	1.35	3.734
2.171	1.818	30.056	47.004	1.46	3.837

Pressure : 5 bar (cont'd)

Major axis.a. in mm.	Minor axis.b. in mm.	Volume in mm^3	Surface area in mm^2	Velocity in m/s	Diameter in mm.
Position V.					
2.182	1.882	32.373	49.308	1.55	3.939
2.193	1.892	32.918	49.358	1.48	3.967
2.171	1.072	31.868	48.795		3.919
Position VI					
2.374	1.630	24.616	44.112	1.69	3.620
2.364	1.658	27.221	44.687	1.61	3.655
2.310	1.700	27.964	45.263	1.65	3.707
2.385	1.679	28.163	45.693		3.698
2.280	1.636	25.562	42.74	1.56	3.588
2.226	1.700	27.431	44.603	1.63	3.690
2.214	1.765	28.891	45.934	1.694	3.774
2.278	1.700	27.577	44.783		3.695
2.257	1.690	27.002	44.145	1.470	3.670
2.203	1.829	30.870	47.873	1.604	3.869
2.193	1.904	33.301	50.230	1.54	3.978

Pressure : 6 bar.

Major axis.a. in mm.	Minor axis.b. in mm.	Volume in mm^3	Surface area in mm^2	Velocity in m/s.	Diameter in mm.
Position I.					
2.545	1.863	37.000	54.582	2.28	4.067
2.513	1.895	37.801	55.207	2.14	4.108
2.428	1.938	38.198	55.329	2.13	4.142
2.311	1.996	38.566	55.408	2.04	4.176
2.289	2.034	39.668	56.385		4.221
Position II.					
2.186	1.854	31.474	48.435	1.543	3.899
2.412	1.822	33.540	54.968	1.543	3.948
2.347	1.800	31.853	49.177		3.886
2.251	1.800	30.550	47.665	1.60	3.846
2.203	1.856	31.788	48.775	1.73	3.910
2.210	1.878	32.649	49.627	1.65	3.947
2.223	1.835	31.355	48.391		3.888
2.223	1.824	30.980	48.024		3.871
Position III.					
2.298	1.862	33.373	50.510	1.816	3.964
2.309	1.808	31.616	48.848	1.633	3.883
2.320	1.667	27.005	44.332	1.735	3.665
2.337	1.775	30.763	48.080		3.839
2.276	1.917	35.035	52.043	2.14	4.039
2.287	1.851	32.822	49.956	2.06	3.942
2.331	1.841	33.093	50.323		3.946
Position IV.					
2.289	1.706	27.906	45.144	2.883	3.709
2.257	1.749	28.902	46.070	2.883	3.766
2.226	1.780	29.543	46.012	2.883	3.803
2.176	1.812	29.927	46.882		3.830
Position V.					
2.444	1.890	36.569	53.881	1.822	4.072
2.423	1.873	35.606	52.932	1.65	4.036
2.423	1.884	36.025	53.320	1.91	4.054
2.401	1.884	35.698	52.958		3.751
2.177	1.761	28.279	45.235	1.94	3.772
2.166	1.782	28.811	45.748	1.63	3.692
2.124	1.739	26.906	43.721	1.89	3.857
2.026	1.884	30.122	46.861		3.894
2.121	1.873	37.168	48.024	1.68	3.816
2.035	1.852	29.237	45.967	1.66	3.[illegible]

Pressure : 6 bar (cont'd)

Major axis a. in mm.	Minor axis b. in mm.	Volume in mm^3	Surface area in mm^2	Velocity in m/s.	Diameter in mm.
Position VI.					
2.157	1.810	29.600	46.521		3.818
2.201	1.756	28.429	45.440	1.69	3.754
2.233	1.713	27.447	44.530	1.75	3.698
2.046	1.765	26.698	43.363		3.694
1.994	1.817	27.576	44.207	1.89	3.743
1.921	1.879	28.410	45.030	1.906	3.785
2.108	1.630	23.460	40.079		3.512
2.066	1.651	23.509	40.120	1.62	3.528
2.066	1.672	24.193	40.764	1.68	3.561

APPENDIX II

Values of Physical Properties used in the Calculation of Evaporating Drops.

Values for the Nusselt number, drag coefficient and Reynolds number have been calculated on the basis of physical property values of the surrounding superheated steam and on the basis of mean conditions.

Mean conditions for evaporating drops are taken to be the arithmetic average between 100% vapour at the evaporative zone at the surface temperature of the drop and superheated steam at the surrounding temperature.

Superheated Steam.

Pressure in bar.	2 bar.	4 bar.	5 bar.	6 bar.
Temperature in °C.	200°C	200°C	200°C	200°C
Thermal Conductivity k in 10^{-2} $\frac{W}{m.°K.}$	3.33	3.35	3.36	3.37
Dynamic Viscosity in 10^{-6} $\frac{kg}{m.s}$	16.15	16.09	16.06	16.03
Density in $\frac{kg}{m^3}$	1.03	1.82	2.35	2.85
Specific Heat Capacity in $\frac{kj}{kgK.}$	2.124	2.295	2.32	2.35

Saturated Steam.

Pressure in bar.	2 bar.	4 bar.	5 bar.	6 bar
Steam temperature in °C	120	143	149	159
Thermal Conductivity in $\frac{10^{-2} \ W}{°Km.}$	26.74	28.90	28.98	30.08
Density in $\frac{kg}{m^3}$	1.12	2.11	2.55	3.26

Pressure in bar	2 bar	4 bar	5 bar	6 bar
Dynamic Viscosity in 10^{-6} $\frac{kg}{m.s}$	12.80	13.65	13.85	14.23
Specific Heat Capacity in $\frac{kj}{kg.K.}$	2.120	2.243	2.313	2.397

Water.

Pressure in bar.	2 bar	4 bar	5 bar	6 bar.
Evaporation Temperature $^{o}C.$	120	143	149	159
Latent Enthalpy in $\frac{kj}{kg}$	2203	2135	2118	2086
Thermal Conductivity in 10^{-2} $\frac{W}{Km}$	68.7	68.76	68.72	68.5
Density in $\frac{kg}{m^3}$	943	923	917	908
Specific Capacity in $\frac{kj}{kg.K.}$	4.245	4.289	4.309	4.335

APPENDIX III.

Examples of Calculations.

1. Calculation of Nusselt' Number:

(a) Physical properties based on boundary layer conditions, evaluated at mean temperature:

$$\overline{Nu}_m = \frac{1}{4} \frac{L \cdot \rho_L}{k_m (T_A - T_S)} \cdot \frac{d(D^2)}{dt}$$

$$= \frac{1}{4} \frac{2203 \cdot 943}{3.02 \cdot 10^{-5} \, 80} = 2149.6 \cdot 10^5$$

$\frac{dD^2}{dt}$ obtained from drop size record, a typical result was

$$\frac{dD^2}{dt} = \frac{0.6 \cdot 10^{-6}}{0.029}$$

$$\overline{Nu}_m = 4447.5$$

(b) Physical properties based on water calculated at mean temperature in the boundary layer:

$$= \frac{1}{4} \frac{2203 \cdot 943}{68.7 \cdot 10^{-5} \cdot 80} \cdot \frac{0.6 \cdot 10^{-6}}{0.029}$$

$$\overline{Nu}_m = 195$$

Drag coefficient:

Velocity and diameter were measured for every drop and the corresponding drag coefficient calculated from:

$$C_D = \frac{4}{3} \frac{(\rho_D - \rho_A) \cdot D \cdot g}{v_m^2 \cdot \rho_A}$$

C_D has been calculated using physical properties of the surrounding atmosphere.

A typical result was:

$D = 4.306$ mm. $V = 2.04$ m/s.

$$C_D = \frac{4(943 - 1.03) \cdot 4.306 \cdot 10^{-3} \cdot 9.81}{3 \cdot (2.04)^2 \cdot 1.03}$$

$$= \frac{12.36}{12.36}$$

Reynolds Number.

Re has been calculated using the kinetic viscosity of the surrounding evaluated at the corresponding pressure.

$$Re = \frac{V \cdot D \cdot \rho_A}{0} = \frac{2.04 \cdot 4.306 \cdot 1.03}{16.15} = 560$$

See Appendix II. for the values of the physical properties.

APPENDIX IV.

Contribution by Radiation to total heat received by drop.

Consider a drop 4.22 mm in diameter, evaporating into a superheated steam atmosphere at 200°C. The heat energy transferred by radiation is given by

$$Ra = \alpha_D \cdot \varepsilon_W \cdot \sigma \times A(T_W^4 - T_D^4)$$

Ra	=	energy transferred by radiation
α_D	=	absorbtivity of eater drop.
ε_W	=	emissivity of wall.
σ	=	Stefan-Boltzman constant
A	=	Surface area of drop
T_W	=	wall temperature
T_D	=	Drop temperature

Substituting into this equation the values:-

A	=	$58.77 \cdot 10^{-6}$ m^2
T_W	=	200°C
T_D	=	120°C
σ	=	$56.7 \cdot 10^{-12}$ $\frac{kw}{m^2\ ^oK}$
ε_W	=	0.79 (steel walls at 200°C)
α_D	=	0.04
R_a	=	$2.51 \cdot 10^{-5}$ kW

Now, $\frac{dm}{dt}$ for a 4.22 mm drop in superheated steam at 200°C found in the experiment of this study to be $0.39 \cdot 10^{-3}$ $\frac{kg}{s}$

$\therefore$ Radiation absorbed per gramm evaporated

$$\frac{2.5110^{-5} \quad kW}{0.39 \cdot 10^{-3} \frac{kg}{s}} = 6.43 \quad \frac{kj}{kg}$$

For water, $L = 2203 \frac{kj}{kg}$, and hence heat energy by radiation received by the drop is negligible.

APPENDIX V.

```
      SUBROUTINE DSIMQ%A,B,N,KS<
      DOUBLE PRECISION A,B,BIGA
      DIMENSION A%1<,B%1<
C        FORWARD SOLUTION
      TOL#0.0
      KS#0
      JJ#-N
      DO 65 J#1,N
      JY#J&1
      JJ#JJ&N&1
      BIGA#0
      IT#JJ-J
      DO 30 I#J,N
C        SEARCH FOR MAXIMUM COEFFICIENT IN COLUMN
      IJ#IT&I
      IF%DABS%BIGA<-DABS%A%IJ<<< 20,30,30
   20 BIGA#A%IJ<
      IMAX#I
   30 CONTINUE
C        TEST FOR PIVOT LESS THAN TOLERANCE %SINGULAR MATRIX<          SI
      IF%DABS%BIGA<-TOL< 35,35,40
   35 KS#1
      RETURN
C        INTERCHANGE ROWS IF NECESSARY
   40 I1#J&N*%J-2<
      IT#IMAX-J
      DO 50 K#J,N
      I1#I1&N
      I2#I1&IT
      SAVE#A%I1<
      A%I1<#A%I2<
      A%I2<#SAVE
C        DIVIDE EQUATION BY LEADING COEFFICIENT
   50 A%I1<#A%I1</BIGA
      SAVE#B%IMAX<
      B%IMAX<#B%J<
      B%J<#SAVE/BIGA
C        ELIMINATE NEXT VARIABLE
      IF%J-N< 55,70,55
   55 IQS#N*%J-1<
      DO 65 IX#JY,N
      IXJ#IQS&IX
      IT#J-IX
      DO 60 JX#JY,N
      IXJX#N*%JX-1<&IX
      JJX#IXJX&IT
```

```
   60 A%IXJX<#A%IXJX<-%A%IXJ<*A%JJX<<
   65 B%IX<#B%IX<-%B%J<*A%IXJ<<
C          BACK SOLUTION
   70 NY#N-1
      IT#N*N
      DO 80 J#1,NY
      IA#IT-J
      IB#N-J
      IC#N
      DO 80 K#1,J
      B%IB<#B%IB<-A%IA<*B%IC<
      IA#IA-N
   80 IC#IC-1
      RETURN
      END
      SUBROUTINE DGTPRD%A,B,R,N,M,L<
      DOUBLE PRECISION A,B,R
      DIMENSION A%1<,B%1<,R%1<
      IR#0
      IK#-N
      DO 10 K#1,L
      IJ#0
      IK#IK&N
      DO 10 J#1,M
      IB#IK
      IR#IR&1
      R%IR<#0
      DO 10 I#1,N
      IJ#IJ&1
      IB#IB&1
   10 R%IR<#R%IR<&A%IJ<*B%IB<
      RETURN
      END
      SUBROUTINE  PLSQF %X,Y,M,N,U,ERR,A,V<
      DOUBLE PRECISION X,Y,A,U,V,ERR,YC
      DIMENSION X%1<,Y%1<,A%1<,U%1<,V%1<
      DO 3 I#1,M
      A%I<#1.0
      DO 3 J#1,N
      JJ#J*M&I
      J1#JJ-M
    3 A%JJ<#A%J1<*X%I<
      CALL DGTPRD %A,Y,U,M,N&1,1<
      CALL DGTPRD %A,A,V,M,N&1,N&1<
      CALL DSIMQ %V,U,N&1,NERR<
      ERR#0
      J1#N&1
      DO 2 I#1,M
      YC#0.0
      DO1 J#1,J1
      JJ#M*%J-1<&I
    1 YC#A%JJ<*U%J<&YC
      A(I) = Y(I)-YC
    2 ERR#A%I<*A%I<&ERR
      RETURN
      END
```

EPLACEMENT OR "CANCEL".

) COMMAND

```
      DOUBLE PRECISION X,Y,A,U,V,ERR,YC
      DIMENSION X(200),Y(200),U(10),A(2000),V(250)
      DATA YES/'YES '/,NO/'NO  '/
      WRITE(6,6010)
 6010 FORMAT(' DO YOU REQUIRE INSTUCTIONS IN THE USE OF THIS PROGRAMME?'
     1/'IF SO PLEASE TYPE YES, IF NOT TYPE NO.'/)
    6 READ(1,1000)ANS
 1000 FORMAT(A4)
      IF(ANS.EQ.YES)GO TO 5
      IF(ANS.EQ.NO)GO TO 1
      WRITE(6,6011)
 6011 FORMAT(' ANSWER IS INCORRECT. PLEASE RETYPE YES OR NO.')
      GO TO 6
    5 WRITE(6,6012)
 6012 FORMAT(' INSTRUCTIONS')
    1 READ(5,5001)M,N
      WRITE(6,6003)
 6003 FORMAT(1H ,25X,'POLYNOMIAL LEAST SQUARES FIT'/)
      READ(5,5000)(X(I),I=1,M)
      READ(5,5000)(Y(I),I=1,M)
.5    DO 8 I=1,M
.55   XL=X(I)
.56   YL=Y(I)
.6    X(I)=ALOG(XL)
.7    8 Y(I)=ALOG(YL)
    3 CALL PLSQF(X,Y,M,N,U,ERR,A,V)
      N1 = N+1
      WRITE(6,6004)
 6004 FORMAT(' CURVE IS OF THE FORM:Y = A0+A1*X+A2*X**2+...+AN*X**N'/)
      WRITE(6,6006)N,M
 6006 FORMAT(' ORDER OF CURRENT FIT = ',I2,10X,'NO. OF POINTS GIVEN = ',
     1I3/)
      DO 2 I=1,N1
      I1=I-1
    2 WRITE(6,6005)I1,U(I)
 6005 FORMAT(' A',I1,' = ',E14.6)
      WRITE(6,6002)
 6002 FORMAT(///8X,'X',12X,'Y',11X,'ERROR'/)
      WRITE(6,6000)(X(I),Y(I),A(I),I=1,M)
      WRITE(6,6007)
 6007 FORMAT('0 ''ERROR'' IS THE ALGEBRAIC DIFFERENCE BETWEEN THE VALUE
     1GIVEN FOR Y AND THAT FOUND FROM THE FITTED CURVE'/)
 5000 FORMAT(8F10.0)
 5001 FORMAT(2I5)
 6000 FORMAT(1H ,3E14.6)
      READ(1,5001)N
      IF(N)4,1,3
    4 STOP
      END
```

FILE

APPENDIX VI

Derived Results

$Re^{0.8}$ Nusselt

		X	Y	ERROR
>	17	0.383787D 03	0.109030D 05	-0.596000D 03
>	19	0.367128D 03	0.101240D 05	-0.729040D 03
>	20	0.368667D 03	0.101240D 05	-0.787660D 03
>	21	0.358051D 03	0.977500D 04	-0.736859D 03
>	22	0.270017D 03	0.746000D 04	-0.135827D 03
>	23	0.272503D 03	0.746000D 04	-0.208395D 03
>	24	0.275396D 03	0.766200D 04	-0.915720D 02
>	25	0.297682D 03	0.833800D 04	-0.973928D 02
>	26	0.288328D 03	0.787400D 04	-0.269651D 03
>	27	0.311782D 03	0.859000D 04	-0.300360D 03
>	28	0.281983D 03	0.787400D 04	-0.763270D 02
>	29	0.282188D 03	0.833800D 04	0.381478D 03
>	30	0.362113D 03	0.101240D 05	-0.539620D 03
>	31	0.344820D 03	0.977500D 04	-0.253057D 03
>	32	0.429063D 03	0.141740D 05	0.790535D 03
>	33	0.434986D 03	0.141740D 05	0.530067D 03
>	34	0.438678D 03	0.141740D 05	0.366079D 03
>	35	0.320167D 03	0.914500D 04	-0.246236D 02
>	36	0.318176D 03	0.787400D 04	-0.122871D 04
>	37	0.331661D 03	0.914500D 04	-0.417901D 03
>	38	0.316979D 03	0.944900D 04	0.386313D 03
>	39	0.270639D 03	0.787400D 04	0.260069D 03
>	40	0.284853D 03	0.914500D 04	0.110770D 04
>	41	0.282598D 03	0.809900D 04	0.130081D 03
>	42			

```
>     43    0.286898D 03  0.787400D 04 -0.225765D 03
>     44    0.308171D 03  0.809900D 04 -0.673111D 03
>     45    0.309576D 03  0.833800D 04 -0.479994D 03
>     46    0.258759D 03  0.914500D 04  0.187066D 04
>     47    0.269602D 03  0.914500D 04  0.156123D 04
>     48    0.303542D 03  0.834400D 04 -0.278278D 03
>     49    0.299099D 03  0.823800D 04 -0.242295D 03
>     50    0.273124D 03  0.723100D 04 -0.455601D 03
>     51    0.250766D 03  0.673200D 04 -0.321153D 03
>     52    0.265653D 03  0.723100D 04 -0.238815D 03
>     53    0.258130D 03  0.697300D 04 -0.283730D 03
>     54    0.263568D 03  0.723100D 04 -0.179252D 03
>     55    0.254560D 03  0.697300D 04 -0.184405D 03
>     56    0.255401D 03  0.697300D 04 -0.207700D 03
>     57    0.261689D 03  0.723100D 04 -0.125890D 03
>     58    0.241219D 03  0.673200D 04 -0.646838D 02
>     59    0.232441D 03  0.650800D 04 -0.602515D 02
>     60    0.253297D 03  0.723100D 04  0.108451D 03
>     61    0.237161D 03  0.638000D 04 -0.310199D 03
>     62    0.283624D 03  0.816900D 04  0.169038D 03
>     63    0.280340D 03  0.810100D 04  0.200130D 03
>     64    0.298290D 03  0.883000D 04  0.375380D 03
>     65    0.264194D 03  0.781000D 04  0.381909D 03
>     66    0.306362D 03  0.899700D 04  0.283688D 03
>     67    0.307970D 03  0.976000D 04  0.994433D 03
>     68    0.234804D 03  0.644400D 04 -0.185043D 03
>     69    0.228994D 03  0.644400D 04 -0.364799D 02
>     70    0.226400D 03  0.636000D 04 -0.551615D 02
```

```
>     71        0.222278D 03  0.619800D 04 -0.114641D 03
>     72        0.241219D 03  0.687500D 04  0.783162D 02
>     73        0.316380D 03  0.976200D 04  0.719289D 03
>     74        0.306563D 03  0.947800D 04  0.758166D 03
>     75        0.180856D 03  0.429900D 04 -0.107009D 04
>     76        0.169338D 03  0.470700D 04 -0.427762D 03
>     77        0.230072D 03  0.686000D 04  0.352175D 03
>     78        0.228994D 03  0.693400D 04  0.453520D 03
>     79        0.158335D 03  0.444700D 04 -0.475319D 03
>     80        0.177878D 03  0.515900D 04 -0.148348D 03
>     81        0.175810D 03  0.496000D 04 -0.304940D 03
>     82        0.177878D 03  0.507700D 04 -0.230348D 03
>     83        0.171193D 03  0.481200D 04 -0.359683D 03
>     84        0.188813D 03  0.496000D 04 -0.578099D 03
>     85        0.195794D 03  0.539600D 04 -0.295163D 03
>     86        0.187908D 03  0.565600D 04  0.137422D 03
>     87        0.188361D 03  0.570700D 04  0.178668D 03
>     88        0.220537D 03  0.537400D 04 -0.895806D 03
>     89        0.193099D 03  0.537400D 04 -0.257541D 03
>     90        0.212221D 03  0.651400D 04  0.444952D 03
>     91        0.203826D 03  0.555900D 04 -0.313819D 03
>     92        0.220101D 03  0.632200D 04  0.628723D 02
>     93        0.208255D 03  0.605500D 04  0.794713D 02
>     94        0.209358D 03  0.675200D 04  0.750596D 03
>     95        0.189265D 03  0.635300D 04  0.805121D 03
>     96        0.173043D 03  0.678800D 04  0.157918D 04
>     97        0.181541D 03  0.560700D 04  0.223587D 03
>     98        0.167943D 03  0.515900D 04  0.517845D 02
>     99      0 'ERROR' IS THE ALGEBRAIC DIFFERENCE BETWEEN THE VALUE GI
#END OF FILE
"
```

Reynolds Number	Drag Coefficient.
637	10.216
587	11.151
859	5.136
854	5.015
540	12.377
624	9.452
615	10.006
624	9.239
595	10.378
672	8.354
703	7.565
668	8.424
670	8.431
815	5.693
691	7.824
777	5.948
739	6.474
813	5.149
759	5.743
764	4.752
674	7.685
603	9.350
640	8.773
584	9.177

Reynolds Number	Drag Coefficient.
1212	4.302
1190	4.411
1063	5.774
956	6.660
1027	5.876
991	6.101
1017	5.566
974	6.013
978	6.083
1008	5.745
911	6.484
870	7.085
968	6.488
892	7.056
1114	4.237
1096	4.276
1186	3.543
1020	4.794
1226	3.462
1234	3.106
881	6.772
854	6.548
842	6.770
823	7.155
911	5.775
1276	2.826
1227	2.980

Reynolds Number	Drag Coeffimient.
1622	3.254
1535	2.919
1543	2.665
1488	4.176
1048	6.813
1060	6.898
1074	6.250
1183	5.43
1137	6.03
1253	5.000
1106	6.057
1107	5.065
1509	3.669
1420	3.864
1863	1.856
1895	1.885
1915	1.903
1295	5.103
1285	6.167
1353	4.623
1279	4.176
1051	5.624
1120	
1109	5.468
1130	5.023
1235	4.359
1247	4.334
994	5.592
1046	5.248

NOMENCLATURE

A	Surface area of drop	L^2
Ap	Projected area of drop	L^2
B	Transfer number	
c	Specific heat at constant pressure	L/θ
c_d	Drag coefficient	
D	Equivalent spherical diameter of drop	L
g	Acceleration due to gravity	L/t^2
h	Heat transfer coefficient	M/L^2t
k	Thermal conductivity of medium	M/Lt
Ko	Evaporation constant	
L	Latent heat of vaporisation	L
m	Mass of drop	M
Nu	Nusselt number	
Pr	Prandtl number	
r	Distance from centre of sphere	L
Re	Reynolds number	
Sc	Schmidt number	
t	Time	t
T	Temperature	T
ΔT	Temperature difference	T
V	Velocity	L/t
ρ	Density	M/L^3
ν	Kinematic viscosity	L^2/t

Subscripts

A	Atmosphere
m,M	Mean conditions
d,D	Drop
L	Liquid
E	Evaporation
O	Stationary drop
-	Let bar denote conditions of intense mass transfer

Units

T - Temperature ^{o}C; ρ - density kg/m^3

L - Latent heat of vaporisation kj/kg

k - Thermal conductivity $W/K.m$

ν - Viscosity $N.s/m^2$

C - Specific heat j/kg

P - Pressure N/m^2

v - Specific volume m^3/kg

Definition:

Mean conditions - for evaporating drops the arithmetic average between 100% vapour at drop temperature and superheated steam at surrounding temperature.

BIBLIOGRAPHY

1. R. Hoyle and D. H. Matthews. "The effect of speed on the condensate layer on a cold cylinder rotating in a steam atmosphere". J. Fluid. Mech. 22, 105, 1965.

2. N. A. Fuchs "Evaporation and droplet growth in gaseous media." Pergamon Press, London, 1959.

3. N.A.C.A. Report, 1300, 1957 "Basic Considerations in the combustion of hydrocarbon fuels with air".

4. Nishiwaki, N., Haghi, S. Proceedings First Japan National Congress for Applied Mechanics.

5. Kobayasi, K. "An experimental study of the combustion of a single fuel drop." Fifth (Int.) Symposium on Combustion. Also Engineers Digest, 15. 463-5. 1954. Also Trans. Japan Soc. Mechn. Engrs. 20, 826-31, 1954.

6. Spalding, D.B. "The combustion of liquid fuels". Fourth (Int.) Symposium on Combustion. 847 - 64, 1953.

7. Frössling, N., "On the evaporation of falling drops". Beiträge zur Geophysik. 52. 170-216. 1938.

8. Ranz, W.E. and Marshall, W.R. "Evaporation from Drops". Chem. Eng. Prog., Part I., Vol. 48 No.3. March, 1952. Part II, Vol. 48, No. 4, April, 1952.

9. Lee, K., and Ryley, D.J. "The Evaporation of Water Drops in Superheated steam." J. Of Heat Transfer, 445-451, Nov., 1968.

10. Kumagi, S., Isoda, H. "Combustion of fuel droplets in a vibrating air field." Fifth (Int)., Symposium on Combustion, 1954.

11. Gohrbrandt, W., "Effect of gas motion on vaporisation and combustion.". N.G.T.E., M.110, April, 1951.

12. Rasbach, D.J. and Stark, I. "On the evaporation of water drops in a bunsen flame." D.S.I.R., F.R., Note 26/1951. August, 1952.

13. Ingebo, R.D. "Drag Coefficients for droplets and solid spheres in clouds accelerating in airstreams." NACA Report, No. 3762.

14. Newton, I., Mathematical Principles of Natural Philosophy, Book III, (Transl. 1729).

15. Waddle, Hokon, "The Coefficient of Resistance as a function of Reynolds' Number for solids of various shapes." J. Franklin Inst., 2 17, 459-490 (1934).

16. Schlichting, H., "Boundary Layer Theory". Pergamon Press, Transl. 1955.

17. Topps, J.E.C. "An experimental study of the evaporation and combustion of falling drops." J. Inst. Peltrol, 37., 535, 1951.

18. Eds, A.J., "An introduction to Heat Transfer." Pergamon Press, 1967.

19. Ingebo, R.D., "Study of pressure on effects of vapourisation rate of drop in gaseous media" NACA Report 2850.

"Vaporisation rates and heat transfer coefficients for pure liquid drops." N.A.C.A. Report, 2368.

20. Davis, E.J., and David, M.V. "Two-Phase Gas-Liquid Convection Heat Transfer." I. and E. Fundamentals, Vol.3. (1964), p.111-118.

21. Meisse, C.C. "Ballisicts of an Evaporating droplet." Jet Propulsion, pp.237 - 244. 1954.

22. Rayleigh, Lord. Proc. Roy. Soc., 29, 71, 1879.

23. Ryley, D.J. and Woods, M.R. "The construction and operating characteristics of a new vibrating capillary atomizer." J. Scient. Instrum. 1963, 40, 33.

24. Schneider, J.M. and Hendricks, C.D. "Source of Uniform-Size Liquid Droplets". Review of Scient. Instrum., 35, 10, 1964.

25. Eisenklam, P., Arunchalam, S., and Weston, J.A., "Evaporation rates and drag resistance of burning drops." 11th Sym. on Combustion, pp.715 - 727. Pittsburg: The Combustion Institution., 1966.

26. Eisenklam, P., "Mass Transfer from drops with Simultaneous heat transfer." NEL Report, 453 May, 1970.

27. Godsave, G.A.E., "The burning of single drops of fuel." Fourth (Int) Symposium on Combustion. 818-830. 1953.
Also N.G.T.E. England Report R-66. 1950.

28. Goldstein, S. "Modern developments in fluid dynamics" Oxford, 1938. Claredon Press.

29. Lapple, S.C.E. et al., Fluid and Particle Mechanics. University of Delaware Press, 1951.

30. Toei, R. Okazaki, M., and Kubota, K., "Evaporation from a water drop in a steam/air mixture." Memoirs of the Faculty of Engineering, Kyoto University, Vol., 28, p. 4., October, 1966. p.413.

31. Kinzer, G.D., and Gunn, R., "The Evaporation, Temperature and thermal relaxation-time of freely falling water drops." Journal of Metrology, Vol.8., No.2., April 1951.

32. Yasuo Mori, et.al., "Unsteady heat and mass transfer from spheres." Int. J. Heat Mass Transfer., Vol. 12., pp.571-585. 1969.

33. Hughes, R.R. and Gilliland, E.R., "Mechanics of Drops." Chemical Eng. Progress Vol., 48, No.19, 1952.

34. Perry, J.H., et al., "Chemical Engineer Handbook." McGraw-Hill Book Company, 1963.

35. Kreith, F., "Principles of Heat Transfer." International Textbook Company, 1965.

36. International Critical Tables. National Research Council, U.S.A., 1933.

37. Properties of Water and Steam in Si-Units, Springer-Verlag, 1969.

38. Thermophysical Properties of Water Substance, Edward Arnold (Publishers) Ltd., 1969.